



Advances in nanoarchitectonics of metal-organic frameworks and metal-/metalloid-containing nanomaterials for antibacterial and antifungal applications

Ahmad Abd-El-Aziz^a, Jian Li^a, Moustafa M.G. Fouda^b, Carmen M. Sharaby^c, Xinyue Zhang^a, Ning Ma^a, Spiros N. Agathos^{a,d}, Alaa S. Abd-El-Aziz^{a,*}

^a Qingdao Innovation and Development Center, Harbin Engineering University, Qingdao 266400, China

^b Pre-Treatment and Finishing of Cellulosic Fabric Department, Textile Research and Technology Institute (TRT), National Research Center, 33- El- Buhouth St, Dokki, Giza, 12622- Egypt

^c Chemistry Department, Faculty of Science (Girls), Al-Azhar University, Cairo, Egypt

^d Earth and Life Institute, Catholic University of Louvain, Louvain-la-Neuve 1348, Belgium

ARTICLE INFO

Keywords:

Antibacterial
Antifungal
Metal-organic frameworks
Nanocomposites
Nanoparticles
Nanoarchitectonics

ABSTRACT

The past two decades have seen exponential growth in the design and applications of nanoparticles in the medical field. This review is focused on recent developments in metal-organic frameworks (MOFs) and nanomaterials as inhibitors of microbial growth. With the development of the field of MOFs at the end of the 20th century, much research has been devoted to their biomedical applications. A brief introduction to the structure and synthetic methodologies of MOFs is described. The antibacterial and antifungal activities of a number of examples of MOFs containing transition metals, inner transition metals, and other metals are explored. Metal- and metalloid-containing nanoparticles and composites have also been surveyed for their antibacterial and antifungal activities. A brief description of green and chemical syntheses of nanoparticles is included. This class of metallic nanomaterials encompasses a vast number of nanoarchitectonic paradigms, however, in this review, we will identify a few examples from each metallic group to illustrate the importance of the antimicrobial properties of these nanoparticles. Although metalloids are comprised of a small number of elements compared to metals, there have been several investigations into their antimicrobial activities, which are highlighted at the end of the review. These new substances demonstrate the viability of this class of materials to overcome the ever-growing threat of antimicrobial resistance.

Abbreviations: ADM, ammonium dimolybdate; AMN, aminomalononitrile; AMPs, antimicrobial peptides; AMR, antimicrobial resistance; APTMS, aminosilane; BFO, bismuth ferrite; BioTe, biogenic tellurium nanorods; BNNS, boron nitride nanosheets; BTB, 1,3,5-tri(4-carboxyphenyl) benzene; Car, carbenicillin; CDT, chemodynamic therapy; CQDs, carbon quantum dots; DPPH, 2,2-diphenyl-1-picrylhydrazyl; ED, *Equisetum diffusum*; FTIR, Fourier transform infrared spectroscopy; GLM-Fe, liquid metal gallium-iron nanomaterials; GO, graphene oxide; GSDMD, gasdermin D; GSDMD-NT, gasdermin D N-terminal domain; H&E, haematoxylin and eosin stain; H₂BDC, terephthalic acid; HAp, hydroxyapatite; HB-PAPES, hyperbranched polyaminopropylalkoxysiloxane; HMDI, hexamethylene diisocyanate; HNTs, halloysite nanotubes; ICG, indocyanine green; IL, ionic liquid; IL-1 β , interleukin 1 β ; IL-6, interleukin 6; IONPs, iron oxide nanoparticles; LMs, liquid metal nanoparticles; MABA, microplate Alamar Blue assay; MBC, minimum bactericidal concentration; MFC, minimum fungicidal concentration; mHNTs, metal-coated HNTs; MIC, minimum inhibitory concentration; MOFs, metal-organic frameworks; MRSA, methicillin-resistant *Staphylococcus aureus*; MTT, 3-[4,5-dimethylthiazol-2-yl]-2,5 diphenyl tetrazolium bromide; nFeS, nano-iron polysulfides; NH₂H₂BDC, 2-aminoterephthalic acid; NIR, near-infrared; NPs, nanoparticles; NPPBs, nanoparticle-pinch polymer brushes; PAA, poly(acrylic acid); PAN, polyaniline; PBPs, penicillin-binding proteins; PBS, phosphate-buffered saline; PCL, polycaprolactone; PEG, polyethylene glycol; PHO, polyhydroxyoctanoate; PLA, polylactic acid; poly(l-lactide), PLLA; Pro-IL-1 β , interleukin 1 β precursor; PTT, photothermal therapy; PVA, polyvinyl alcohol; PVP, polyvinylpyrrolidone; ROS, reactive oxygen species; SA, sodium alginate; SBUs, secondary building units; SEM, scanning electron microscopy; SSZ, sulfasalazine; TBAB, tetra-butyl ammonium bromide; TCPP, meso-tetra(4-carboxyphenyl)porphyrin; TEM, transmission electron microscopy; TMB, tetramethylbenzidine; TNF- α , tumour necrosis factor α ; UV-Vis, UV-visible spectroscopy; WHO, World Health Organization; XRD, X-ray diffraction; ZIF-8, zeolitic imidazolate frameworks-8; ZN, zein

* Corresponding author.

E-mail address: aabelaziz@hrbeu.edu.cn (A.S. Abd-El-Aziz).

<https://doi.org/10.1016/j.apmt.2024.102335>

Received 5 June 2024; Received in revised form 27 June 2024; Accepted 14 July 2024
2352-9407/© 20XX

1. Introduction

In November 2023, the World Health Organization (WHO) report on antimicrobial resistance (AMR) underscored the importance of the continued development of antimicrobial agents. In this document, the crisis

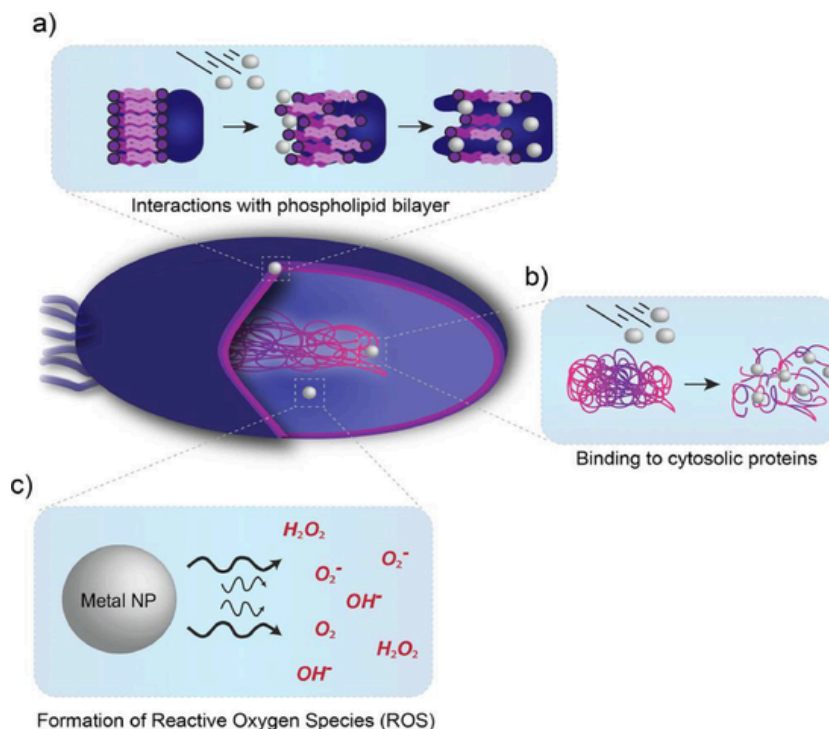


Fig. 1. Mechanisms of antimicrobial activity of nanomaterials via: a) disruption of the phospholipid bilayer, b) binding proteins in the cytosol and c) formation of reactive oxygen species. Reproduced from Ref. [19], with permission from John Wiley & Sons, Copyright © 2018. Wiley-VCH GmbH.

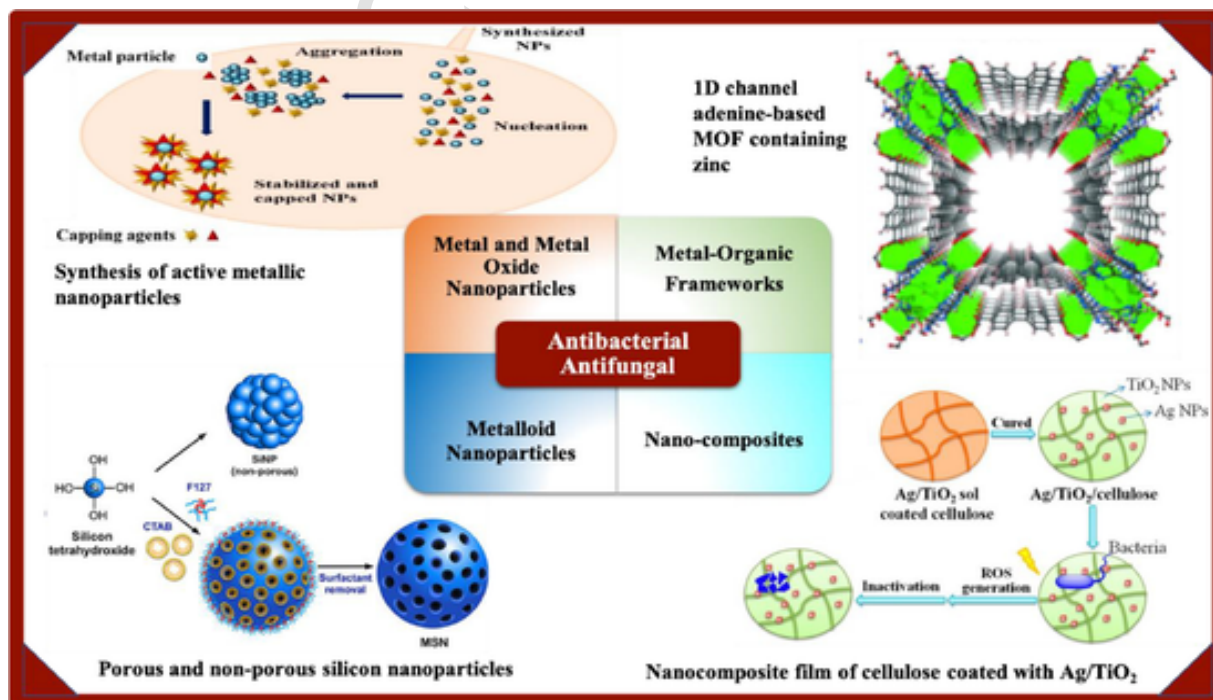


Fig. 2. Classes of antibacterial and antifungal nanomaterials with illustrative examples. Reproduced from Ref. [35] with permission from the Royal Society of Chemistry and from Ref. [36], <https://www.mdpi.com/2079-4991/12/4/673>, Ref. [37], <https://doi.org/10.3389/fchem.2020.00602>, and Ref. [38], <https://doi.org/10.3390/polym10101052>, under the terms of the CC BY 4.0 license, <http://creativecommons.org/licenses/by/4.0/>

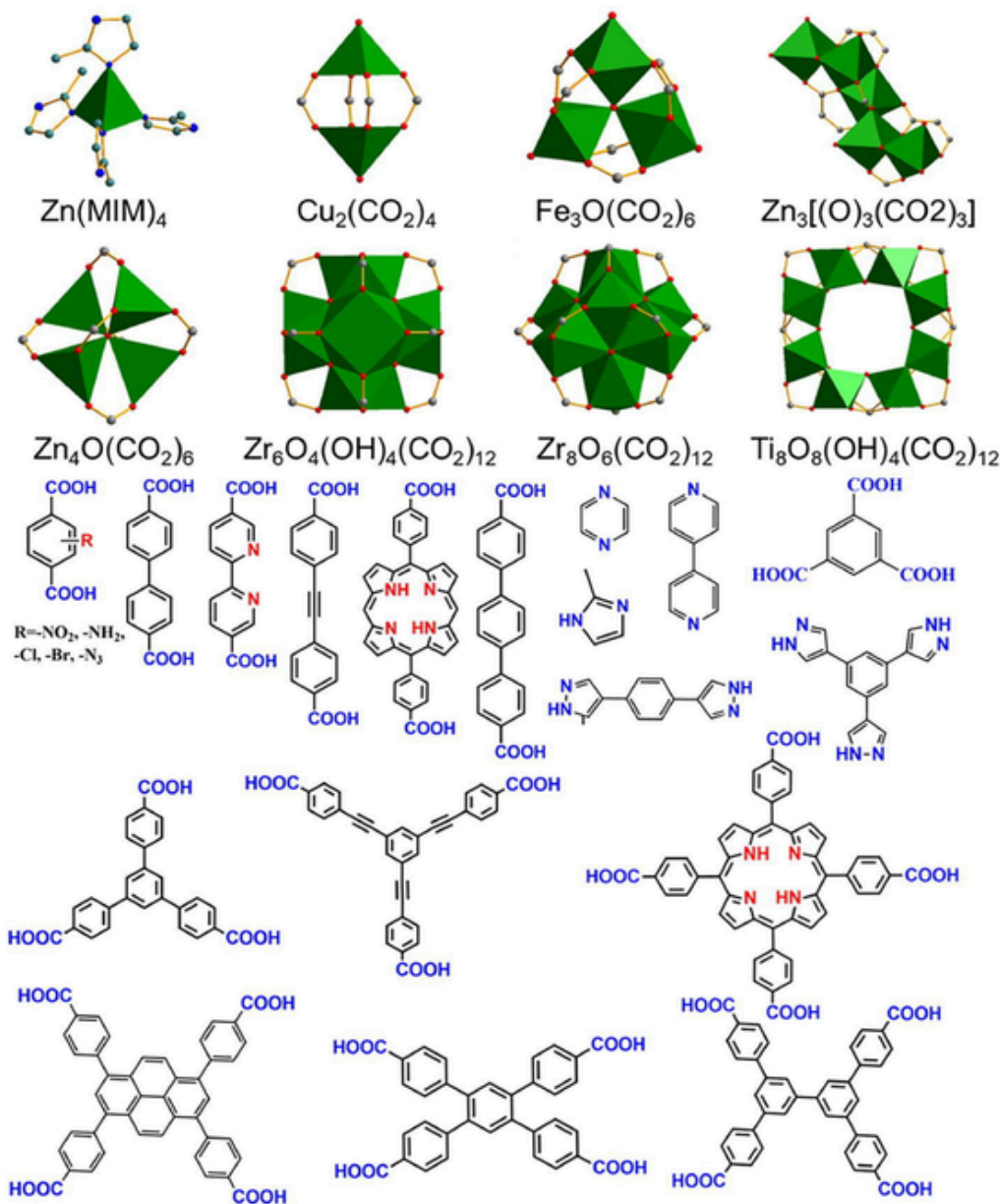


Fig. 3. Example structure of secondary building units (SBUs) and organic linkers used in the construction of MOFs. Reproduced from Ref. [58] with permission from Elsevier, Copyright © 2019.

facing the world in terms of antimicrobial development and clinical trials was analyzed [1]. The report estimated that 1.27 million deaths globally were directly related to AMR in 2019, as an example [1,2]. There has been tremendous interest in the development of metal- and metalloid-containing materials for biomedical applications, including as antimicrobials [3–18]. Some of the mechanisms of antimicrobial activity of nanomaterials are shown in Fig. 1, including phospholipid bilayer interactions, binding of cytosolic proteins, and generation of reactive oxygen species (ROS) [19].

Antimicrobial nanomaterials have been the focus of attention as alternatives to traditional antibiotics, as they have the potential to overcome antibiotic resistance [20–22]. A review by Xie *et al.* described the effects of antibacterial nanomaterials on the development of AMR [23]. Unlike conventional antibiotics, some antibacterial nanomaterials have been shown to have effects that do not result in the development of AMR. However, others do cause AMR evolution due to bacterial resis-

tance mechanisms. The authors therefore proposed four main approaches to try to design antibacterial nanomaterials that would prevent AMR development: design of nanocomposites to diversify the types of interactions and targets in the cell, functionalization of nanomaterials for specific stimuli-responsive behaviour, attaching ligands to the surface of the nanomaterials for species selectivity and ion shielding to reduce non-specific metal ion release. The authors also noted other challenges that hindered the use of antibacterial nanomaterials in different fields, including lower selectivity for target microorganisms, adverse side effects, poor colloidal stability resulting in aggregation and unfavourable reaction kinetics compared to simpler molecules.

In addition to their antibacterial properties, research has also been carried out on the use of nanomaterials for treating fungal infections. In 2020, a review by Xu *et al.* described the progress of investigation of antifungal nanomaterials as potential therapeutic agents [24]. Metal nanoparticles such as silver and zinc oxide, as well as curcumin, chi-

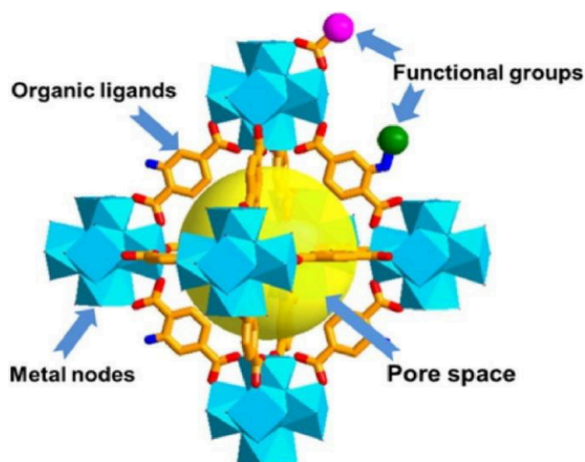


Fig. 4. MOF pore structure. Reproduced from Ref. [58] with permission from Elsevier, Copyright © 2019.

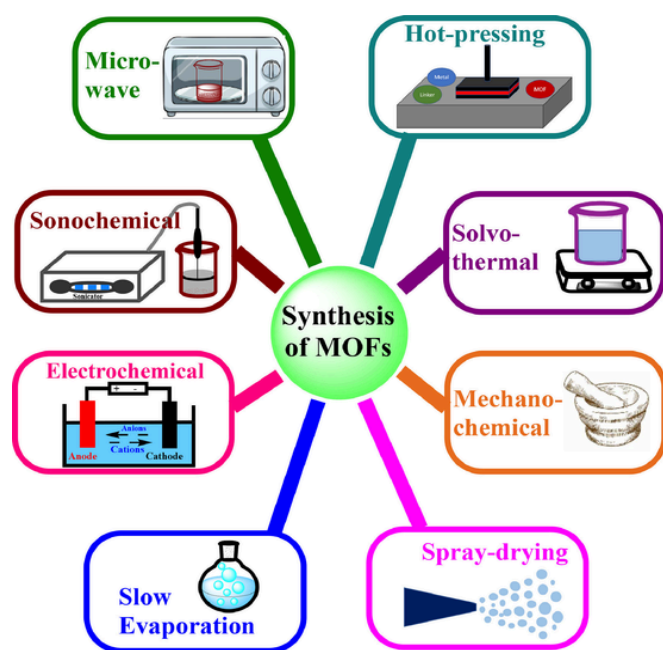


Fig. 5. Different synthetic methods for the preparation of MOFs.

tosan, and SiCl_4 nanoparticles have all shown promise as antifungal agents, although metal nanoparticles have been studied the most for their mechanisms.

Nanocomposites have also been examined for their antibacterial and antifungal activities [25]. Incorporation of inorganic nanoparticles into nanocomposites has been shown to enhance their antimicrobial activity compared to the corresponding bulk materials. The increased activity is a function of greater contact with the bacterial cell surface, due to the nanocomposites' high surface-to-volume ratio. However, further research is needed on their toxicity, details on the mechanism of bacterial interactions, and applications of nanocomposites as antifungal agents.

In an article published in Annual Review of Microbiology in 2021, Li and coworkers surveyed the antimicrobial activities of metals and metalloids like copper and arsenic as well as describing the development of AMR as an evolutionary advantage for microorganisms [26]. In contrast, our review article is focused on metal- and metalloid-containing

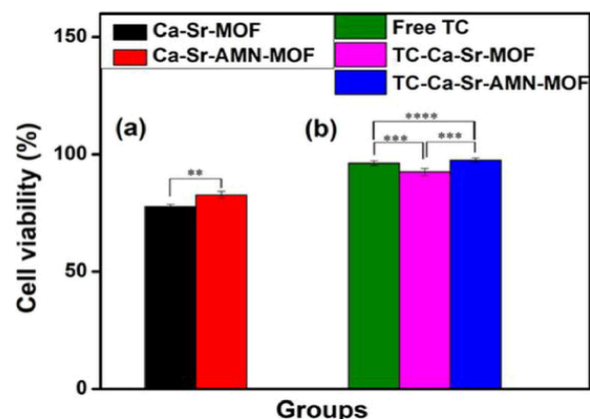


Fig. 6. Cell viability of a) empty and b) tetracycline (TC)-loaded Ca-Sr-MOFs using MTT assays. Reproduced from Ref. [104], <https://doi.org/10.1021/acsomega.3c06991>, under the terms of the CC BY NC ND license, <http://creativecommons.org/licenses/by-nc-nd/4.0/>

materials and their importance in combating bacterial and fungal infections.

Recent reports on nanoarchitectonics have shown the importance of the design of these tunable bioactive materials [27–34]. Fig. 2 is an illustration of the various classes of nanomaterials that are covered in this review. Metal-organic frameworks (MOFs) are composed of metals connected to organic linker groups. As an example, a Zn-containing MOF was prepared with a one-dimensional channel in which adenine residues are immobilized on the interior surface of the channel to facilitate DNA base pairing with thymine [35]. Another class of nanomaterials is metallic nanoparticles. Metal ions can be reduced to metal nanoparticles, then aggregated and stabilized with capping agents to form the active metallic nanoparticles [36]. Metalloid nanoparticles can be prepared similar to metallic nanoparticles and silicon nanoparticles are included in Fig. 2 as an example of this class [37]. Finally, nanocomposites are nanoscale materials that consist of multiple phases. For example, a nanocomposite film was prepared by coating of a cellulose film with Ag and TiO_2 nanoparticles [38]. This review will give a detailed description of the design of these classes of materials and their biological activities, using notable examples.

2. Metal-organic frameworks (MOFs)

Since the 1990's, there has been tremendous interest in the use of metal-organic frameworks (MOFs) in many fields, in light of their extraordinarily high surface areas and their ability to tune their pore size as well as their surface properties [39–54]. A highly cited review by Zhou *et al.* in 2012 thoroughly described the field of MOFs [55]. The development, utilization and challenges of MOFs in biomedicine were examined by Yang and Yang [56] and Wang *et al.* [57]. They reviewed the preparations of MOFs and the ability to functionalize them for use in biomedical fields such as drug delivery, detection of diseases and as antimicrobial agents.

2.1. Structure

Jiao *et al.* described the structure of MOFs and their functional applications in various fields including biomedicine [58]. They highlighted the challenges facing the progress of this area, as it still requires more research to fully understand the process of self-assembly in a closed system. MOFs are porous materials that consist of metals or metal clusters, referred to as secondary building units (SBUs), connected by organic linkers, which contain either nitrogen atoms or car-

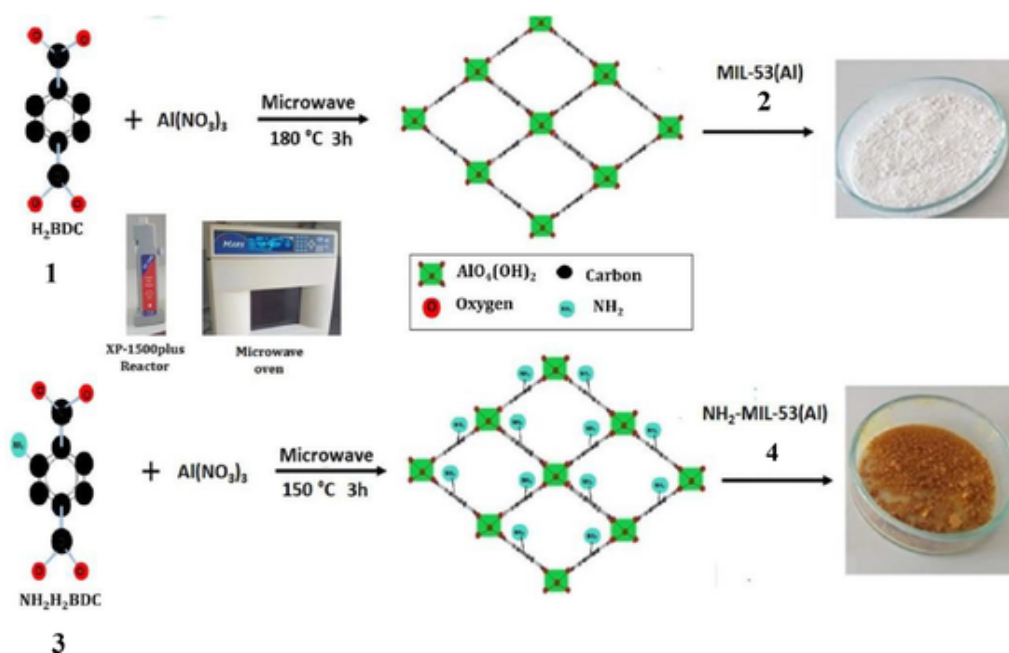


Fig. 7. Microwave synthesis of aluminum-based metal-organic frameworks (MOF). Reproduced from Ref. [112] with permission from Elsevier, Copyright © 2022.

boxylic acid groups. A few examples of SBUs containing Zn, Cu, Fe, Zr, or Ti, as well as several organic linkers, are presented in Fig. 3.

By selecting specific SBUs and organic linkers, MOFs can be tuned for pore size and structure [59–63]. This can provide pore surfaces with different functional sites for a range of potential applications. Functional groups may also be integrated into the organic linkers or added via post-synthetic modification of SBUs or organic linkers. Fig. 4 shows the general structure of a pore in an MOF [58]. Due to the tunable properties of MOFs, these pores can range in size, from accommodating small molecules and metal atoms to larger polymers and even small enzymes.

2.2. Synthetic methodologies

Synthetic methodologies for the preparation of MOFs were summarized in a highly cited review by Stock and Biswas in 2012, as well as several more recent reviews [64–68]. Fig. 5 outlines the main synthetic techniques for MOFs. It was reported that the microwave and ultrasound techniques were the most efficient, with the lowest cost and energy consumption [69]. The microwave approach produces highly porous and crystalline materials [70,71]. It also can allow for smaller particle sizes and greater control over shape [72,73]. The microwave methodology often gave high yields and shorter reaction times [74,75]. Synthesis using ultrasound can reduce the time and temperatures needed for nucleation and crystallization, but requires careful handling to achieve optimal particle size and morphology [76–78]. The methodology for the electrochemical preparation of MOFs first appeared in a patent by Müller *et al.* from BASF Aktiengesellschaft in 2005 [79]. Electrochemical synthesis of MOFs consists of two types: anodic dissolution and cathodic deposition [80,81]. This approach allows for fine control over particle size, but the morphology of the resulting MOFs is highly dependent on concentrations of the SBUs and linkers by the electrode [82–84]. Hot pressing is a rapid solvent-free technique involving the bonding of the SBUs and linkers to the surface of substrates, followed by the application of temperature and pressure to initiate nucleation [85–87]. Another solvent-free or low-solvent synthetic approach is mechanochemical synthesis, which uses mechanical force to assist the chemical reactions, through milling, grinding, or liquid-assisted grind-

ing [88–91]. Spray drying is efficient in preparing microspherical powders, which can be effectively scaled up with a low-cost and simple methodology [92]. The solvothermal method uses heated solvent in a sealed vessel so that it can reach temperatures above its atmospheric boiling point [93,94]. Disadvantages to this approach include high temperatures and lower yields [95]. Lastly, in one of the first effective methods for MOF preparation, the slow evaporation method, the reagents are mixed and the solvent slowly evaporates, resulting in deposition of crystals that promote further nucleation [96].

2.3. Antibacterial and antifungal activities

MOFs can exert antibacterial effects through (1) the release of antimicrobial ligands, (2) the release of metal ions with antibacterial activity like Ag, Cu, and Zn, (3) the release of antibacterial agents carried by the MOF, or (4) the release of antibacterials loaded by post-synthetic modifications into the MOF. Recent progress has been made in developing Zn-based MOFs, Cu-based MOFs, Ag-based MOFs, and Fe-based MOFs for antibacterial applications, both as pure MOFs and composite MOF systems. Strategies like surface modification, core-shell structures, and MOF derivatives have been utilized to enhance antibacterial performance. MOFs show broad-spectrum antibacterial activity against both Gram-positive and Gram-negative bacteria. Proposed mechanisms involve metal ion release, ROS generation, and synergies with co-loaded antibiotics. Challenges remain regarding biocompatibility, controlled degradation, efficient loading, and controlled cargo release. However, continued research to address these will support the translation of MOF antibacterial platforms to clinical applications [97,98]. In addition to their antimicrobial effects, MOFs can also simultaneously be used to promote wound healing while preventing infection at the wound site [99,100]. In this section, we will divide the MOFs based on the metallic moieties and provide some recent examples of the use of this class of materials as antimicrobial and antifungal agents.

2.3.1. Alkaline earth metals

Alkaline earth metal-containing MOFs have been utilized in various applications, including the biomedical field [101–103]. Here we describe an example of this class of materials. Aminomalononitrile

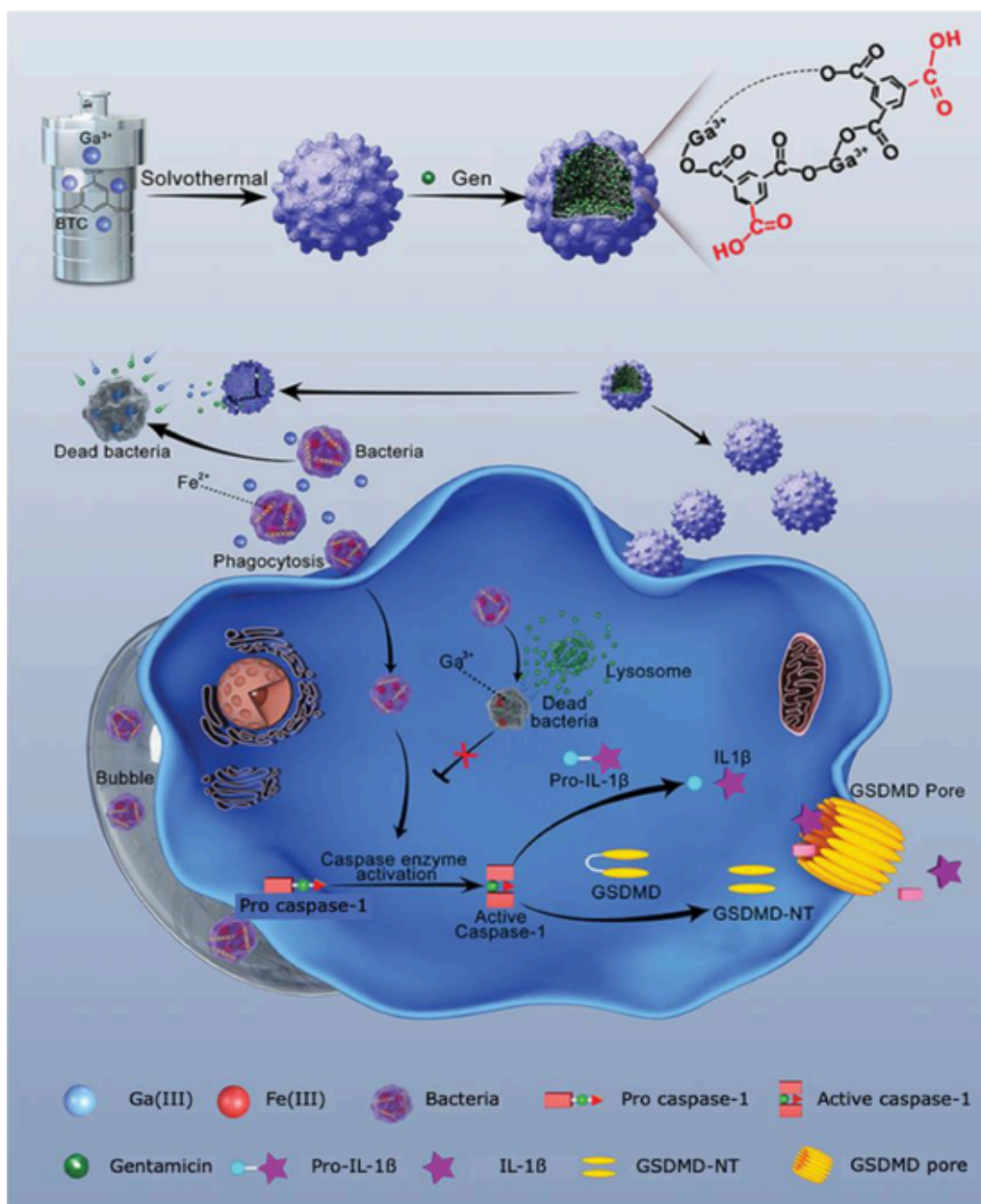


Fig. 8. Illustration of cellular mechanisms for GaMOF inhibition of intracellular bacterial growth and pyroptosis, as well as anti-inflammatory activity. Pro-IL-1 β = interleukin 1 β precursor, IL-1 β = interleukin 1 β , GSDMD = gasdermin D, GSDMD-NT = gasdermin D N-terminal domain. Reproduced from Ref. [113], with permission from John Wiley & Sons, Copyright © 2022.

(AMN)-coated MOFs with calcium, strontium, and organic ligands were developed by Vadivelmurugan *et al.*, and their applications as antibacterial agents and drug carriers of tetracycline were investigated [104]. In this study, tetracycline was loaded on the MOFs in high capacity. Drug release studies showed 55.15 % cumulative release from Ca-Sr-MOF and 9.1 % from Ca-Sr-AMN-MOF over 24 h. The cytotoxicity assays demonstrated that both MOFs (Ca-Sr-MOF and Ca-Sr-AMN-MOF) showed good biocompatibility with fibroblast cells. The relative cell viability was over 80 % for both empty Ca-Sr-MOF and Ca-Sr-AMN-MOF, as well as for tetracycline (TC)-loaded TC-Ca-Sr-MOF and TC-Ca-Sr-AMN-MOF, as shown in the results from MTT (3-[4,5-dimethylthiazol-2-yl]-2,5 diphenyl tetrazolium bromide) assays in Fig. 6. Antibacterial testing against *E. coli* revealed enhanced inhibition zones for tetracycline-loaded MOFs compared to free tetracycline, indicating improved antibacterial performance. It was therefore

concluded that Ca-Sr-based MOFs are promising drug carriers for tetracycline delivery with sustained release and improved antibacterial activity, in which the AMN polymer coating allowed for the modulation of the drug release profile.

2.3.2. Aluminum and gallium

Multiple metals such as aluminum and gallium have gained attention as components of MOFs in light of their low cost and toxicity, as well as their industrial and biomedical applications [105–111]. To demonstrate the antibacterial and antifungal activities of Al and Ga, a few examples are presented.

An aluminum-based metal-organic framework, the porous aluminum terephthalate (MIL-53(Al)) (2), and its amine-functionalized form, NH₂-MIL-53(Al) (4), were synthesized using a microwave method from terephthalic acid (H₂BDC) (1) or 2-aminoterephthalic acid

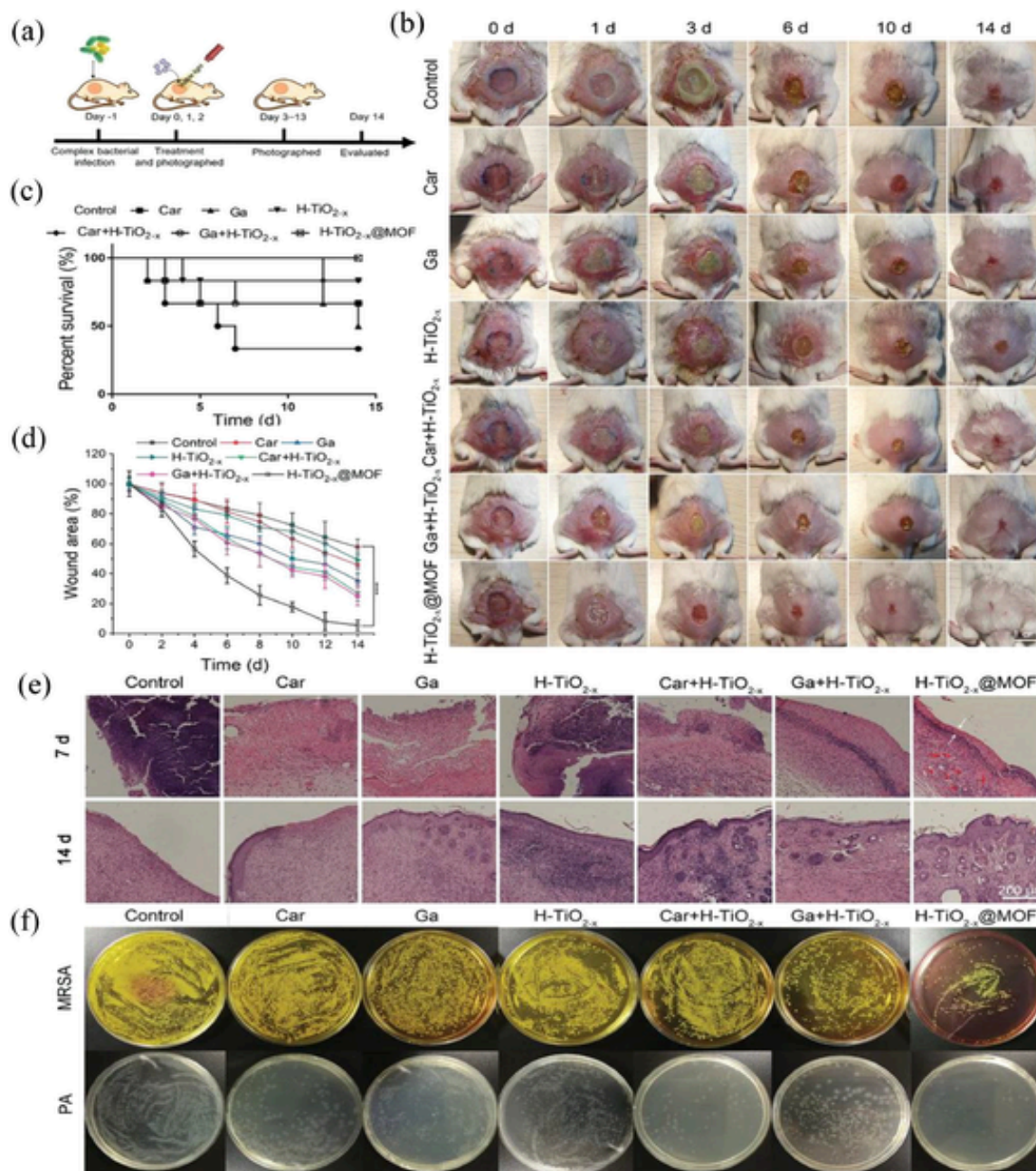


Fig. 9. Mouse model of wound healing *in vivo*. a) Illustrated outline of wound healing experiment design, b) photographs of infected wounds up to 14 days after treatments (Car = carbenicillin, H-TiO_{2-x} = titanium oxide nanoshells, Car + H-TiO_{2-x} = carbenicillin-coated nanoshells, Ga + H-TiO_{2-x} = gallium-coated nanoshells, H-TiO_{2-x}@MOF = gallium MOF-coated nanoshells), c) survival rates of mouse groups, d) reduction of wound area size over time (data = means ± standard deviation; n = 3; **** p < 0.0001), e) microscope images of wound tissue sections stained with hematoxylin and eosin at days 7 and 14 (white arrows indicate the epidermis, red arrows indicate blood vessels, f) photographs of agar plates inoculated with bacterial colonies from the infected wounds of mice in each treatment group. Reproduced from Ref. [115] with permission from John Wiley & Sons, Copyright © 2020 Wiley-VCH GmbH.

(NH₂H₂BDC) (3), as shown in Fig. 7 [112]. The materials were characterized and found to have crystalline, microporous structures. Functionalization with amine groups increased the surface charge but decreased particle size and surface area of 4 compared to 2. The biological activities of the MOFs were tested, and 4 showed better antioxidant ability to scavenge 2,2-diphenyl-1-picrylhydrazyl (DPPH) radicals (48.6 % at 500 mg/L) and metal chelating capacity (63.3 % at 500 mg/L) compared to MIL-53(Al). In tests with plasmid DNA, both 4 and 2 demonstrated DNA cleavage. MOF 4 also exhibited stronger antimicrobial properties against bacteria and fungi tested, with minimum inhibitory

concentrations as low as 8 mg/L against *Enterococcus hirae*. The MOFs, especially 4, displayed excellent anti-biofilm activity against *S. aureus*, inhibiting up to 79 % of biofilm formation at 500 mg/L concentration. The results indicate that aluminum MOFs have promising biological activities and could be used as antioxidant, antimicrobial, and anti-biofilm agents in various applications pending further research. Functionalization with amine groups enhanced some of these activities.

Huang *et al.* described how gallium MOFs form into nanoparticle “bombs” that can enter cells and activate apoptosis via the caspase pathway [113]. The gallium MOFs can carry antibiotics across cell

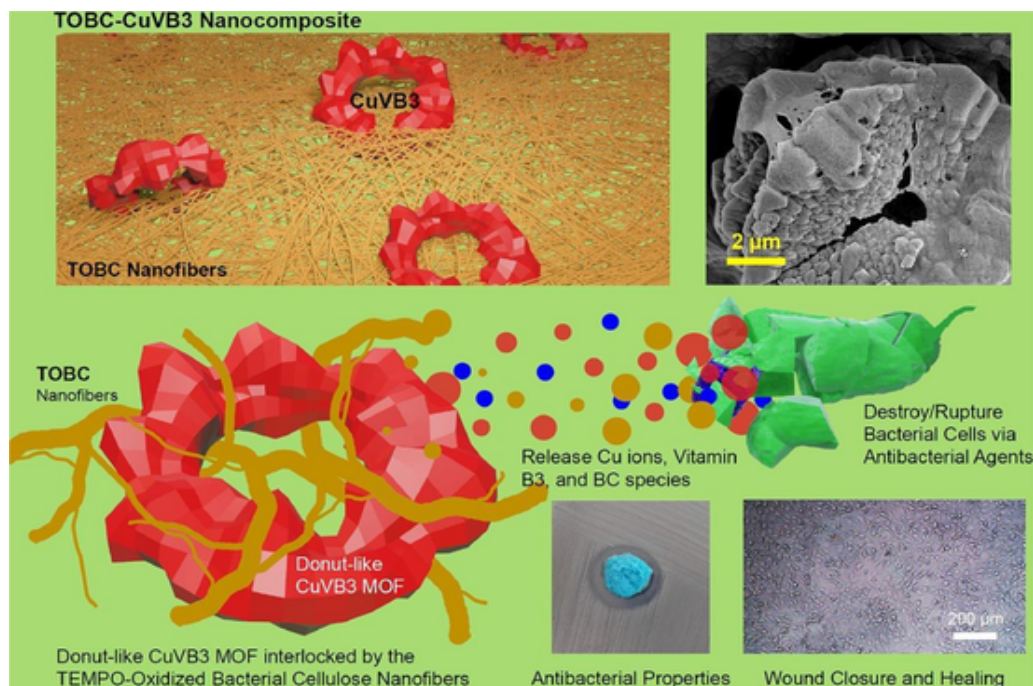


Fig. 10. Summary of structure and activity of the copper-cellulose CuVB3 MOF. Reproduced from Ref. [126] with permission from Elsevier, Copyright © 2023.

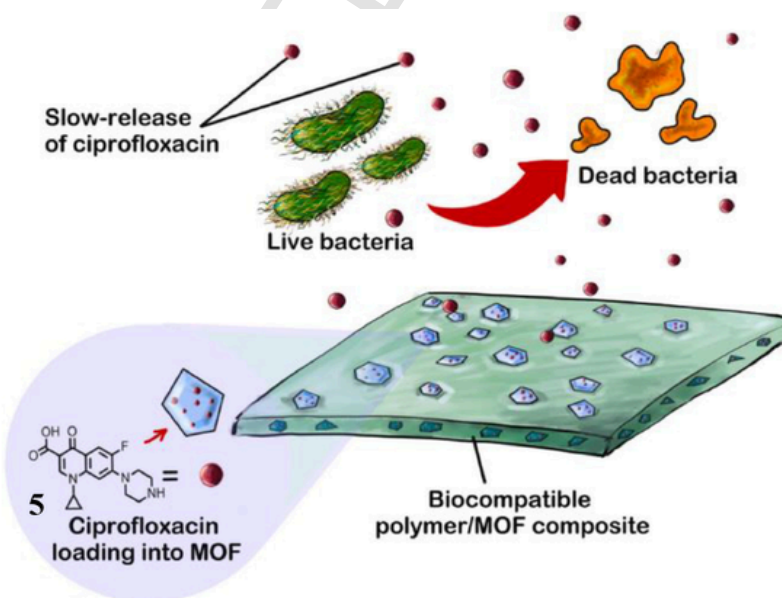


Fig. 11. Schematic illustration of the loading of ciprofloxacin into PCL-MOF composites and sustained release of the antibiotic. Reproduced from Ref. [127], <https://doi.org/10.1016/j.jddst.2023.104894>, under the terms of the CC BY 4.0 license, <http://creativecommons.org/licenses/by/4.0/>

membranes and interfere with iron metabolism using the Ga^{3+} mechanism. The *in vivo* inflammation-associated pyroptosis caused by infections with intracellular *S. aureus* bacteria was also reduced by the gallium MOFs and even further reduced by a combination of gallium MOFs with conventional antibiotics. The anti-pyroptosis mechanism is shown in Fig. 8.

Liu *et al.* prepared MOFs containing gallium and loaded with antimicrobial peptides (AMPs) to use as a combination therapy for targeting methicillin-resistant *Staphylococcus aureus* (MRSA) and *E. coli* bacteria [114]. The resulting nanocomposites not only showed antibacterial ef-

fects from both the gallium and AMPs, but also a synergistic effect that was stronger than each individually. Other advantages of the nanocomposites included the downregulation of proinflammatory cytokines IL-6 (interleukin 6) and TNF- α (tumour necrosis factor α), which improved wound healing, as well as being biocompatible.

A gallium-carbenicillin framework containing coated defect-rich hollow titanium oxide nanoshells, referred to as $\text{H-TiO}_{2-x}\text{/MOF}$, was prepared by Yang *et al.* [115]. The framework was also sensitive to degradation under acidic pH, such as that present in the environment of bacterial infections. This framework synergistically generated ROS

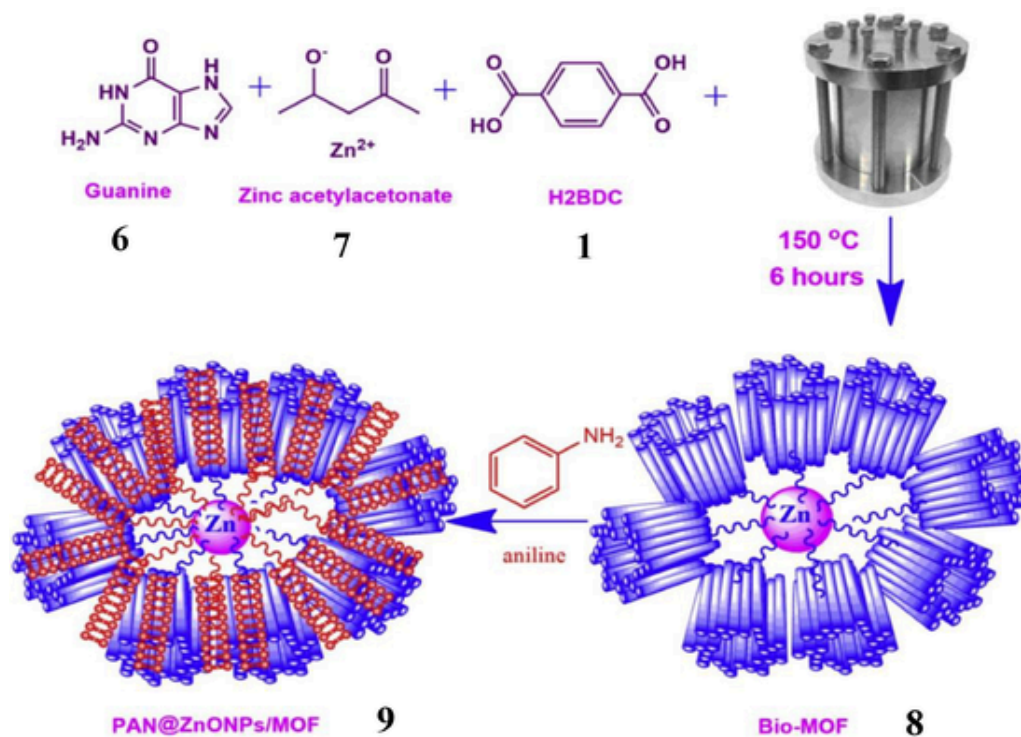


Fig. 12. Synthesis of PAN@ZnONPs/MOF (9). Reproduced from Ref. [128] with permission from Elsevier, Copyright © 2020.

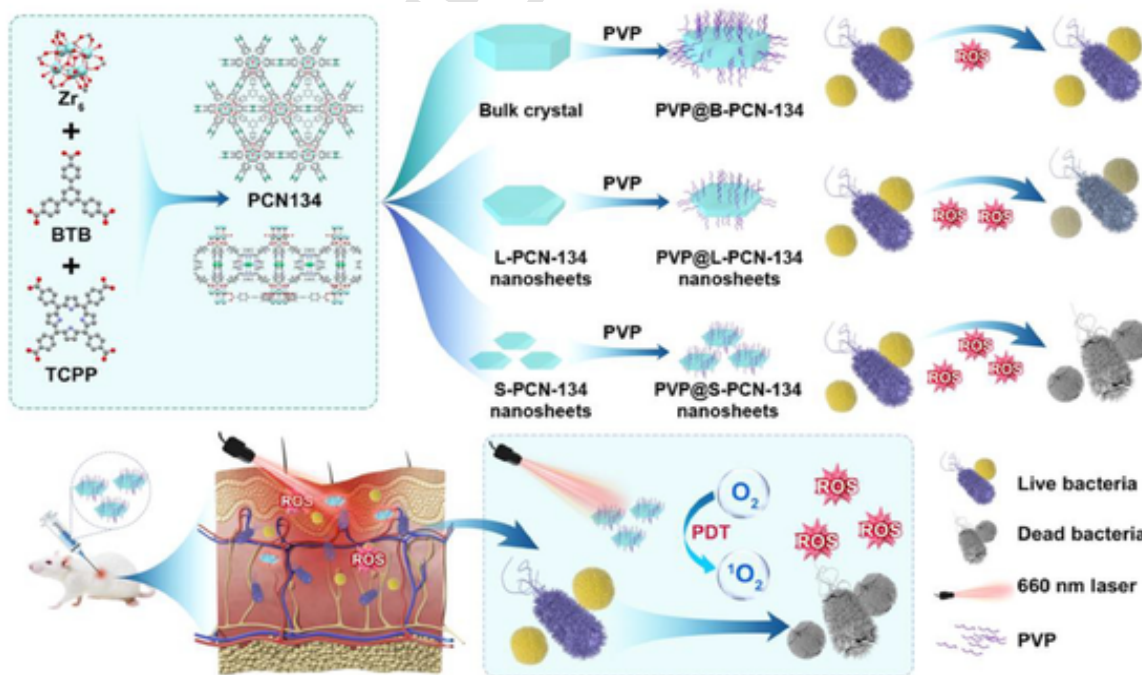


Fig. 13. Summary of the synthetic preparation of PCN-134 MOFs and their use in photodynamic therapy. Reproduced from Ref. [129] with permission from Elsevier, Copyright © 2023.

from both the Ga and TiO₂, in addition to the antibacterial properties of carbenicillin. Due to these factors, improved antibacterial properties were observed for the MOFs *in vitro* against MRSA and *P. aeruginosa*. An *in vivo* mouse model outlined in Fig. 9a was then used to study their wound healing and antibacterial effects. In addition to reduced bacter-

ial load, which was determined by growth of bacterial colonies on plates inoculated with the bacteria from infected tissue (Fig. 9f), the wounds closed faster due to the MOF compared to any combination of the individual components (Fig. 9b and d). The survival rate (Fig. 9c) was also highest for the H-TiO_{2-x}@MOF. The authors proposed that the

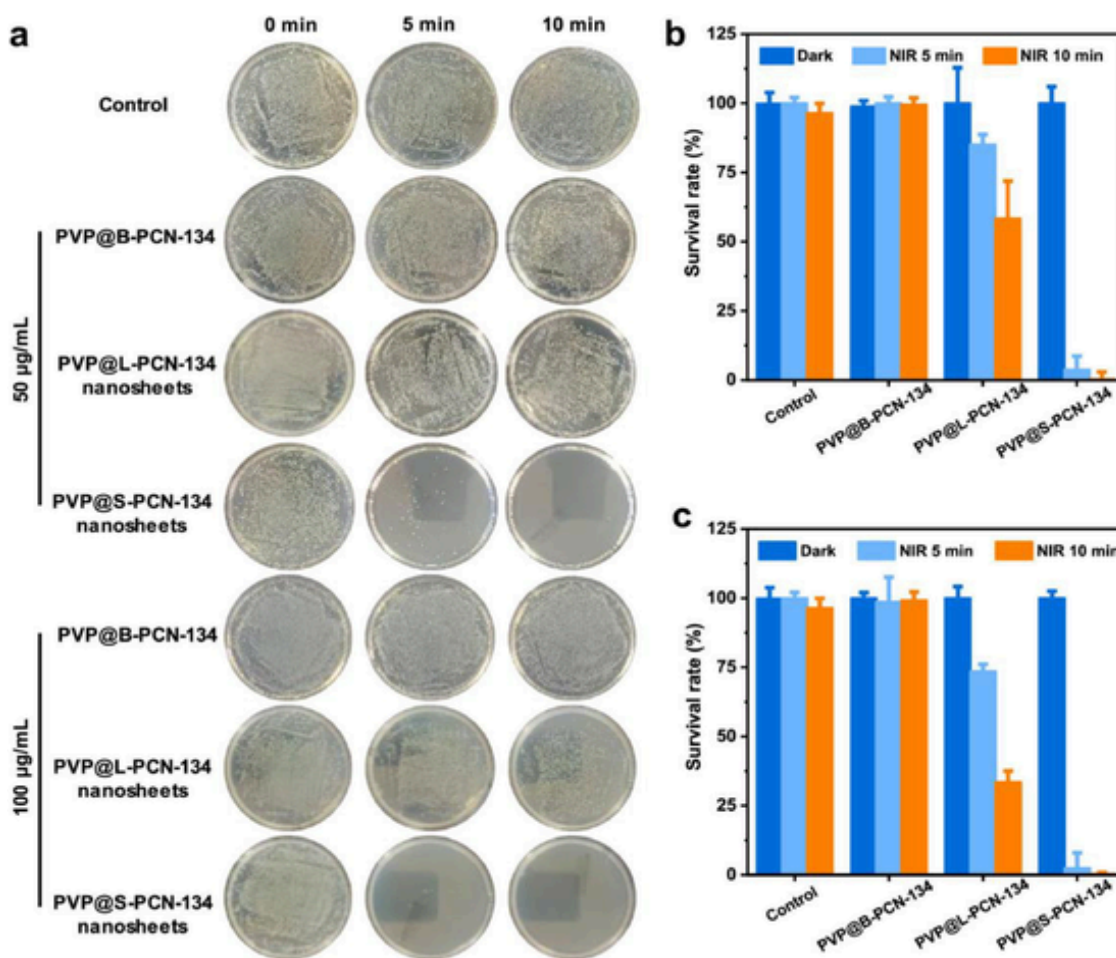


Fig. 14. Antibacterial studies of photodynamic therapy against *S. aureus* using containing polyvinylpyrrolidone (PVP) of PCN-134 MOFs and 660 nm near infrared (NIR) laser irradiation. a) *S. aureus* plates treated with 0 (control), 50, or 100 µg/mL PCN-134 MOFs. Graphs of the survival rates are shown for the b) 50 µg/mL and c) 100 µg/mL concentrations of PCN-134. Reproduced from Ref. [129] with permission from Elsevier, Copyright © 2023.

absence of inflammatory cells due to infection would improve healing. Further, the MOF encouraged vascularization of the wound site, which could recruit different mediators at the site to also improve wound healing (Fig. 9e).

2.3.3. Transition metals

Transition metal-containing MOFs have seen considerable attention due to their wide range of uses including renewable energy, biomedical, catalytic and environmental applications [116–125]. A nanocomposite wound dressing was prepared using a copper MOF of TEMPO-oxidized bacterial cellulose nanofibers with vitamin B3 (TOBC-CuVB3) [126]. An agar diffusion method was used to measure antibacterial activity against Gram-positive *S. aureus* and Gram-negative *E. coli*. In addition, in cellular scratch assays, over 98 % of wounds treated with the copper nanocomposite closed. This combination showed that the nanocomposite not only prevented infection, but also promoted wound healing. A summary of the findings is shown in Fig. 10.

Researchers developed composites of MOFs loaded with the antibiotic ciprofloxacin integrated into polycaprolactone (PCL) polymer membranes with UiO-66 and UiO-66-NH₂ zirconium-based MOFs [127]. Ciprofloxacin (5) was loaded into the MOFs post-synthetically and then integrated into PCL membranes using a solvent casting method. Drug release studies showed pH-dependent drug discharge with sustained delivery over seven days from the PCL-MOF composites, with concentrations remaining effective against bacteria. Antimicrobial

testing demonstrated inhibition of both Gram-positive *S. aureus* and Gram-negative *E. coli* bacterial growth. The ciprofloxacin-loaded PCL-MOF composites showed promise as an antimicrobial platform for controlled and sustained drug delivery at effective doses, as shown in the illustration in Fig. 11. The authors suggested these composite systems could be useful for developing medical devices or implants for the treatment of infections.

Shouei *et al.* prepared guanine-MOF (Bio-MOF) (8) by ultrasonic mixing of guanine (6) with zinc acetylacetonate (7) and terephthalic acid (1) for 30 min, followed by heating for 6 h at 150 °C [128]. Polyaniline (PAN) was encapsulated within a bio-compatible metal-organic framework (Bio-MOF) containing zinc oxide nanoparticles. The resulting PAN@ZnONPs/MOF composite (9) was investigated for its antimicrobial properties. The composite photocatalyzed the degradation of ciprofloxacin from hazardous pharmaceutical waste. The PAN formed a fibrous network with diameters around 20 nm and lengths from 180–450 nm. The Bio-MOF particles were rod-shaped with diameters of 55–130 nm (Fig. 12). Combining PAN and Bio-MOF led to a rougher surface and more porous structure.

The PAN@ZnONPs/MOF (9) composite was able to degrade 97.2 % of ciprofloxacin (5) after 70 min under visible light irradiation. The increased photocatalytic activity was attributed to improved charge separation from the ZnO and conductivity of the PAN. Antimicrobial testing showed the PAN@ZnONPs/MOF (9) composite had enhanced inhibition zones under light compared to dark conditions against *S. aureus*, *E.*

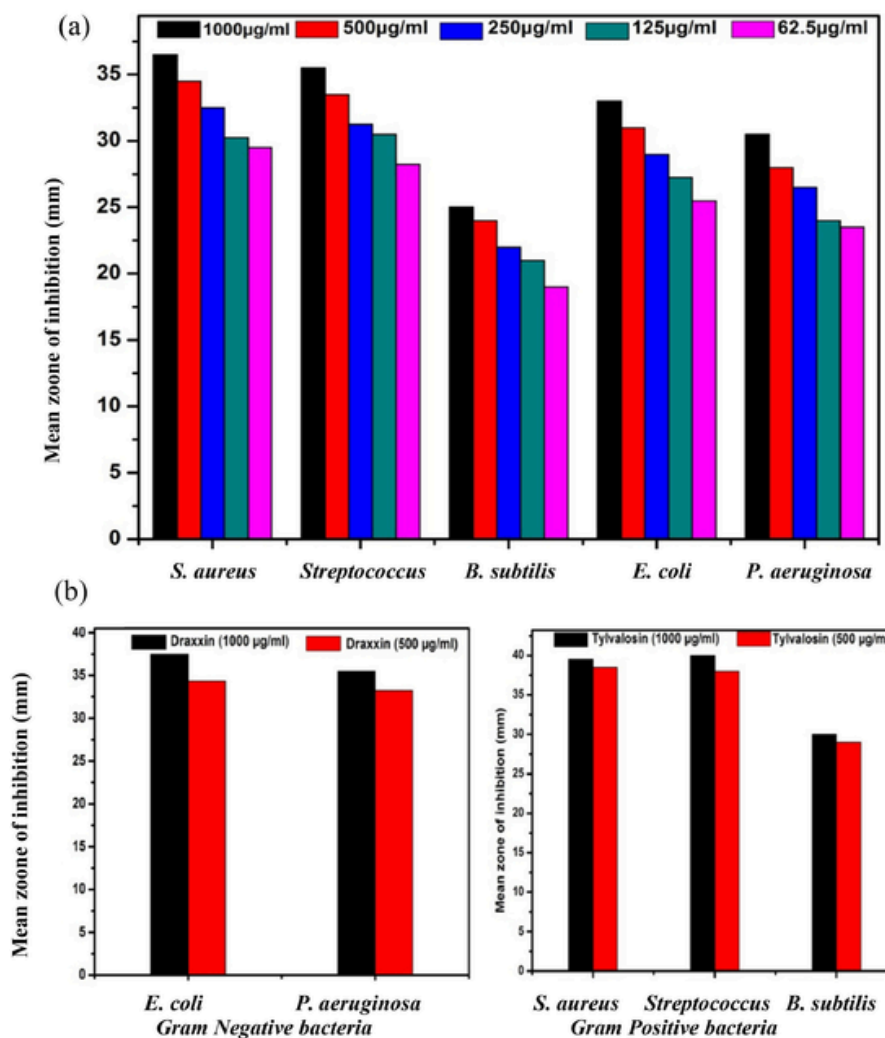


Fig. 15. Inhibition zones for a) *S. aureus*, *Streptococcus*, *B. subtilis*, *E. coli*, *P. aeruginosa* treated with Ni-gallate MOFs and b) *E. coli* and *P. aeruginosa* treated with draxxin, as well as *S. aureus*, *Streptococcus*, and *B. subtilis* treated with tyvalosin. Reproduced from Ref. [130], <https://doi.org/10.1186/s12645-023-00207-5>, under the terms of the CC BY 4.0 license, <http://creativecommons.org/licenses/by/4.0/>

coli, *C. albicans* and *Aspergillus niger*, demonstrating a photo-activated antimicrobial effect. The fast photocatalytic degradation of ciprofloxacin and photo-activated antimicrobial properties make the PAN-encapsulated Bio-MOF an interesting material for disinfection and sterilization applications.

Xue *et al.* designed size-controlled synthesis of two-dimensional (2D) porphyrin-based metal-organic framework (MOF) PCN-134 nanosheets and explored the effect of size on their photodynamic performance for enhanced photodynamic antimicrobial therapy [129]. 2D PCN-134 MOF nanosheets with different lateral sizes and thicknesses were synthesized by a two-step solvothermal method by controlling the reaction temperature (Fig. 13). Zirconium salts were reacted with 1,3,5-tri(4-carboxyphenyl) benzene (BTB) at low temperature, followed by reaction with meso-tetra(4-carboxyphenyl)porphyrin (TCPP) at high temperature, yielding PCN-134 MOF. Different types of nanosheets were produced by changing the temperature, organic acid, and type of zirconium salt in the first step. These nanosheets were then modified with polyvinylpyrrolidone (PVP).

Small PCN-134 (S-PCN-134) nanosheets (lateral size 160–180 nm, thickness 9.1–9.7 nm) exhibited higher catalytic activity for ROS generation under 660 nm laser irradiation compared to bulk PCN-134 crystals and large PCN-134 (L-PCN-134) nanosheets. After modification

with PVP, PVP@S-PCN-134 nanosheets showed excellent photodynamic antibacterial activity against *S. aureus* (Fig. 14). These nanosheets also promoted wound healing in a mouse model under 660 nm laser irradiation. Bacteria were taken from the wound tissue after 3 days and the lowest level of bacteria was observed from the samples from the group treated with the nanosheets and irradiation. Sections of tissue were also obtained after 9 days of treatment and showed growth of granulation tissue, as demonstrated by haematoxylin and eosin (H&E) staining. The antibacterial effect was also demonstrated by measuring the degree of inflammation. The level of inflammatory cytokine TNF- α was determined using staining with anti-TNF- α antibodies and, as expected, the lowest level of TNF- α was also observed in the group treated with the nanosheets and irradiation.

In summary, the PVP@S-PCN-134 nanosheets acted as efficient photosensitizers for photodynamic antimicrobial therapy and the optimization of 2D MOF nanosheet size allowed for enhanced photodynamic performance for antibacterial applications.

The synthesis and characterization of a nickel-based metal-organic framework (Ni-gallate MOF) using the natural antioxidant gallic acid as a linker was described in an article by El-Shahawy *et al.* [130]. The Ni-gallate MOF displayed antibacterial activity against both Gram-positive (*S. aureus*, *Streptococcus*) and Gram-negative (*E. coli*, *P. aeruginosa*) bac-

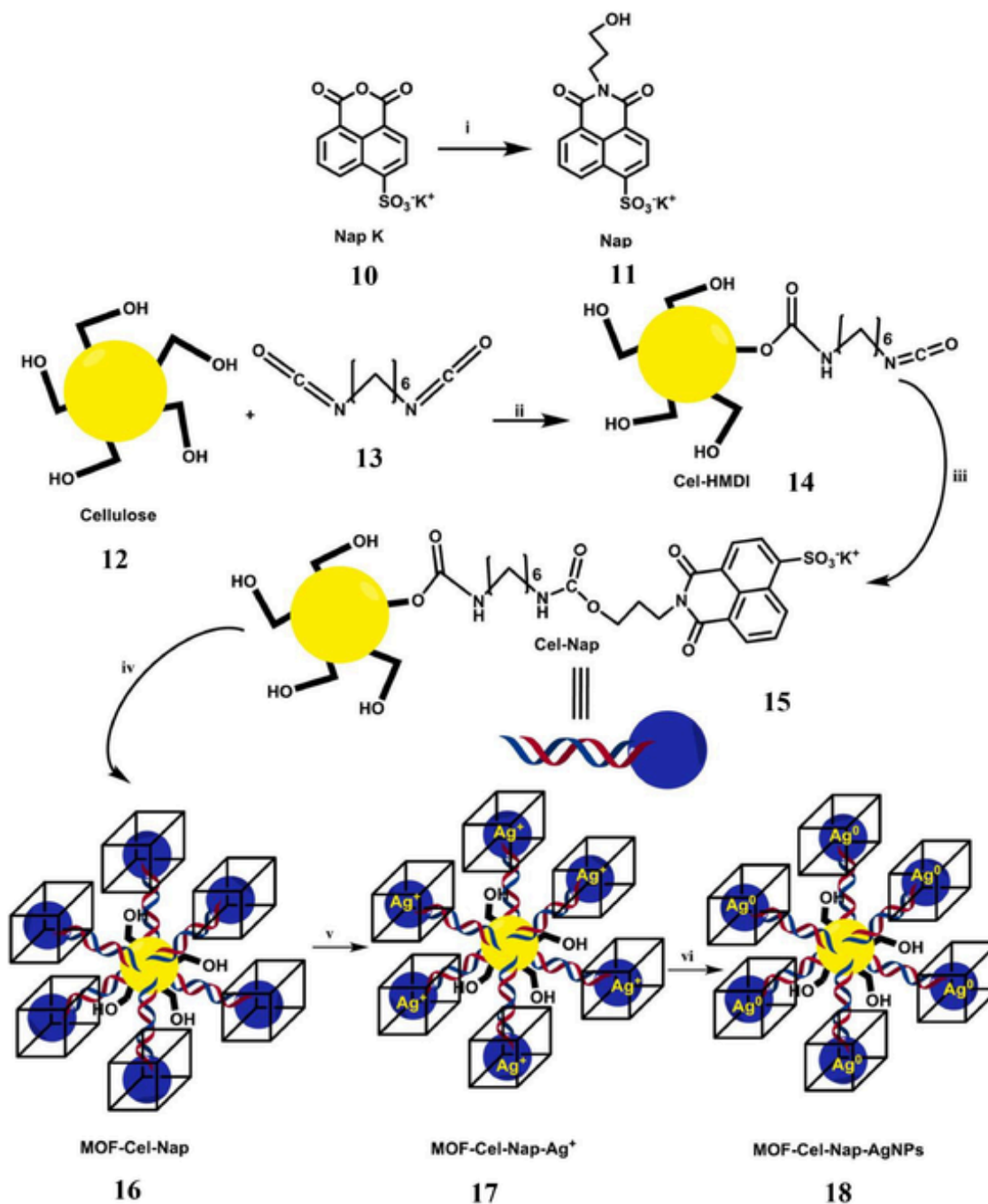


Fig. 16. Synthetic methodology for the preparation of cellulose-based fluorescent sensor (Cel-Nap). (i) 3-amino-1-propanol, H₂O, 90 °C, 4 h; (ii) HMDI, DMF, 70 °C, 4 h; (iii) DMF, RT, 24 h; (iv) 1,4-benzene dicarboxylic acid, Cel-Nap, DMF, 120 °C, 24 h (for UiO-66 MOFs) or 4-methylimidazole, Cel-Nap, methanol, RT, 2 h (for ZIF-8 MOFs); (v) AgNO₃, RT, 3 h; (vi) NaBH₄, 3 h, RT. Reproduced from Ref. [131] with permission from Elsevier, Copyright © 2023.

teria, antifungal activity against two fungal strains (*Aspergillus flocculosus* and *Aspergillus nigricans*), and anticancer activity against human rhabdomyosarcoma (RMS) cells. The Ni-gallate MOF inhibited cell growth in a concentration-dependent manner (Fig. 15). Its anticancer efficacy was comparable to the chemotherapy drug doxorubicin. The mechanisms behind the antimicrobial and anticancer activities are unknown but may involve reactive oxygen species generation by the gallic acid component. Further studies are needed to elucidate the mechanisms. Overall, the results demonstrate that the synthesized Ni-gallate MOF has broad-spectrum antimicrobial effects and anticancer potential, warranting further investigation for therapeutic applications.

Yilmaz and coworkers reported the development of a cellulose-based fluorescent sensor (Cel-Nap) using a naphthalimide group for detecting chromium (VI) ions [131]. This group also previously described the use of the UiO-66 MOF modified with naphthalimide for detection of chromium ions as well as its antimicrobial activity [132]. The synthetic approach of modifying cellulose with naphthalimide is shown in Fig. 16. The 4-sulfo-1,8-naphthalic anhydride potassium salt (10) was reacted with 3-amino-1-propanol to produce Nap (11). Cellulose (12) was then modified with hexamethylene diisocyanate (HMDI) (13) to give the modified cellulose (14), which then reacted with Nap (11) to yield Cel-Nap (15). Cel-Nap showed high sensitivity and selectivity for

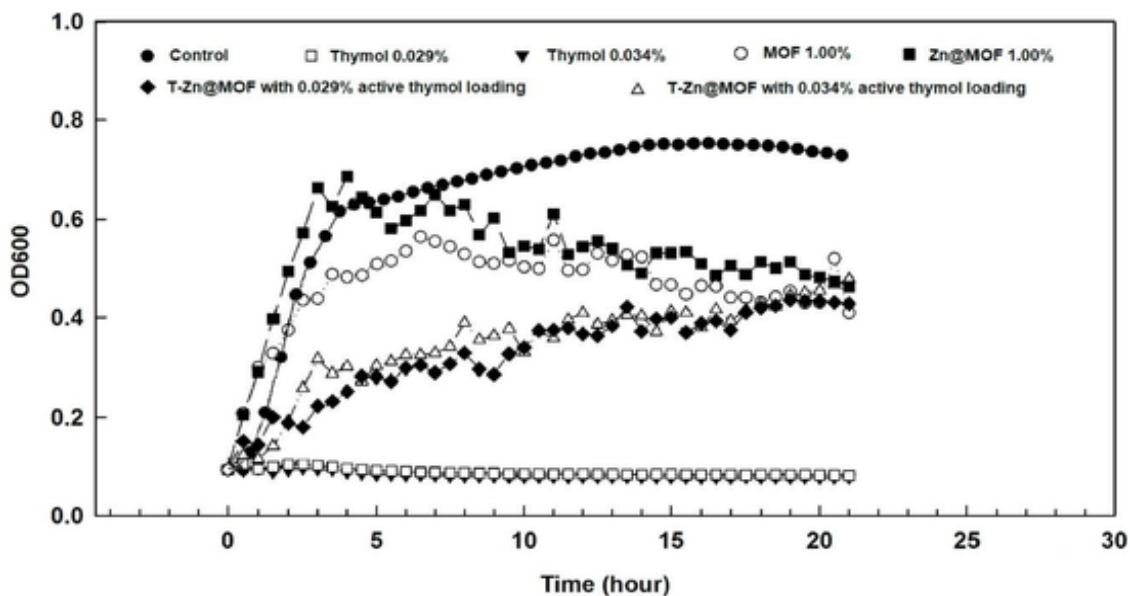


Fig. 17. Effect of T-Zn@MOF with thymol loading on growth of *E. coli*, measured by OD₆₀₀. Reproduced from Ref. [133] with permission from Elsevier, Copyright © 2019.

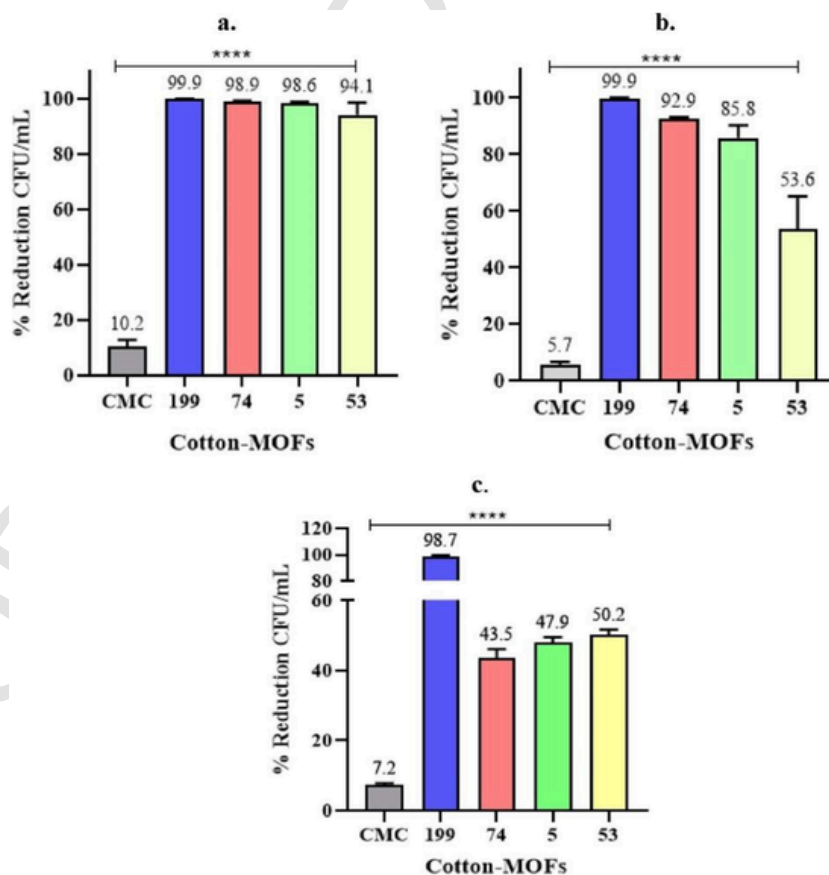


Fig. 18. Reduction in bacterial colony formation (in CFU/mL) by cotton-MOFs for a) *E. coli* ATCC 25922, b) *K. pneumoniae* ATCC 13882, and c) *S. aureus* ATCC 6538. Results = means \pm standard deviation; n = 3. Reproduced from Ref. [134], <https://doi.org/10.1016/j.ica.2022.120955>, under the terms of the CC BY NC ND license, <http://creativecommons.org/licenses/by-nc-nd/4.0/>

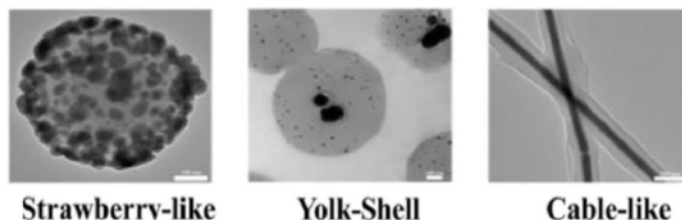
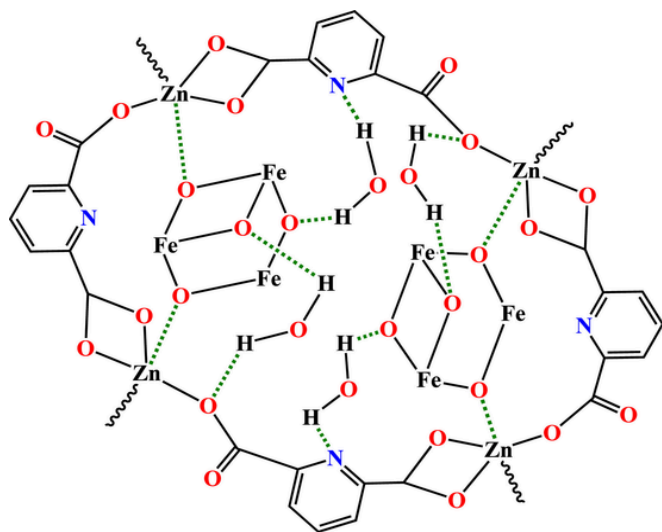


Fig. 19. SEM micrographs of three nanostructures of Ag@PRV. Reproduced from Ref. [135] with permission from Elsevier, Copyright © 2023.



Scheme 1. Structure proposed for Fe₃O₄/Zn-metal organic framework (19).

detecting Cr(VI), with a low detection limit of 1.07 μM . Cel-Nap (15) was encapsulated into two metal-organic framework structures - UiO-66 and ZIF-8. The antimicrobial properties of these MOF-encapsulated materials (16) were tested and then further modified by adding silver ions (17) or silver nanoparticles (18). Either form of silver enhanced

antimicrobial activity against bacteria (*E. coli*, *P. aeruginosa*, *K. pneumoniae*, *S. aureus*, *S. enteritidis*, *S. lutea* and *B. cereus*) and yeast (*C. albicans*). ZIF-8 based materials showed better antimicrobial effects than UiO-66, while silver ions were more effective than silver nanoparticles. The best antimicrobial activity was seen for ZIF-8 encapsulated Cel-Nap loaded with silver ions, which showed a minimum inhibitory concentration of 0.0024 mg/mL against *E. coli*. In summary, the cellulose-based probe was selective and sensitive for Cr(VI) detection, while MOF encapsulation allowed for antibacterial functionality with excellent effects from silver ion loading.

Wu *et al.* investigated the use of metal-organic frameworks (MOFs) as carriers for volatile antimicrobial essential oils like thymol [133]. Zinc metal-organic framework (Zn@MOF) was synthesized and its porous structure was confirmed. Thymol was loaded into the pores at 3.96 % by weight. The morphology and crystal structure of the Zn@MOF were analyzed with SEM (scanning electron microscopy) and XRD (X-ray diffraction) spectroscopy. The Zn@MOF had a cubic structure with a pore size of 30 Å. Antibacterial testing showed thymol-loaded Zn@MOF (T-Zn@MOF) inhibited *E. coli* O157:H7 growth without an exponential phase, likely due to sustained release of thymol from the MOF pores where it was incorporated via noncovalent interactions. A graph of the antibacterial assay results is shown in Fig. 17. The results demonstrate that MOFs could potentially be used as carriers for volatile antimicrobial oils like thymol to enhance their antimicrobial effects, although further research is needed on applications in food and efficacy against other pathogens.

Sierra and coworkers described the synthesis and antibacterial activity of metal-organic frameworks (MOFs) immobilized on cotton fi-

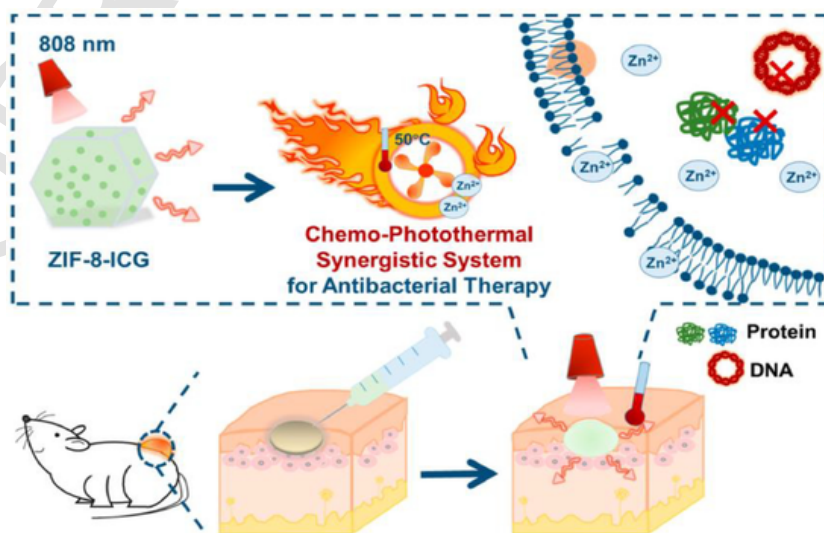


Fig. 20. Schematic diagram of synergistic chemo-photothermal antibacterial therapy for ZIF-8-ICG nanoparticles irradiated at 808 nm. Reproduced from Ref. [137], <https://doi.org/10.3390/pharmaceutics11090463>, under the terms of the CC BY 4.0 license, <http://creativecommons.org/licenses/by/4.0/>

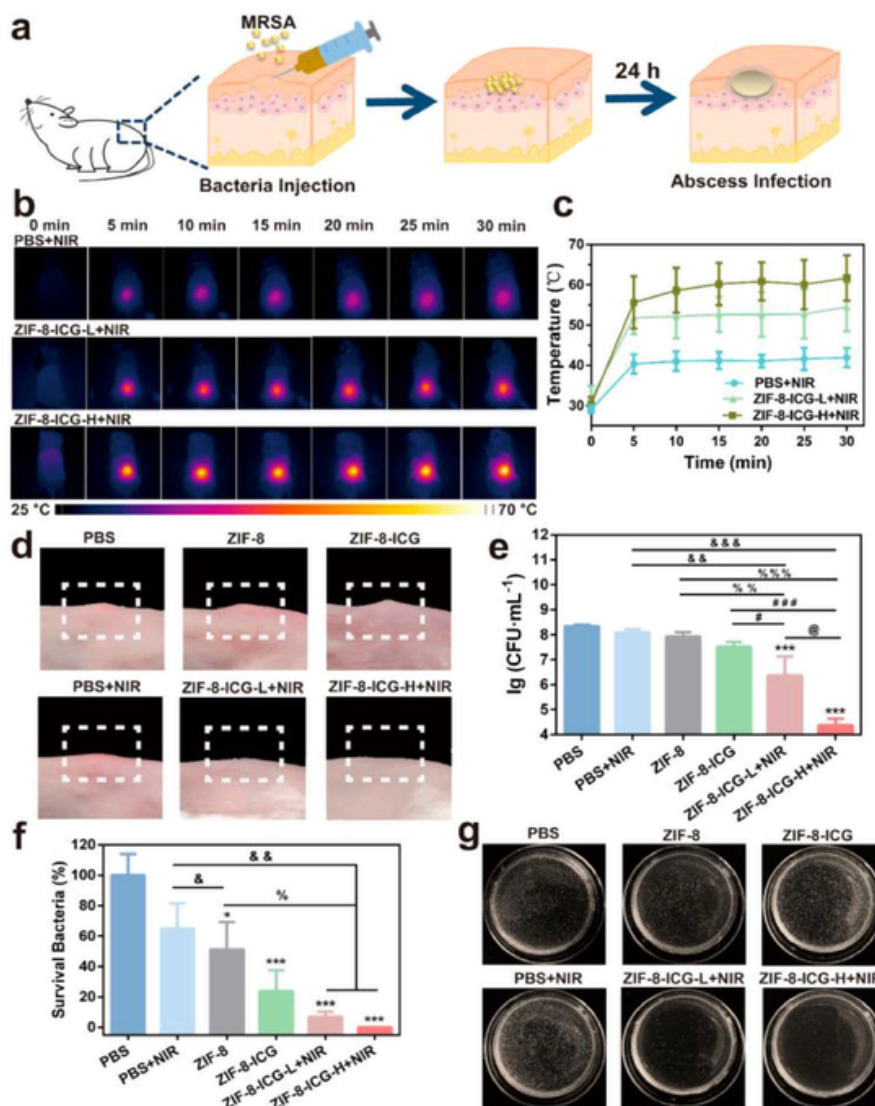


Fig. 21. a) Outline of *in vivo* mouse model of photothermal therapy with ZIF-8 and ZIF-8-ICG nanoparticles. b) Thermal imaging of mice infected with MRSA and irradiated with a 808 nm laser for 0–30 min. Mice in the ZIF-8-ICG-L (low dose) group were given 1 mg/mL, while those in the ZIF-8-ICG-H (high dose) group were given 10 mg/mL. c) Local temperature measurements over time. d) Photographs of skin from the infected region after different treatments. e) MRSA growth of bacteria taken from the infected area of mice in each treatment group. f) Percent survival of bacteria from each group. (p-values: *p < 0.05 vs. PBS (phosphate-buffered saline control); *** p < 0.001 vs. PBS; & p < 0.05 vs. PBS+NIR; && p < 0.01 vs. PBS+NIR; &&& p < 0.001 vs. PBS+NIR; % p < 0.05 vs. ZIF-8; %% p < 0.01 vs. ZIF-8; %%% p < 0.001 vs. ZIF-8; # p < 0.05 vs. ZIF-8-ICG; ### p < 0.001 vs. ZIF-8-ICG; @ p < 0.05 vs. ZIF-8-ICG-L+NIR) g) Photographs of agar plates inoculated with MRSA from mice in each group. Reproduced from Ref. [137], <https://doi.org/10.3390/pharmaceutics11090463>, under the terms of the CC BY 4.0 license, <http://creativecommons.org/licenses/by/4.0/>

bres [134]. Copper, zinc, and aluminum-based MOFs (MOF-199, MOF-74, MOF-5, and MIL-53) were successfully synthesized on carboxymethylated cotton fibres using an *in situ* method. SEM and XRD analysis confirmed the MOF crystals were present on the cotton fibres and remained stable after sterilization by autoclaving. All the cotton-MOF systems displayed antibacterial activity against the tested nosocomial bacteria *E. coli*, *S. aureus*, and *K. pneumoniae*, as shown by the graphs of bacterial growth inhibition in Fig. 18. Gram-negative bacteria (*E. coli* and *K. pneumoniae*) were more susceptible to the MOF systems than the Gram-positive *S. aureus*. Cotton-MOF-199 showed the highest broad-spectrum antibacterial activity. The MOFs appear stably bound to the fibers, with no leaching of MOF components. This suggests a direct contact-based antibacterial mechanism rather than one based on leaching. The environmentally friendly synthesis method and high antibacterial activity make these cotton-MOF systems promising for

reusable anti-infective hospital textiles to help prevent healthcare-associated infections.

Polyphosphazene modified with silver nanoparticles (Ag@PRV) exhibited an antibacterial effect against *E. coli* and *S. aureus* [135]. Ag@PRV Strawberry-like nanoparticles showed better activity relative to Ag@PRV Yolk-Shell nanoparticles and Ag@PRV Cable-like nanofibers. SEM micrographs of each nanofiber are shown in Fig. 19. These three nanoparticles or nanofibers were tested against Gram-positive bacteria and Gram-negative bacteria, and they had higher activities against Gram-positive bacteria.

Bashar *et al.* reported on the synthesis and characterization of a novel Fe₃O₄/Zn-metal organic framework (MOF) magnetic nanostructure (19) using a microwave-assisted method [136]. Characterization of the nanostructures confirmed their crystallinity, thermal stability, high

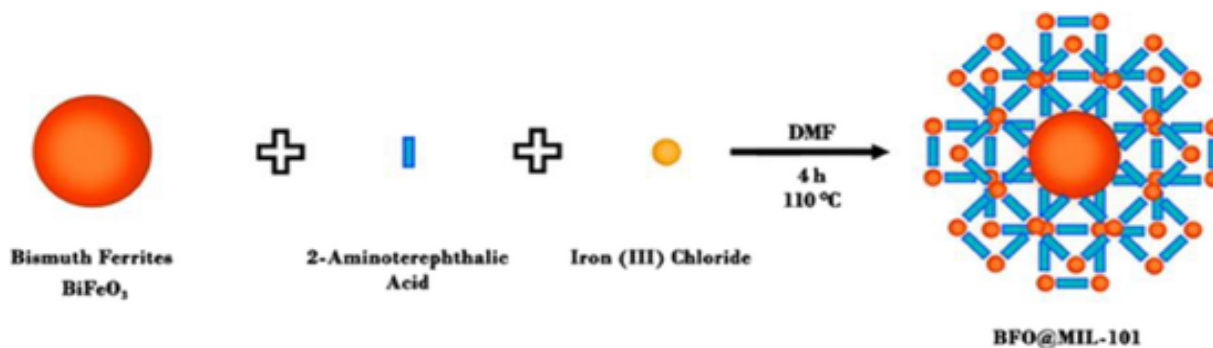


Fig. 22. Assembly of BFO@MIL-101 hybrid nanomaterials. Reproduced from Ref. [139], <https://doi.org/10.1186/s11671-023-03883-9>, under the terms of the CC BY 4.0 license, <http://creativecommons.org/licenses/by/4.0/>

Table 1

Summary of antimicrobial activities for Cu/Co-hybrid MOF/PVA fibers. Reproduced from Ref. [140], <https://doi.org/10.3389/fmats.2023.1214426>, under the terms of the CC BY 4.0 license, <http://creativecommons.org/licenses/by/4.0/>

| Product/Drug | Gram-Positive Strain | | | | | | Gram-negative Strain | | | | | | Fungal Strain | | | | | |
|------------------------|----------------------|----|-----|-----|----|----|----------------------|-----|-----|------|----|----|---------------|-----|-----|-----|----|-----|
| | a | | b | | c | | d | | e | | f | | g | | h | | i | |
| | I | II | I | II | I | II | I | II | I | II | I | II | I | III | I | III | I | III |
| Copper-containing MOFs | 32 | 64 | 64 | 128 | 16 | 64 | 128 | 256 | 512 | 1024 | - | - | 16 | 64 | 256 | 512 | 32 | 64 |
| Cobalt-containing MOFs | 64 | 64 | 128 | 256 | 32 | 64 | 256 | 512 | - | - | - | - | 64 | 128 | 256 | 256 | 32 | 64 |
| Cu/Co-hybrid MOFs | 32 | 64 | 64 | 128 | 16 | 32 | 64 | 128 | 512 | 1024 | - | - | 64 | 64 | 128 | 256 | 32 | 32 |
| Cu/Co-hybrid MOFs/PVA | 16 | 32 | 64 | 64 | 16 | 32 | 64 | 128 | 256 | 512 | - | - | 32 | 64 | 128 | 256 | 32 | 32 |
| j | - | - | 4 | 16 | 16 | 16 | 4 | 8 | 16 | 32 | - | - | 32 | 64 | 64 | 64 | 16 | 32 |
| k | 4 | 8 | 2 | 4 | 4 | 8 | 8 | 16 | 8 | 16 | 32 | 64 | - | - | - | - | - | - |

a: *B. cereus*; b: *S. aureus*; c: *Streptococcus*; d: *Proteus mirabilis*; e: *E. coli*; f: *Acinetobacter*; g: *Fusarium oxysporum*; h: *C. albicans*; i: *A. fumigatus*. I: MIC ($\mu\text{g/mL}$); II: MBC ($\mu\text{g/mL}$); III: MFC ($\mu\text{g/mL}$); Drugs for bacteria: j: cefazolin, k: gentamicin; drug for fungi: J: terbinafine, K: tolnaftate. (n = 3) \pm SD.

surface area, and magnetic properties. Based on the structural characterization, the authors proposed a structure presented in Scheme 1.

The nanostructures showed strong antimicrobial activity against Gram-positive (*Rhodococcus equi* and *Streptococcus agalactiae*) and Gram-negative bacteria (*P. aeruginosa* and *Shigella dysenteriae*) as well as fungi (*C. albicans*), with minimum inhibitory concentration (MIC) values ranging from 16–128 $\mu\text{g/mL}$. The antimicrobial activity was higher than some commercial antimicrobial drugs. The high surface area also imparted good catalytic activity to the nanostructures in synthesizing new spiro[indoline-pyranopyrimidine] heterocyclic compounds via a multicomponent reaction. Twelve derivatives were synthesized in 10–20 min with yields above 85 %. The magnetic nanostructures could be easily separated by a magnet after the reaction due to their magnetic properties and reused for five cycles without significant loss of activity. In summary, microwave synthesis imparted unique properties like high surface area to the magnetic MOF nanostructures, making them efficient as antimicrobial agents and catalysts for organic synthesis.

An article from 2019 by Wu *et al.* described the development of an MOF-based system for combined chemo and photothermal therapy against antibiotic-resistant bacteria [137]. Zeolitic imidazolate frameworks-8 (ZIF-8) were loaded with the photothermal agent indocyanine green (ICG) to form ZIF-8-ICG nanoparticles. These nanoparticles have high ICG loading capacity and stability. ZIF-8-ICG nanoparticles efficiently convert near-infrared light into heat, allowing precise and rapid

photothermal killing of bacteria. The heat also accelerates the release of zinc ions from the degrading ZIF-8 framework. The zinc ions permeabilize bacterial cell membranes, inhibit bacterial growth, and reduce heat resistance - enhancing the antibacterial efficacy by combining photothermal ablation with chemotherapeutic effects. A summary of the mechanisms for this combination therapy is shown in Fig. 20.

ZIF-8-ICG showed potent antibacterial activity *in vitro* against both Gram-positive and Gram-negative species, completely eradicating MRSA and *P. aeruginosa* even at low nanoparticle doses with mild heating. *In vivo* tests using a mouse model of MRSA skin infection (Fig. 21a) demonstrated that ZIF-8-ICG treatment under near-infrared (NIR) irradiation could almost completely eliminate skin abscesses caused by the infection, as shown in the photographs in Fig. 21d. The antibacterial activity was due to photothermal heating, as demonstrated by both the thermal images in Fig. 21b and the temperature graph in Fig. 21c. The growth of MRSA (as illustrated by the graphs in Fig. 21e and photographs of plates in Fig. 21g) and percent bacterial survival (Fig. 21f) were both significantly decreased due to irradiation after ZIF-8-ICG treatment. The ZIF-8-ICG system was biocompatible and safe for antimicrobial therapy in cell culture and animal models. The results indicate this chemo-photothermal approach has strong potential to combat multidrug-resistant bacteria.

Zhan *et al.* synthesized a cobalt-MOF composite (Co-MOF) using a solvothermal method [138]. SEM and TEM (transmission electron microscopy) analysis showed the Co-MOF had a layered, folded structure

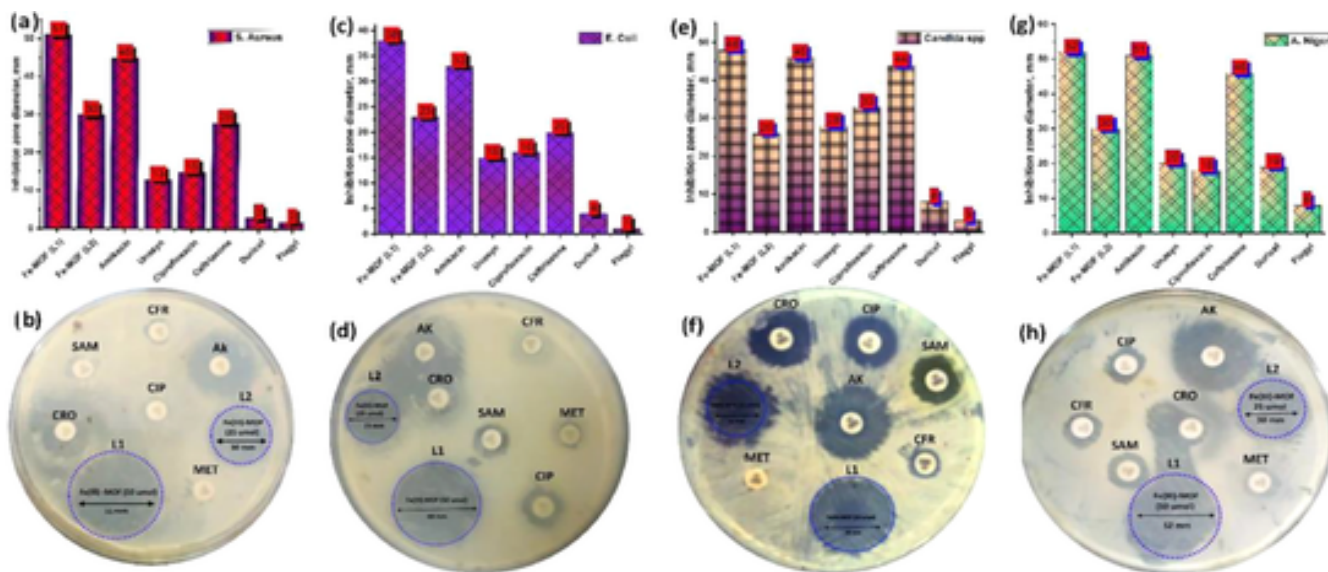


Fig. 23. Antibacterial activities measured using the agar well diffusion method for (a, b) *S. aureus*, (c, d) *E. coli*, (e, f) *Candida* spp., or (g, h) *A. niger*, treated with two Fe(III)-MOFs, amikacin, Unasyn (ampicillin/sulbactam), ciprofloxacin, ceftriaxone, Duricef (cefadroxil), or Flagyl (metronidazole). Reproduced from Ref. [141], <https://doi.org/10.1557/s43578-022-00644-9>, under the terms of the CC BY 4.0 license, <http://creativecommons.org/licenses/by/4.0/>

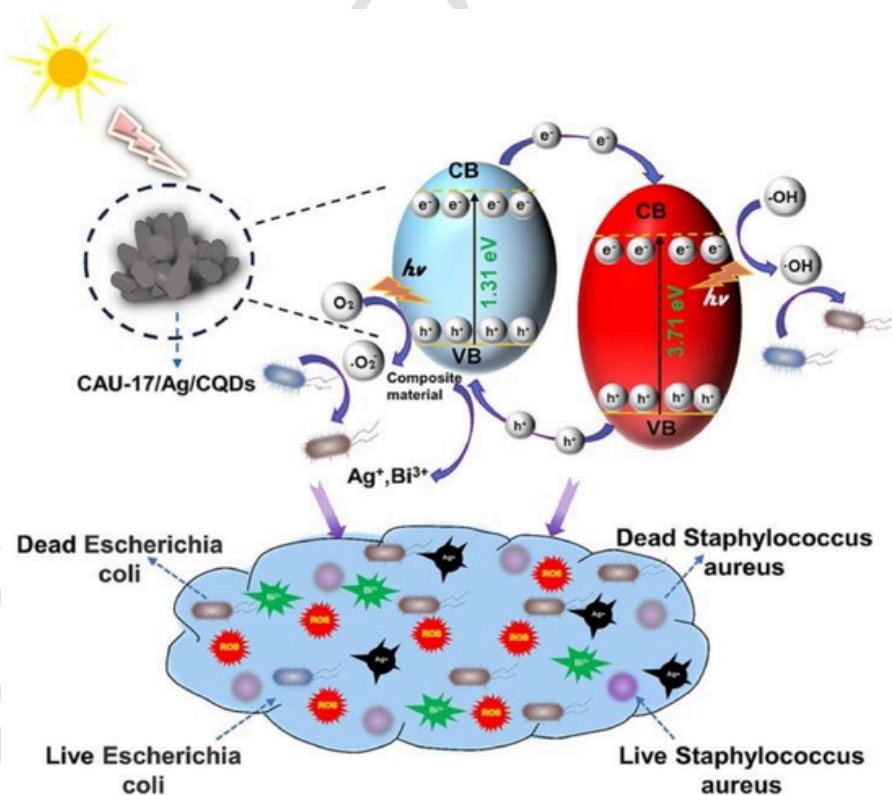


Fig. 24. Schematic diagram of the photocatalytic mechanism of the antibacterial effect of CAU-17/Ag/CQDs nanocomposites against *E. coli* and *S. aureus*. Reproduced from ref. [144] with permission from Elsevier, Copyright 2023.

with rough, uneven surface morphology. Tests showed the Co-MOF exhibited peroxidase-like activity, catalyzing the oxidation of tetramethylbenzidine (TMB) by hydrogen peroxide. This activity could allow it to produce reactive oxygen species that are toxic to bacteria. Bacterial infection experiments revealed the Co-MOF showed excellent antibac-

terial activity against *P. aeruginosa* in the presence of low concentrations of hydrogen peroxide, reducing bacterial colony survival to less than 10 %. Further exploration is still needed on aspects like the specific ROS involved, dose-response effects, broad antibacterial spectrum,

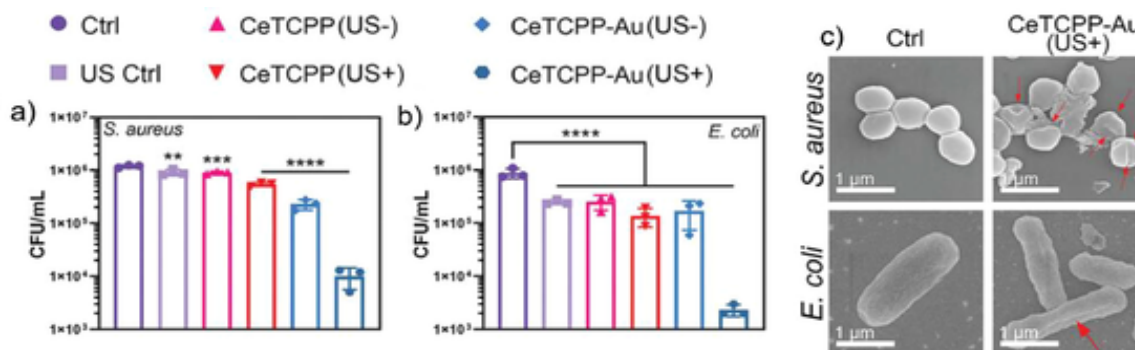


Fig. 25. Inhibition of bacterial growth by CeTCPP and CeTCPP-Au, with and without ultrasound (US) irradiation, for a) *S. aureus* and b) *E. coli*. c) SEM micrographs of *S. aureus* and *E. coli* treated with CeTCPP-Au under ultrasound (red arrows show damage to the cell membranes). Adapted from Ref. [149], with permission from John Wiley & Sons, Copyright © 2023. Wiley-VCH GmbH.

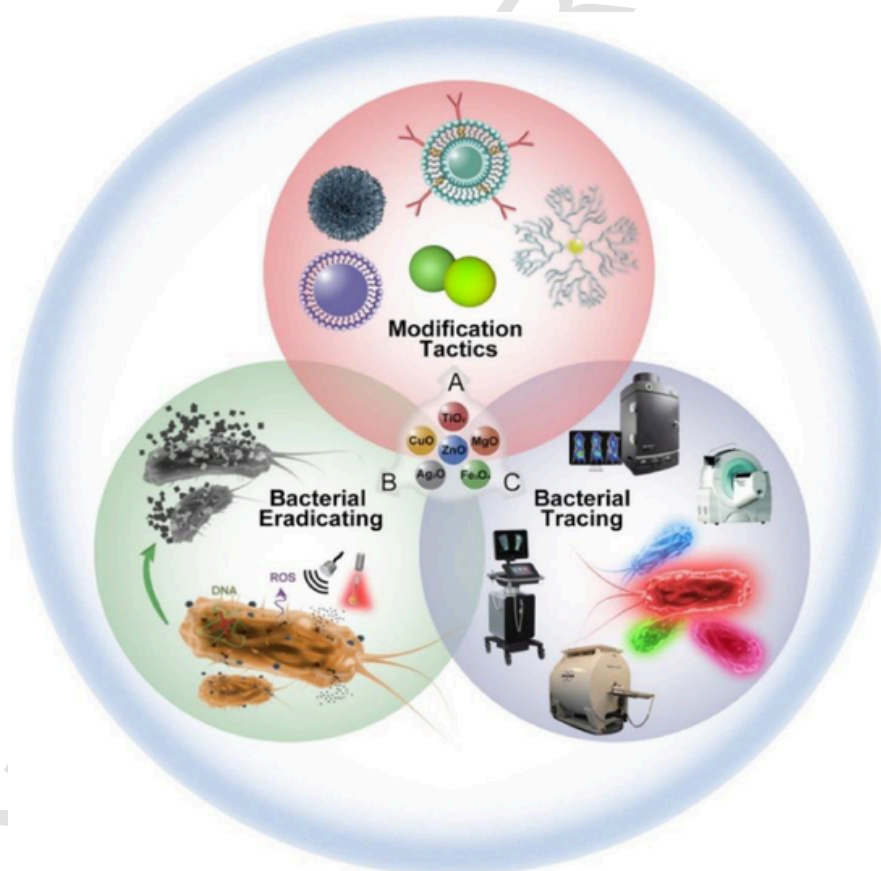


Fig. 26. Bacterial tracing and eradication by metal oxide nanoparticles, and modification tactics used to reduce immunogenicity and toxicity of these nanoparticles. Reproduced from Ref. [197], <https://doi.org/10.1002/VIW.20200052>, under the terms of the CC BY 4.0 license, <http://creativecommons.org/licenses/by/4.0/>

and toxicity, but initial results indicated this Co-MOF's potential as an antibacterial agent via its peroxidase-like activity.

A new hybrid photocatalytic material consisting of bismuth ferrite (BFO) nanoparticles was modified with the growth of an iron-based MOF called MIL-101 formed from the reaction of 2-aminoterephthalic acid with iron (III) chloride. BFO nanoparticles were synthesized via a sol-gel method shown in Fig. 22 [139]. MIL-101 was then grown on the surface of the BFO nanoparticles using BFO as the source of metal ions. Characterization with XRD, TEM, and FTIR (Fourier transform infrared spectroscopy) confirmed the successful growth of crystalline MIL-101

on the BFO while retaining the BFO crystalline structure. The coating thickness increased with longer growth time. The new BFO@MIL-101 nanocomposite showed enhanced visible light-induced antimicrobial activity compared to bare BFO nanoparticles when tested against *S. aureus*, *Staphylococcus haemolyticus* and *E. coli* strains. Specifically, BFO@MIL-101 had MIC and minimum bactericidal concentration (MBC) values, indicating increased antibacterial potency. The improved activity was attributed to the MIL-101 coating enhancing the intrinsic photocatalytic properties of BFO by reducing electron-hole recombination. In summary, the new BFO@MIL-101 hybrid nanomaterial

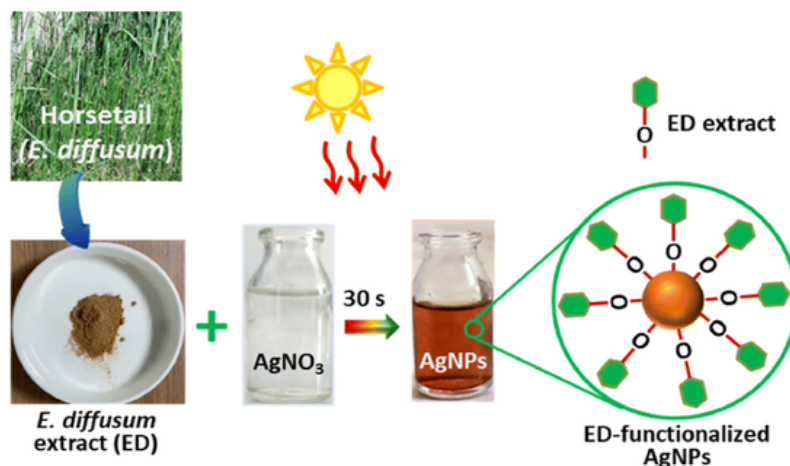


Fig. 27. Synthesis of Ag NPs using sunlight and ED extract. Reproduced from Ref. [219], <https://doi.org/10.1039/D3RA05070J>, under the terms of the CC BY NC ND license, <http://creativecommons.org/licenses/by-nc-nd/4.0/>

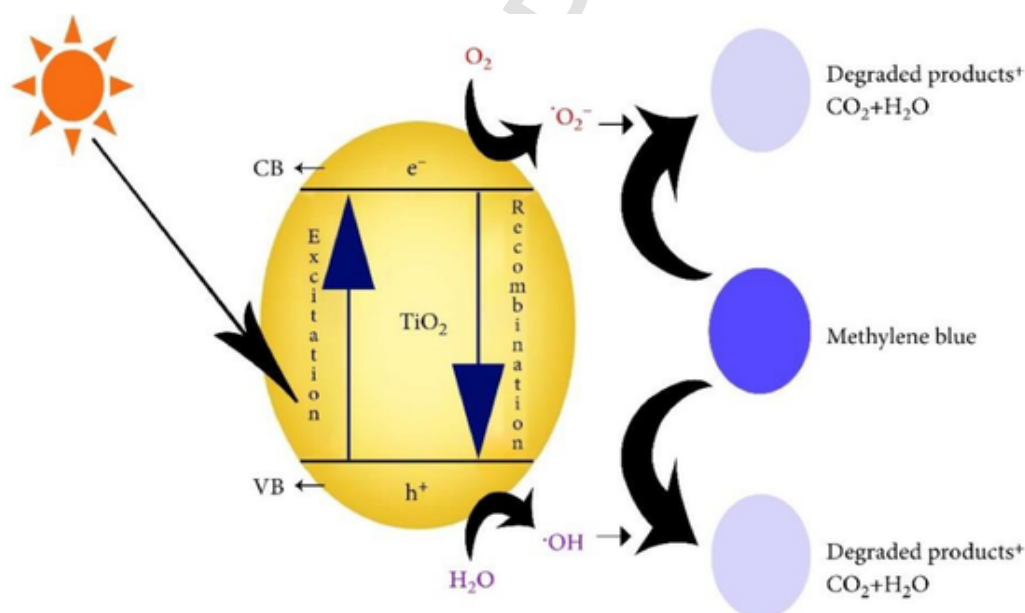


Fig. 28. Photodegradation of methylene blue catalyzed by TiO_2 NPs. Reproduced from Ref. [247], <https://doi.org/10.1155/2022/7060388>, under the terms of the CC BY 4.0 license, <http://creativecommons.org/licenses/by/4.0/>

shows potential as an efficient antibacterial agent under mild sunlight irradiation, making it promising for disinfection applications.

Asiri *et al.* synthesized and characterized novel Cu/Co-hybrid MOFs and Cu/Co-hybrid MOF/polyvinyl alcohol (PVA) fibre nanostructures [140]. Cu-containing MOF, Co-containing MOF, and Cu/Co-hybrid MOF nanostructures were synthesized using an ultrasonic approach. The Cu/Co-hybrid MOF/PVA fibre nanostructures were then produced by electrospinning. The Cu/Co-hybrid MOF/PVA fibers showed a higher surface area and porosity compared to the individual MOFs. The Cu/Co-hybrid MOF nanostructures could also be used as recyclable catalysts to synthesize pyrano [2,3-*c*] pyrazole derivatives. The reactions had higher efficiency and faster rate compared to other reported catalysts.

The nanostructures showed cytotoxic activity against breast cancer cells, with the Cu/Co-hybrid MOF/PVA fibers having the highest activity. They also demonstrated antibacterial activities superior to the com-

mercial antibacterial drugs cefazolin and gentamicin, and antifungal activities superior to the commercial antifungal drugs terbinafine and tolnaftate. A summary of the antibacterial and antifungal activities of the hybrid fibers in MIC, MBC, and MFC (minimum fungicidal concentration) is shown in Table 1. The high activities were attributed to the presence of bioactive metals, high surface area and porosity of the nanostructures. The combination of Cu/Co-hybrid MOF into PVA fibres further enhanced these properties. In summary, the synthesized nanostructures have significant catalytic, antitumor, antimicrobial and antifungal properties due to their composition, porous structure and high surface area. The results highlight their potential for applications in various fields.

A novel iron(III)-based MOF with superior antimicrobial properties was recently synthesized and characterized. The Fe(III)-MOF was prepared by Sheta *et al.* by reacting an organic linker compound with ferric sulfate [141]. Analyses confirmed the high crystallinity and purity of

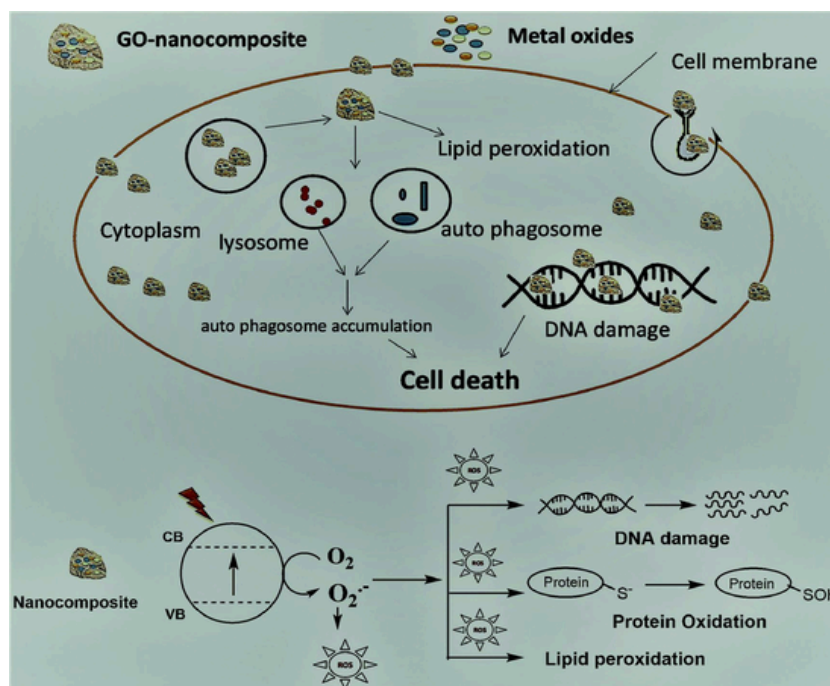


Fig. 29. Nanocomposites containing graphene oxide and zinc oxide, silver and titanium dioxide nanostructures and their oxidative effects leading to cell death. Reproduced from Ref. [248], <https://doi.org/10.1039/c8ra09788g>, under the terms of the CC BY 3.0 license, <http://creativecommons.org/licenses/by/3.0/>

the Fe(III)-MOF, as well as its octahedral structure. Tests showed the Fe(III)-MOF had excellent antimicrobial efficacy against various bacteria, fungi and yeast, with inhibition zones of 40–46 mm and 22–24 mm at concentrations of 50 $\mu\text{g}/\text{mL}$ and 25 $\mu\text{g}/\text{mL}$ respectively (Fig. 23). The antimicrobial mechanism involves the release of Fe^{3+} ions that interact and bind to cell wall components of microorganisms, disturbing the cell membrane integrity. The high surface area porous MOF structure also contributes to antimicrobial activity. The Fe(III)-MOF displayed higher antimicrobial activity than standard antimicrobial drugs. The results indicate the novel affordable Fe(III)-MOF has the potential to be an efficient antimicrobial agent for treating drug-resistant pathogens.

The development of a novel drug delivery system using an MOF modified with sodium alginate-zein (SA-ZN) biopolymer composites was reported by Asadollahi *et al.* [142]. A Zn-based MOF called $\text{Zn}_2(\text{BDC})_2(\text{DABCO})$ was synthesized and characterized, then modified by coating with sodium alginate (SA), zein (ZN) - a natural protein isolated from corn, or a SA-ZN composite. The modified MOFs were loaded with the anti-inflammatory drug sulfasalazine (SSZ) and characterized by FTIR, XRD, SEM, etc. Loading was around 60–78 % depending on the coating. Sustained release was observed over 24 h from the SA-ZN coated MOF, compared to rapid release from uncoated MOFs. The coating protected the stability and controlled SSZ delivery. Antibacterial testing showed the SSZ-loaded SA-ZN coated MOF had enhanced activity against *S. aureus* compared to free SSZ or unloaded MOFs, attributed to synergistic effects. The authors concluded that the SA-ZN coated MOF was a promising drug delivery system for SSZ, providing high loading, sustained release, and improved antibacterial efficacy. The coating improves the MOF's biocompatibility and stability for biological applications.

Bouson *et al.* investigated the antifungal activity of copper-based MOFs (Cu-BTC MOFs) against several fungal species [143]. Cu-BTC MOFs were synthesized using a hydrothermal method. The MOFs had an octahedral morphology with cubic pore structures and were water-stable. Against the yeast *Candida albicans*, Cu-BTC MOFs showed 96–100 % growth inhibition at concentrations of 300–500 ppm after 60 min of incubation. SEM micrographs revealed cell membrane dam-

age in treated *C. albicans*. For the moulds *Aspergillus niger*, *Aspergillus oryzae* and *Fusarium oxysporum*, Cu-BTC MOFs showed 30–32 % mycelial growth inhibition at 500 ppm concentration. The MOFs significantly reduced spore germination and changed spore morphology and color, indicating toxicity. The antifungal activity is likely due to ROS generation via the reduction of oxygen gas by the Cu-BTC MOFs. The water-stable Cu-BTC MOFs show potential as antifungal agents, especially against *C. albicans* yeast and inhibitory effects against *Aspergillus* and *Fusarium* moulds.

A recent report by Li *et al.* demonstrated the antibacterial efficiency of a new composite generated from the doping of bismuth MOF (CAU-17) with silver and carbon quantum dots (CQDs) [144]. The bismuth MOF had previously been prepared by Ding *et al.* in 2023 [145]. The resulting CAU-17/Ag/CQD materials have shown good activity against *S. aureus* and *E. coli* and were also effective against drug-resistant bacteria, namely MRSA. Fig. 24 shows the photocatalytic mechanism of CAU-17/Ag/CQDs composite against bacteria. The doping allowed for enhancement of the absorption of visible light, as well as the reduction of the band gap between the valence band and the conduction band. These effects enhanced the photocatalytic ability of the composite, resulting in the production of ROS including $\bullet\text{OH}$, and $\bullet\text{O}_2^-$. Another factor that contributed to the efficiency of this composite was the slow release of Ag^+ and Bi^{3+} , which can cause bacterial cell death through the denaturation of membrane proteins and penetration of membranes. While these ions can enhance the antibacterial activity, Ag^+ has the potential to be toxic to host cells. However, when the authors measured the release rates of these ions, there was a fast initial release in the first 24 h, followed by a slow release that could maintain a long-term antibacterial effect with a minimal increase in toxic ion levels for human cells.

2.3.4. Inner transition metals

Inner transition metal MOFs have been developed for various activities including chemical and biological sensors and catalysis [146–148]. One example of inner transition metal MOFs that showed antibacterial activity was the use of cerium MOFs decorated with Au nanoparticles

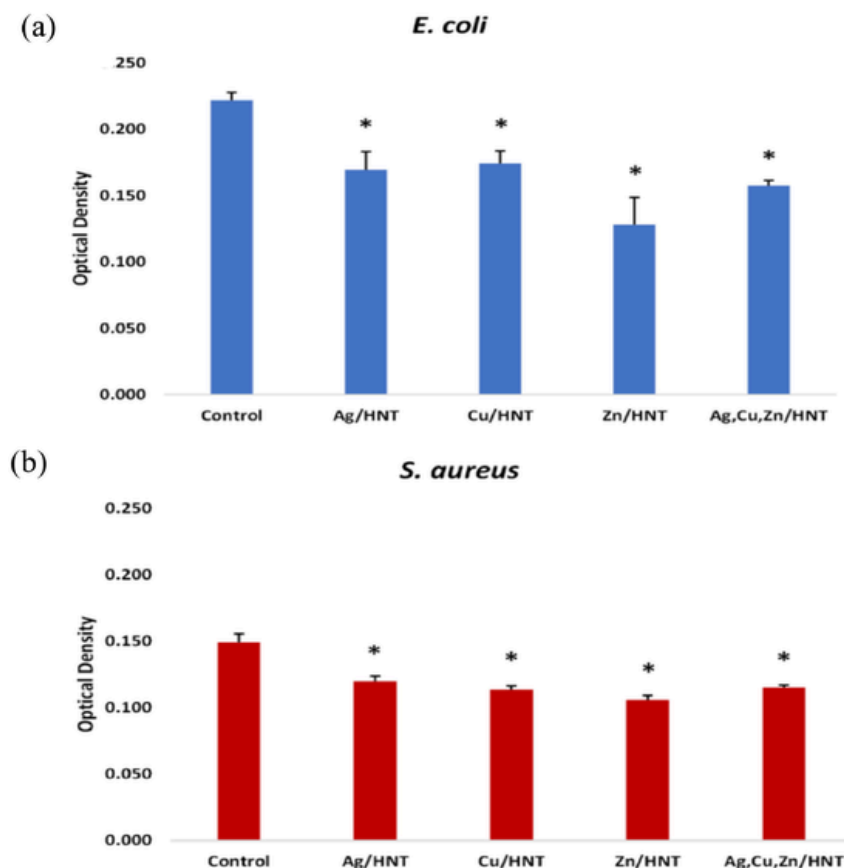


Fig. 30. Inhibition of growth by PLA with incorporated mHNTs (containing Ag, Cu, Zn, or all three) for a) *E. coli* and b) *S. aureus*. Reproduced from Ref. [251], <https://doi.org/10.3390/polym14081603>, under the terms of the CC BY 4.0 license, <https://creativecommons.org/licenses/by/4.0/>

(CeTCPP-Au) for the treatment of osteomyelitis using ultrasound [149]. These MOFs exhibited >99 % inhibitory activity after ultrasound irradiation against Gram-negative *E. coli*, as shown in Fig. 25a, and Gram-positive *S. aureus*, as shown in Fig. 25b. SEM of the bacteria showed wrinkles and damage to the bacterial membranes of both species after treatment with ultrasound and CeTCPP-Au (Fig. 25c). This damage was demonstrated to be due to ROS generation after exposure to ultrasound.

3. Metal/metal oxide nanoparticles and composites

3.1. Nanoparticles and composites

Advancements in nanotechnology continue to be of great importance in many fields, including biomedical research [150–156]. Research into metallic nanoparticles (NPs) has seen an exponential increase in the past few decades in light of their utility in diagnostic and therapeutic applications [157–163]. Nanoparticle sizes can range between 1–100 nm, which can be suitable for a variety of biomedical applications [164,165]. Metallic nanoparticles such as magnetic nanoparticles, silver and gold nanoparticles, as well as quantum dots, have been employed as drug carriers, bioimaging contrasts, and chemodynamic anticancer therapies [166–190]. In addition to single nanoparticles, bimetallic and trimetallic nanoparticles have also been examined for biomedicine [191,192]. Metal oxides have applications including bioimaging, diagnostics, therapeutics, drug delivery and biosensors [193–195]. In particular, the antimicrobial effects of metal oxide nanoparticles have been an area of interest, as they have multiple targets within cells, including cell membrane, cell wall and cytoplasmic components, as well as generating ROS [196,197]. Fig. 26 shows the

applications of metal oxide nanoparticles in bacterial tracing and eradication, as well as examples of techniques used to modify the nanoparticles to reduce immunogenicity and toxicity.

Nanocomposites are materials composed of multiple phases, at least one of which is on the nanoscale (> 100 nm) [198,199]. Due to their high surface-to-volume ratio, local interactions between the phases are increased, providing nanocomposites with improved mechanical and optical properties as well as smaller distances between the phases. Generally, nanocomposites can be divided into three categories: polymer matrix, metal matrix, or ceramic matrix nanocomposites [200].

Green nanocomposites made from natural polymers have been a focus of research, as they are renewable and biodegradable [201,202]. Nanocomposites have also been studied for biomedical applications due to their physical, chemical, and biological properties such as self-healing, sustained drug release, and biocompatibility [203–207].

3.2. Preparation of nanoparticles

Nanoparticle preparation approaches can be broadly divided into physical, chemical and biological methods [208–210]. These methods can also be described as top-down, i.e. breaking down nanostructures or bulk material to yield nanoparticles, or bottom-up, building nanoparticles from individual atoms or ions [211]. The three groups are described in more detail below:

A. Physical Methods

Physical Vapor Deposition (PVD): A metal vapour is generated by sputtering or evaporation, followed by deposition onto a substrate, where nanoparticles can form. However, this approach requires a high temperature to generate the vapour. This is a very useful approach for

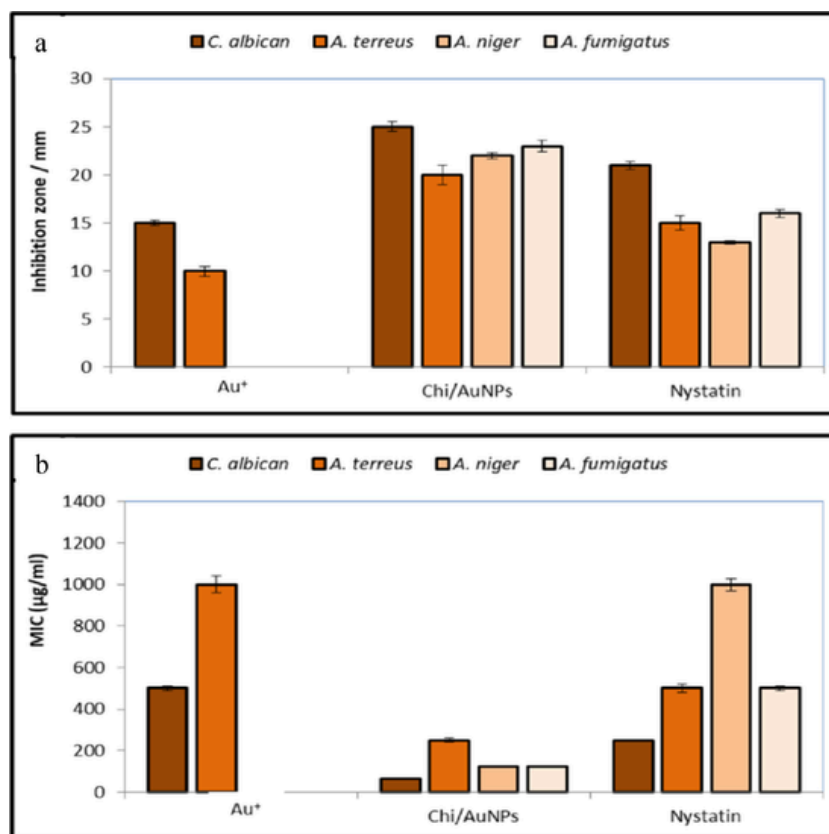


Fig. 31. Antifungal activity measured by (a) inhibition zones and (b) MIC for *C. albicans*, *Aspergillus terreus*, *A. niger*, and *Aspergillus fumigatus* treated with Au⁺, Chi/AuNPs, and control drug nystatin. Reproduced from Ref. [252], <https://doi.org/10.3390/polym14112293>, under the terms of the CC BY 4.0 license, <http://creativecommons.org/licenses/by/4.0/>

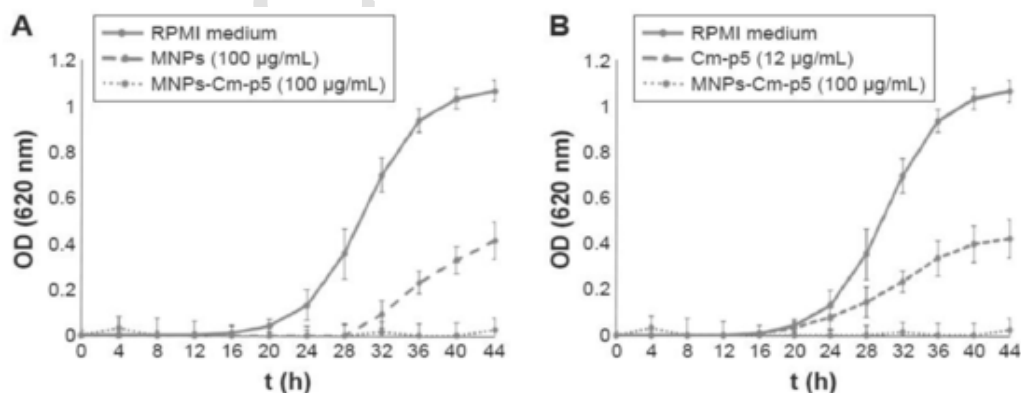


Fig. 32. Inhibition of *C. albicans* growth by MNP-Cm-p5 compared with A) MNP and B) Cm-p5 alone. Reproduced from Ref. [262], <https://doi.org/10.2147/IJN.S107561>, under the terms of the CC NC 3.0 license, <https://creativecommons.org/licenses/by-nc/3.0/>

the preparation of thin films, as it can obtain high purity as well as control over film thickness and morphology.

Laser Ablation: A laser is used to generate either a metal vapour containing nanoparticles from a metal target or a plasma containing nanoparticles from a metal target submerged in a liquid. This is a simple synthetic method that produces ligand-free nanoparticles and allows for size control by adjusting laser parameters. While this is often used to produce high-purity nanoparticles, it is an expensive process that requires a high-powered laser and may have lower production rates compared to chemical or biological methods.

Ball Milling: A top-down approach to nanoparticle synthesis, in which large particles are mechanically ground into smaller ones using high-energy collisions from milling balls within a rotating chamber. This is a relatively simple technique that does not require complex equipment or reactions, making it easily scalable for large-scale production and suitable for the preparation of a wide range of materials, including metals, ceramics, and composites. It also operates at room temperature, making it suitable for temperature-sensitive materials that cannot withstand high-temperature methods. Adjusting parameters such as milling time, speed, and ball-to-powder ratio can influence

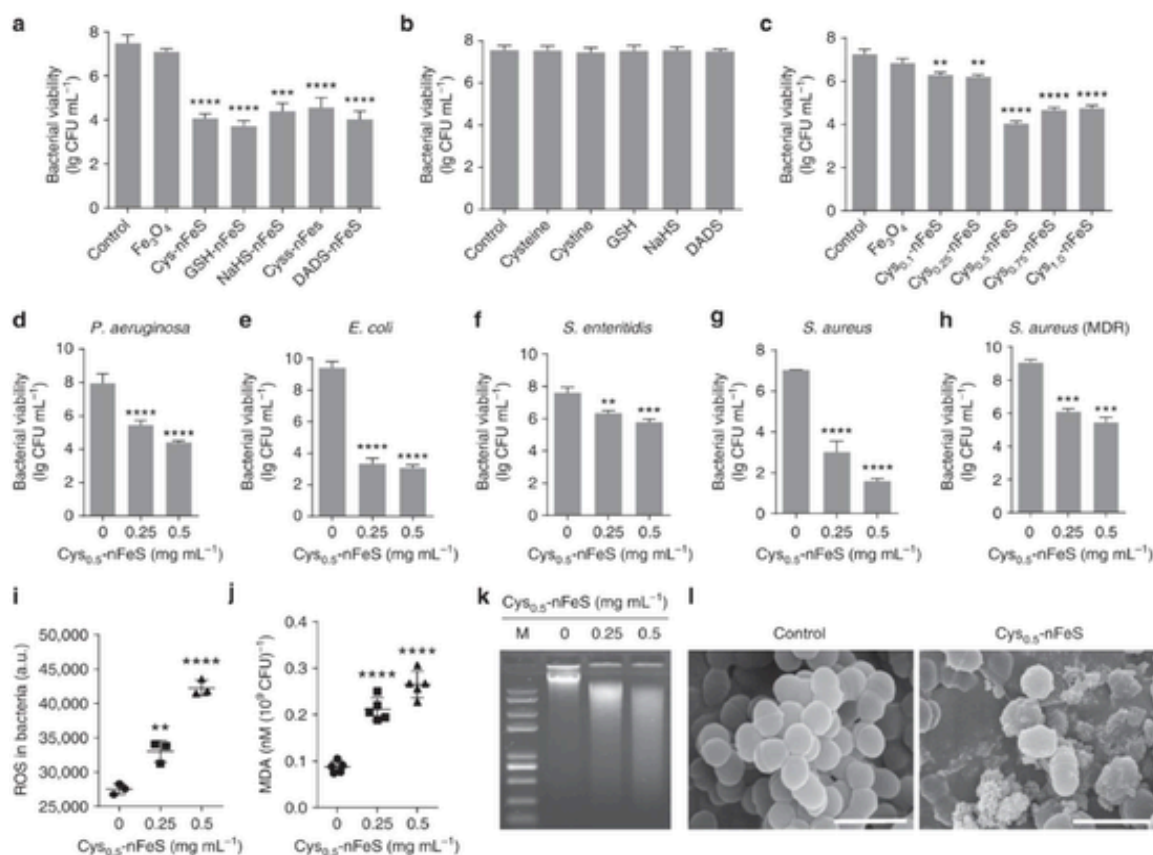


Fig. 33. a) Antibacterial activity of nFeS from various organosulfur compounds against *S. mutans*. b) Antibacterial activity of the organosulfur compounds. c) Effect of cysteine content in Cys-nFeS on antibacterial efficacy. Antibacterial activity of Cys_{0.5}-nFeS against d) *P. aeruginosa*, e) *E. coli*, f) *S. enteritidis*, g) *S. aureus*, and h) multidrug-resistant *S. aureus*. i) ROS production in *S. mutans* treated with Cys_{0.5}-nFeS. j) Lipid peroxidation in *S. mutans* treated with Cys_{0.5}-nFeS measured by malondialdehyde (MDA) concentration. k) DNA gel electrophoresis showing degradation of *S. mutans* genomic DNA after treatment with different concentrations of Cys_{0.5}-nFeS (M = DNA marker standard). l) SEM micrographs of *S. mutans* given Cys_{0.5}-nFeS. n=3 **p < 0.01, ***p < 0.001 and ****p < 0.0001. All scale bars = 1 μ m. Reproduced from Ref. [263], <https://doi.org/10.1038/s41467-018-06164-7>, under the terms of the CC BY 4.0 license, <http://creativecommons.org/licenses/by/4.0/>

nanoparticle size. Although contamination and agglomeration can occur, the use of hard materials like tungsten carbide or zirconia for the milling balls can mitigate these processes.

B. Chemical Methods

Chemical Reduction: This is one of the earliest and most common methods of nanoparticle synthesis. A metal precursor (salt) is dissolved in a solvent, and a reducing agent is added to reduce the metal ions to form nanoparticles of the metal in its atomic form. This technique is simple, cost-effective, and allows for size control by adjusting reaction parameters, but may leave residual reducing agents on the surface of the nanoparticles, impacting their properties.

Sol-Gel Synthesis: A metal precursor is dissolved in a solvent forming a liquid colloidal solution ("sol"), and a gel is formed through hydrolysis and condensation, trapping the metal precursors within the network. The gel is then dried and heated to form nanoparticles. The resulting nanoparticles are distributed homogeneously within the matrix with high purity, and this approach allows for control over the composition. On the other hand, this is a multi-step process that requires high temperatures for the final annealing step.

Microemulsion Technique: Metal precursors are encapsulated in water droplets within an oil phase that form into micelles, to which reducing agents are then added, creating nanoparticles within the droplets. The confined space of the micelles yields uniform and well-dispersed nanoparticles. As a result, the ability to synthesize nanoparticles with excellent size control and narrow size distributions can be

obtained by this technique, however, surfactant removal can be challenging, and scalability can be limited.

C. Biological Methods (Green synthesis)

Bio-reduction: Using microorganisms, enzymes, or biomolecules to reduce metal ions into nanoparticles. This is an environmentally friendly approach with the potential for large-scale production, however, it also requires optimization of microbial growth conditions. The reaction times may also be longer.

Plant-mediated Synthesis: Plant extracts are used to reduce nanoparticles. This approach is environmentally friendly, cost-effective, and often utilizes readily available materials, especially from local or common plants. However, this method may have less control over the size and shape of the resulting nanoparticles when compared to other methods, and characterization of the extract can be complex due to the complex mixture of components.

A number of factors can influence nanoparticle synthesis, including the metal precursor, reducing agents, stabilizing (or capping) agents, solvents, temperature, time and pH, with varying effects based on the synthetic method employed. The choice of precursor directly impacts the pathway and kinetics leading to the product, with highly reactive precursors resulting in faster but less controllable nanoparticle formation, while less reactive precursors may require harsher reaction conditions. Higher concentrations of precursors and reducing agents, as well as stronger reducing agents, lead to faster reaction kinetics and therefore smaller nanoparticle sizes. Stabilizing agents such as surfactants,

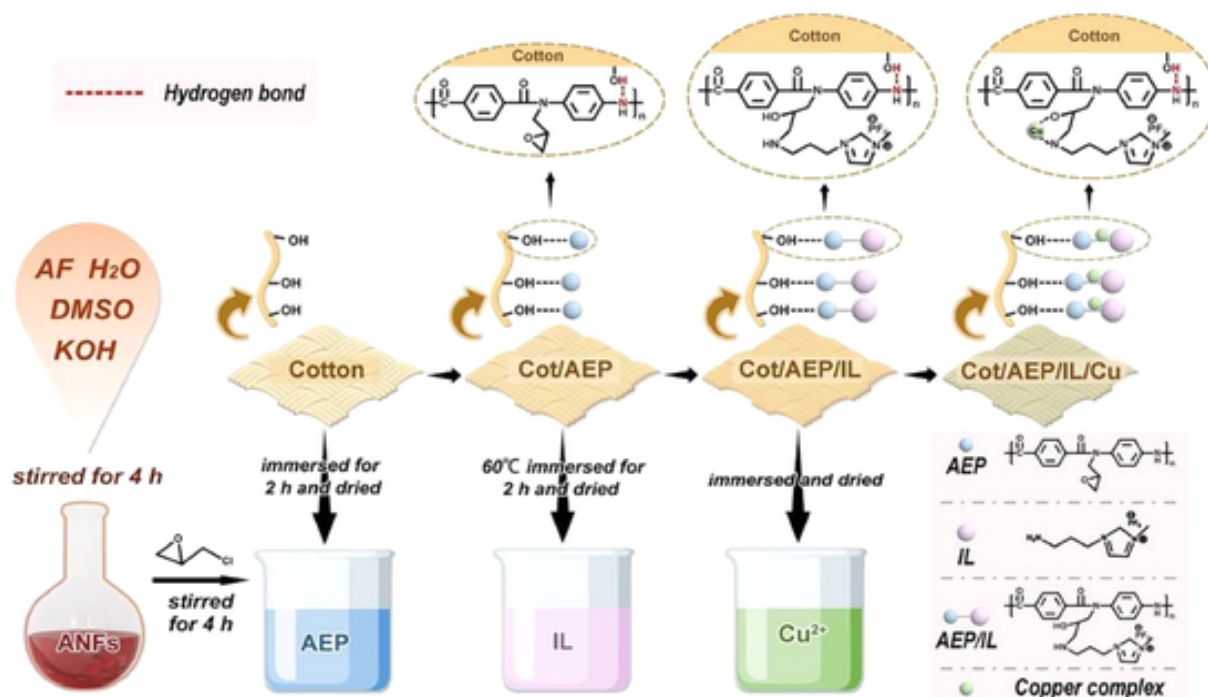


Fig. 34. Preparation of Cot/AEP/IL/Cu. Reproduced from Ref. [264] with permission from Elsevier, Copyright © 2023.

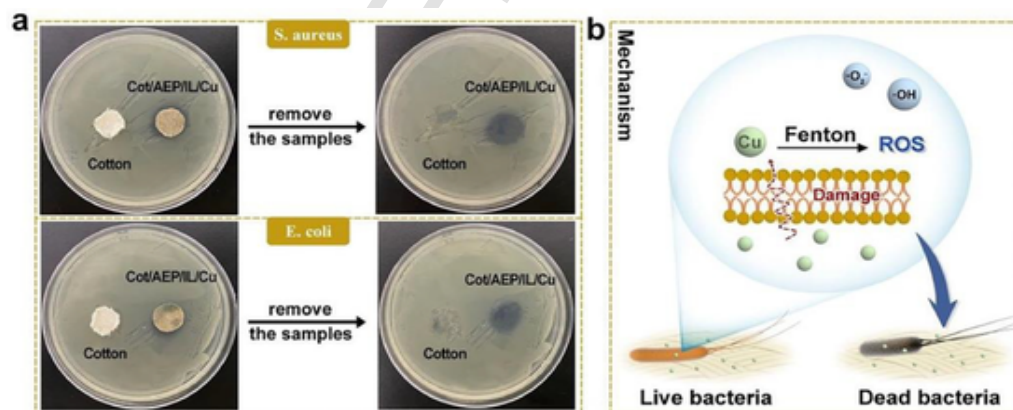


Fig. 35. a) Antibacterial assays for Cot/AEP/IL/Cu against *S. aureus* and *E. coli*. b) Mechanism of ROS-mediated antibacterial activity of Cot/AEP/IL/Cu. Reproduced from Ref. [264] with permission from Elsevier, Copyright © 2023.

ligands, or polymers may be added to adsorb to the nanoparticle surfaces to prevent agglomeration and control growth. The solvent, pH and temperature for the reaction can influence precursor solubility, reaction kinetics, activity of stabilizing and reducing agents and growth rates of the nanoparticles. Finally, longer reaction times can allow for larger nanoparticles, but increase the risk of aggregation occurring.

Green synthesis of metal and metalloid nanoparticles has been a particular focus of research thanks to its low cost, renewable reagents, and lower production of toxic wastes [212–217]. A review by Ahire and Kasabe discussed the synthesis of silver (Ag) and gold (Au) nanoparticles, especially using green methods [218]. Biological materials such as plant parts, tea, coffee, polyphenols, proteins, enzymes, bacteria, yeast, algae, and viruses have been used as reducing and capping agents in the synthesis of nanoparticles. In particular, the synthesis of silver nanoparticles has been explored using a number of sources, including the plants *Solanum xanthocarpum* L., *Hibiscus rosa sinensis*, green algae, brown al-

gae, microalgae, geranium plants, serum albumins, DNA, cashew nuts, banana pith extract, and the fungus *Fusarium oxysporum*.

Jabbar *et al.* described the green synthesis of silver nanoparticles (Ag NPs) using a polar extract of *Equisetum diffusum* (ED) leaves [219]. The AgNPs were synthesized by mixing the ED extract with AgNO_3 solution and exposing the mixture to sunlight for 30–60 sec, as seen in Fig. 27. The synthesized ED-functionalized AgNPs were characterized by UV-visible spectroscopy (UV-Vis), FTIR, XRD, SEM, etc. Analysis showed successful capping of AgNPs (avg size 63 nm) with phytochemicals from the ED extract. The functionalized AgNPs were shown to act as a highly selective colorimetric sensor for detecting Hg^{2+} ions in water. The sensor showed excellent sensitivity and rapid response, with a detection limit of 70 nM Hg^{2+} . It could reliably detect spiked Hg^{2+} in experimental water samples.

Other examples of published green synthetic methods include the use of *Albizia saman* leaf extract for copper oxide nanoparticles (CuO

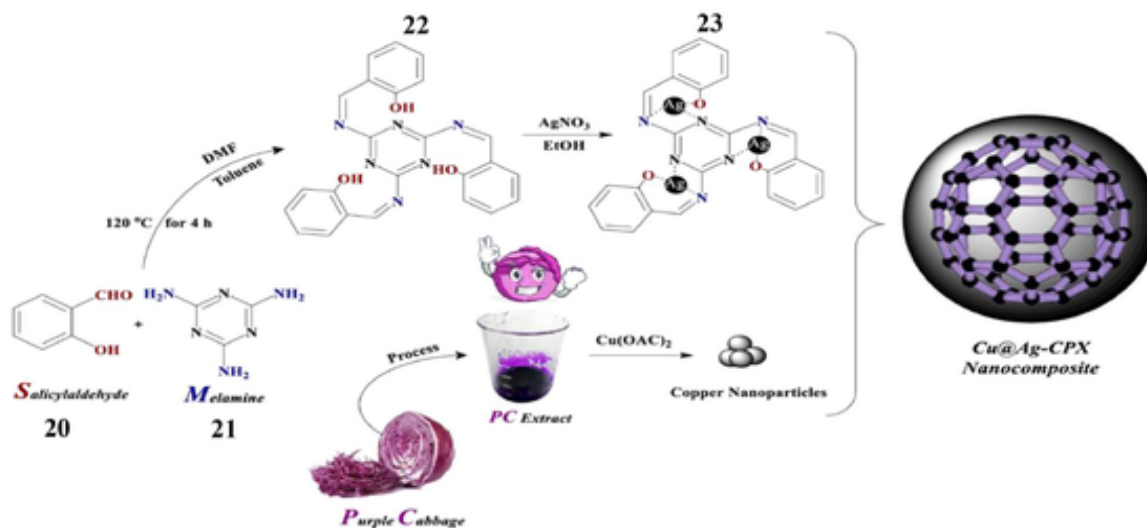


Fig. 36. Illustrated synthesis of Cu@Ag-CPX nanocomposite. Reproduced from Ref. [265], <https://doi.org/10.1038/s41598-023-47358-4>, under the terms of the CC BY 4.0 license, <https://creativecommons.org/licenses/by/4.0/>

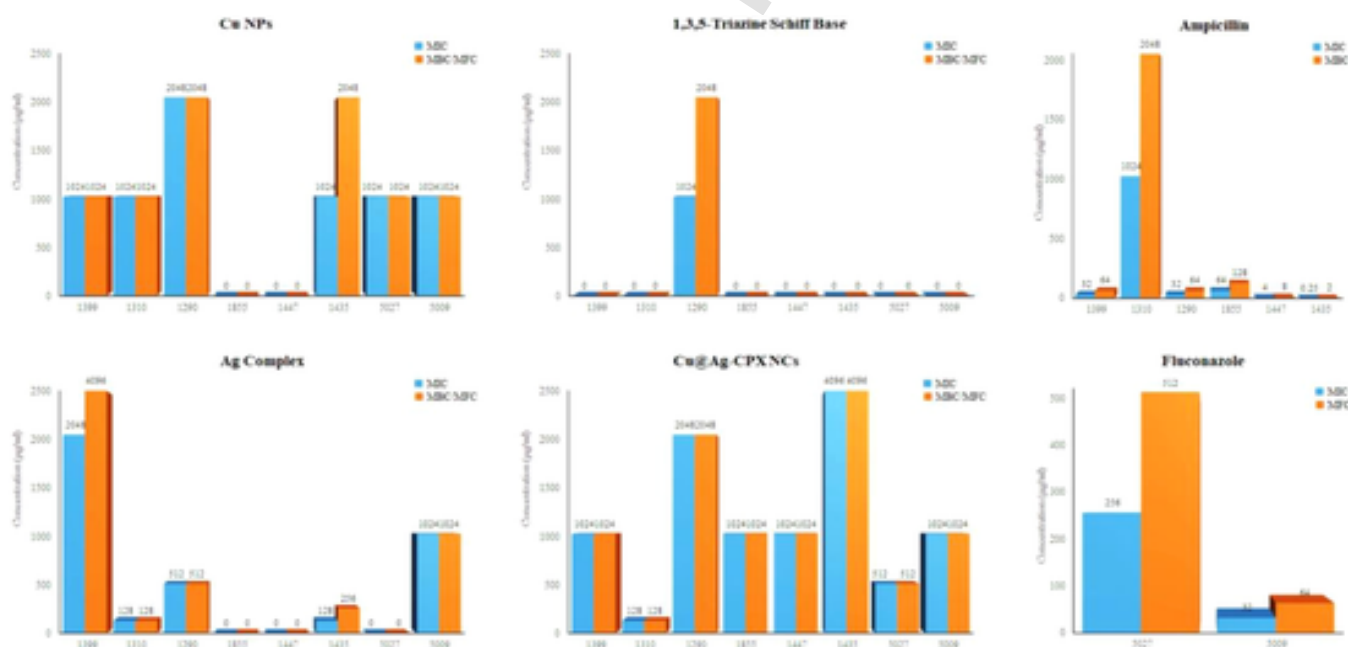


Fig. 37. MIC and MBC/MFC of Cu NPs, the 1,3,5-triazine Schiff base, the Ag complex, and Cu@Ag-CPX, as well as conventional agents against the following species: 1399: *E. coli*, 1310: *P. aeruginosa*, 1290: *K. pneumoniae*, 1855: *A. baumannii*, 1447: *S. pyogenes*, 1435: *Staphylococcus epidermidis*, 5027: *C. albicans*, 5009: *A. fumigatus*. Reproduced from Ref. [265], <https://doi.org/10.1038/s41598-023-47358-4>, under the terms of the CC BY 4.0 license, <https://creativecommons.org/licenses/by/4.0/>

NPs), chitosan from the exoskeleton of marine crustaceans for silver nanoparticles, leaf extract of *Ziziphus spina-christi* for NiO NPs, ginger root or cardamom seed extracts for bimetallic CoFe nanoparticles and *Daphne oleoides* extract for ZnO NPs, which were then dispersed on a silica gel matrix [220–224].

3.3. Antibacterial and antifungal activities

Metal nanoparticles and composites have been studied for their antibacterial and antifungal applications [225,226]. The high surface-to-volume ratio and other physicochemical properties of metal and metal

oxide nanoparticles have garnered a great deal of attention. For example, metal/metal oxide nanoparticles can have strong interactions with cell membranes and cell walls of bacteria and fungi, leading to inhibition of microbial growth [227]. Metal nanoparticles can also act as carriers for drugs, including antibiotics [228].

Silver nanoparticles have been well studied for their activities against both Gram-positive and Gram-negative bacteria as well as fungi [229,230]. AgNPs can release Ag⁺ ions, which can generate ROS, disrupt cell membranes, and inhibit the function of respiratory enzymes, leading to cell death [231]. In addition to their antimicrobial effects, AgNPs can also inhibit microbial adhesion and biofilm formation [232].

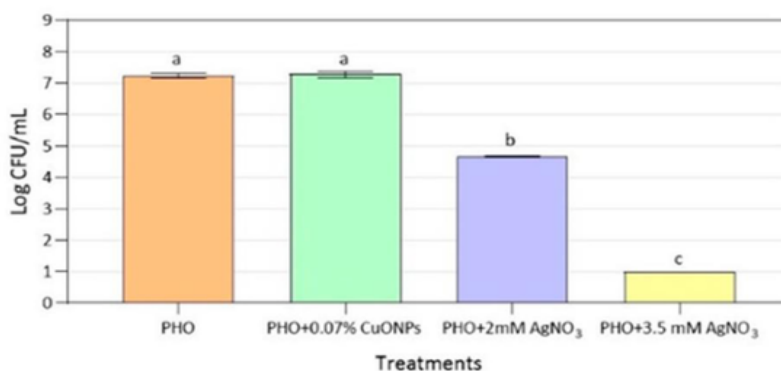


Fig. 38. Reduction in MRSA growth by various PHO with or without embedded Cu or AgNO₃ nanoparticles. Reproduced from Ref. [267], <https://doi.org/10.3390/polym15040920>, under the terms of the CC BY 4.0 license, <https://creativecommons.org/licenses/by/4.0/>

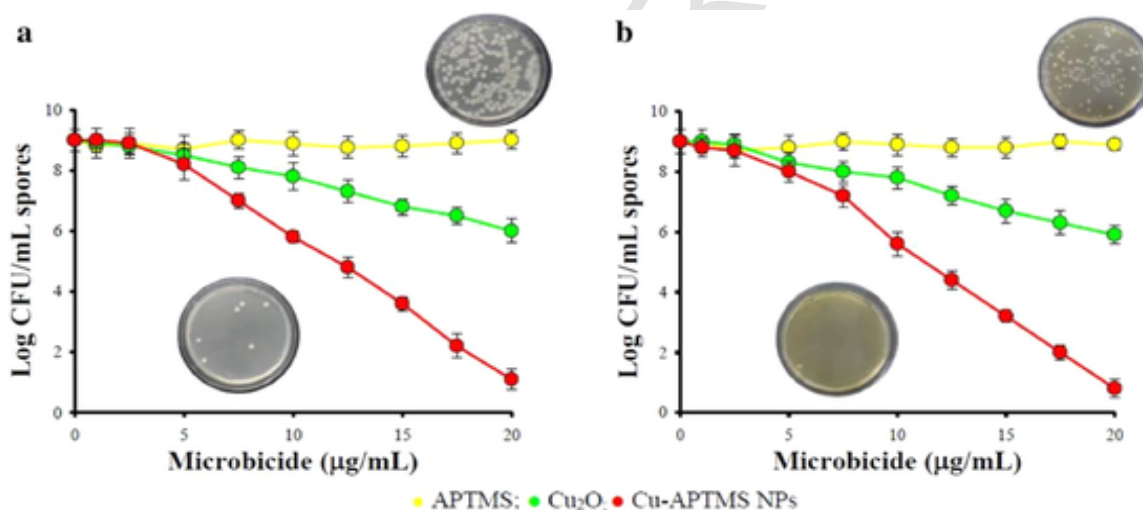


Fig. 39. Disinfection by Cu₂O, APTMS and Cu-APTMS NPs for spores of a) *B. subtilis* and b) *Clostridium perfringens*. n = 3, data = means ± standard error. Photographs in insets are agar plates for (top) untreated bacterial spores and (bottom) spores treated with 80 µM Cu-APTMS NPs for each strain. Reproduced from Ref. [268] with permission from Springer Nature.

Zinc oxide (ZnO), titanium dioxide (TiO₂) and copper oxide (CuO) nanoparticles have also been investigated as antibacterial and antifungal agents [233–235]. Similar to AgNPs, CuO NPs can induce oxidative stress, perturb membranes, and interfere with enzymatic processes [236]. ZnO and TiO₂ NPs have been demonstrated to have photocatalytic activity, meaning that they produce ROS in response to irradiation with various wavelengths of visible and ultraviolet light, allowing them to target drug-resistant microbial strains [237].

Recent advances in the synthesis and production of metal/metal oxide nanoparticles have been employed to control the shape, size and surface chemistry of the resulting NPs. Some of these approaches include chemical reduction using synthetic chemicals or natural products, physical deposition and sol-gel techniques [238]. Further, the functionalization of nanoparticle surfaces has allowed for improvements to their stability, biocompatibility, and targeting. As an example, biosurfactants have been used as an environmentally friendly approach for coating nanoparticles to prevent agglomeration [239].

In addition to being used as antimicrobial agents, metal/metal oxide nanoparticles may also be utilized as adjuvants for existing antimicrobial agents to yield synergistic effects in order to enhance the overall antimicrobial activity and prevent the evolution of antimicrobial resistance [240].

This section will describe the study of a few examples of metal and metal oxide nanoparticles and their antibacterial and antifungal effects. While this is a large field of study, this review will only cover a few recent representative examples.

3.3.1. Industrial settings

Antimicrobial materials containing metal/metal oxide nanoparticles have been shown to have industrial applications such as methods for wastewater remediation as well as antimicrobial textiles/surfaces for healthcare settings [241–243]. Metal oxide nanoparticles and composites have been extensively studied for remediation of wastewater, targeting heavy metals and organic matter, although the commercial applications have been limited due to cost-efficacy and potential toxicity [241]. Fabrics with embedded metal/metal oxide nanoparticles, such as AgNPs, and metal oxide NPs, such as ZnO NPs, have been employed in prevention of nosocomial (hospital-acquired) infections [244]. Not only can these fabrics prevent the spread of multidrug-resistant pathogens, but they can also inhibit biofilm growth, which helps to avoid the development of drug resistance. It was noted, however, that these fabrics have been examined mainly for their antibacterial properties, rather than the physical properties such as tensile strength, permeability to air, flexibility, durability, etc. that are necessary for daily use

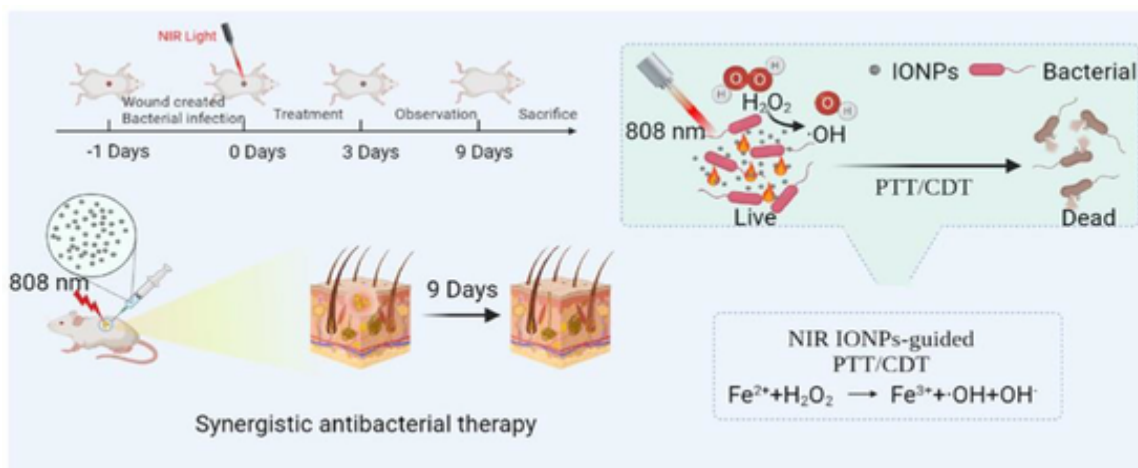


Fig. 40. In vivo antibacterial therapy experiment using mice treated with IONPs and irradiation at 808 nm for synergistic photothermal (PTT) and chemodynamic (CDT) therapies. Reproduced from Ref. [269], <https://doi.org/10.1093/rb/rbac041>, under the terms of the CC BY 4.0 license, <http://creativecommons.org/licenses/by/4.0/>

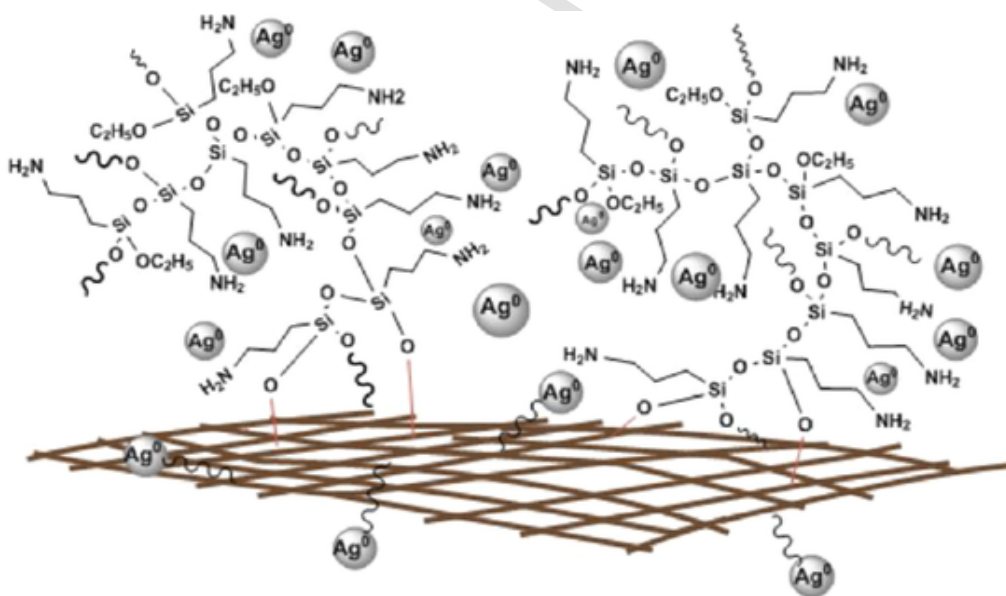


Fig. 41. Ag NPs/HB-PAPES/cotton nanocomposites. Reproduced from Ref. [270], <https://doi.org/10.3390/pharmaceutics15030809>, under the terms of the CC BY 4.0 license, <https://creativecommons.org/licenses/by/4.0/>

and comfort. In addition, as fabric in hospital settings often comes into contact with human skin, the lack of literature focused on the biocompatibility of metallic NP-containing fabrics is a major limitation of this field of study. Some examples of these applications are given below.

Poly(l-lactide) (PLLA)-based materials have excellent mechanical and biological properties but are difficult to process due to the properties of the polylactic acid (PLA) matrix, including its high melting point, poor resistance to environmental factors such as light and moisture, and low thermal stability. Metal oxide nanoparticles have not only been shown to possess antibacterial and antioxidant properties, but also prevent yellowing of their host matrix due to exposure to UV light. Therefore, nanocomposites of nanolignin, PLA, and metal oxides Ag₂O, TiO₂, WO₃, Fe₂O₃, and ZnFe₂O₄ have been developed for use as antibacterial and antioxidant films [245]. The PLLA-based films showed significant antibacterial activity against *S. aureus* and *E. coli*, although the effect

was retained for over 24 hours against *S. aureus*, but not for *E. coli*. In terms of metal oxides, the strongest antibacterial effects were observed for films containing Ag₂O or TiO₂ for either bacterial species. These properties could make these films ideal for applications in food and drug packaging or for biomedical applications.

MgO nanoparticles were investigated for applications in wastewater treatment, using photocatalytic degradation of industrial pollutants and antibacterial effects to target bacterial contamination [246]. The common industrial pollutant Victoria blue dye was used as a model for degradation under UV light. The antibacterial activity demonstrated moderate activity against Gram-negative *E. coli* and Gram-positive *S. aureus* and *S. pyogenes*.

As described in Section 3.1 above, Choudhary *et al.* prepared CuO NPs using *Albizia saman* leaf extract [220]. The removal efficiency of the CuO NPs for Congo Red dye was 33.33 %, while the removal effi-

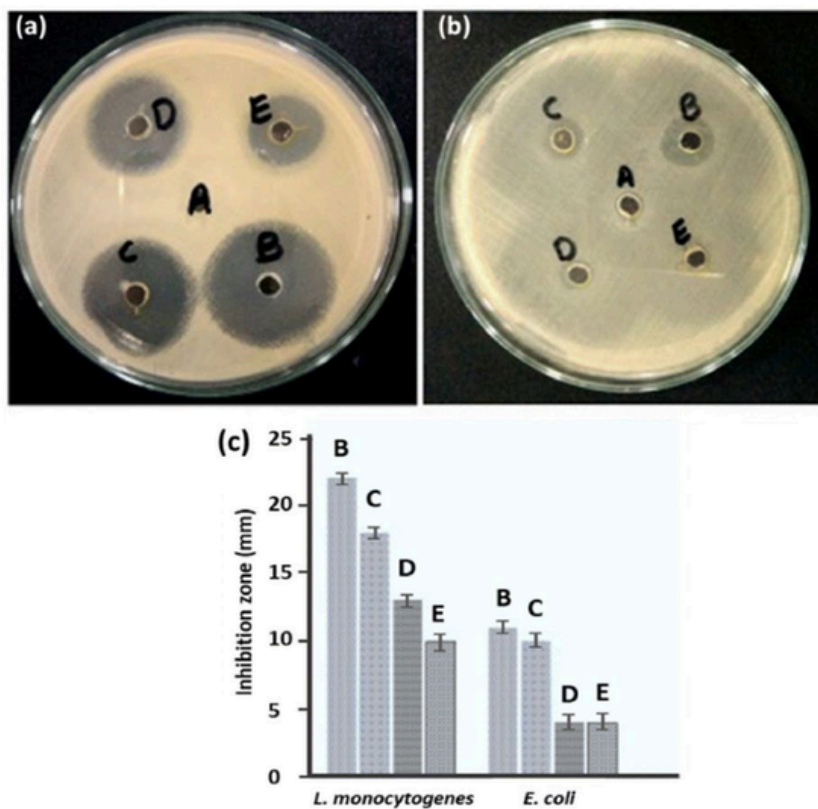


Fig. 42. Inhibition of a) *L. monocytogenes* and b) *E. coli*, and c) their corresponding inhibition zone measurements (in mm). Reproduced from Ref. [219], <https://doi.org/10.1039/D3RA05070J>, under the terms of the CC BY NC ND license, <http://creativecommons.org/licenses/by-nc-nd/4.0/>

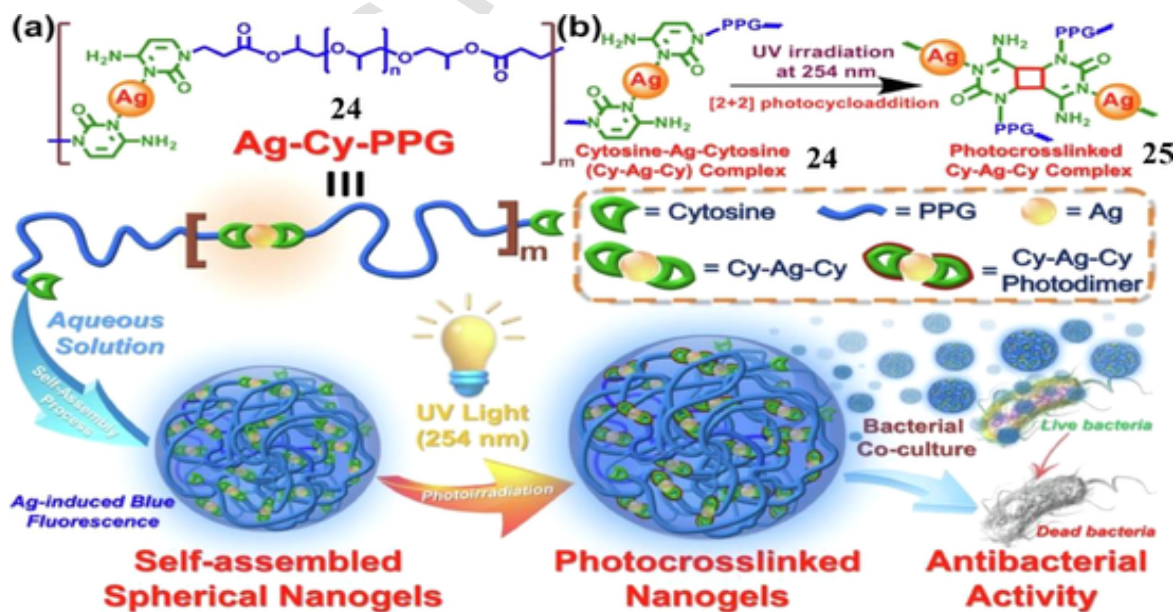


Fig. 43. Self-assembly and photocrosslinking of Ag-Cy-PPG nanoparticles for use as antibacterial agents. Reproduced from ref. [272] with permission from Elsevier, Copyright 2023.

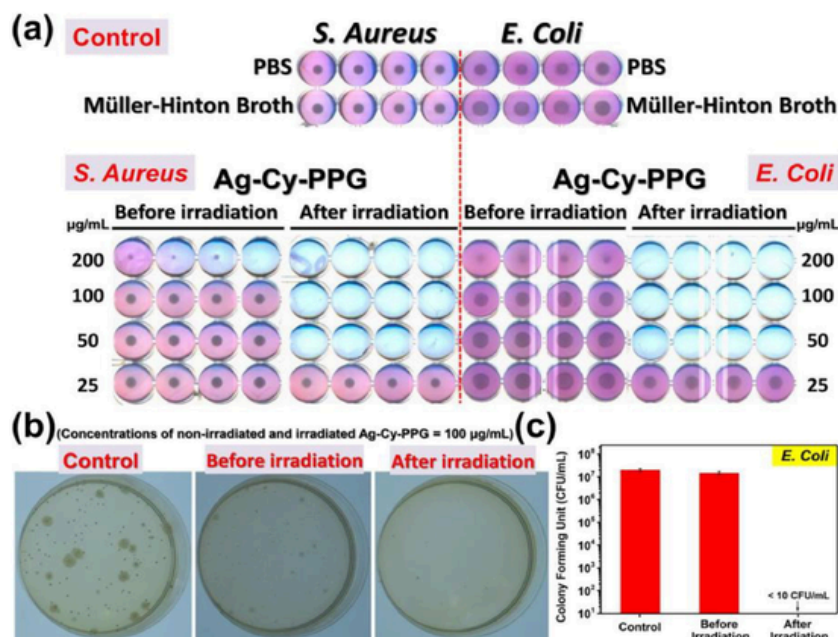


Fig. 44. a) MIC measurements using irradiated and non-irradiated Ag-Cy-PPG nanogels against *E. coli* and *S. aureus*. b) Antibacterial effect and c) quantification (in CFU/mL) for *E. coli* exposed to 100 µg/mL irradiated Ag-Cy-PPG nanogels for 48 h compared with non-irradiated nanogels and a negative control. Reproduced from ref. [272] with permission from Elsevier, Copyright 2023.

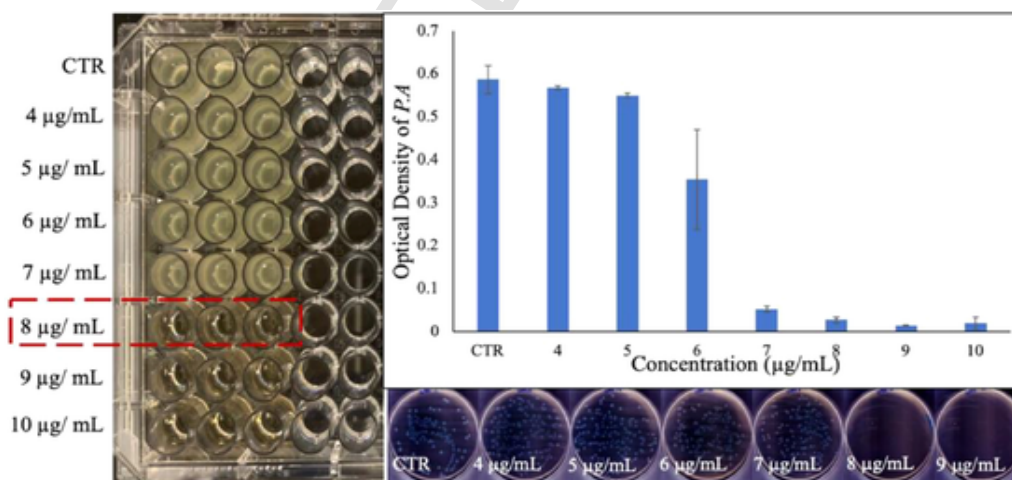


Fig. 45. MIC values for *P. aeruginosa* treated with different concentrations of PVP-coated NPs (CTR = negative control). Reproduced from Ref. [273], <https://doi.org/10.3390/antibiotics12111578>, under the terms of the CC BY 4.0 license, <https://creativecommons.org/licenses/by/4.0/>

ciency of the phytonanofabricated CuO for the same dye decreased to 16 % after four cycles. The antimicrobial activities of CuO NPs against Gram-negative *E. coli*, Gram-positive *S. aureus*, and fungus *C. albicans* were evaluated and showed zones of inhibition of 15, 14, and 12 mm, respectively.

Similarly, TiO₂ nanoparticles have also been studied for use in wastewater treatment for their antibacterial activity and photocatalysis, with water remediation and biomedical applications. Shimi *et al.* prepared TiO₂ nanoparticles using mulberry plant extract and examined their antibacterial activity and photocatalysis of methylene blue dye [247]. Fig. 28 shows the photocatalytic degradation process of methylene blue using these TiO₂ NPs. The TiO₂ NPs exhibited an 8 mm zone of inhibition against *E. coli* and 10 mm against *S. aureus*, which was larger than the mulberry extract alone, but slightly lower than the

reference drug gentamicin (12 mm against *E. coli* and 14 mm against *S. aureus*). The specificity for *S. aureus* is suspected to be a consequence of the drug, plant extract and nanoparticles all being more capable of penetrating the Gram-positive cell wall. The mechanism for the antibacterial activity was believed to be a result of ROS production by Ti³⁺ released from the TiO₂.

Nanocomposites GO-Ag, GO-TiO₂@ZnO and GO-Ag-TiO₂@ZnO composed of graphene oxide (GO) nanosheets decorated with ZnO nanoflowers, silver NPs, and TiO₂ NPs were prepared by El-Shafai *et al.* [248]. Graphene oxide is simple and cost-effective to fabricate, as well as having low toxicity to mammalian cells. The GO, TiO₂, ZnO nanoflowers, and Ag NPs can all produce ROS, which results in synergistic antibacterial activity via DNA damage, protein oxidation and lipid peroxidation. An illustrated summary of the antibacterial mecha-

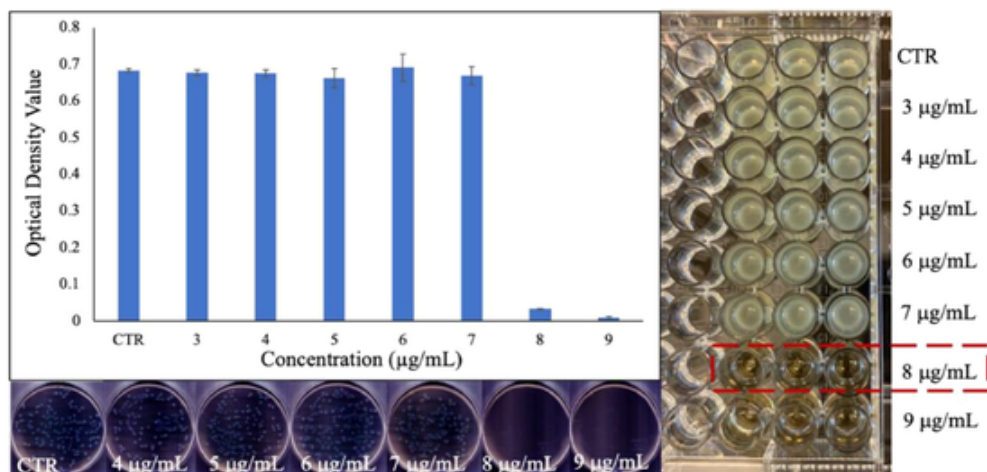


Fig. 46. MIC values for *P. aeruginosa* treated with different concentrations of PEG-coated NPs (CTR = negative control). Reproduced from Ref. [273], <https://doi.org/10.3390/antibiotics12111578>, under the terms of the CC BY 4.0 license, <https://creativecommons.org/licenses/by/4.0/>

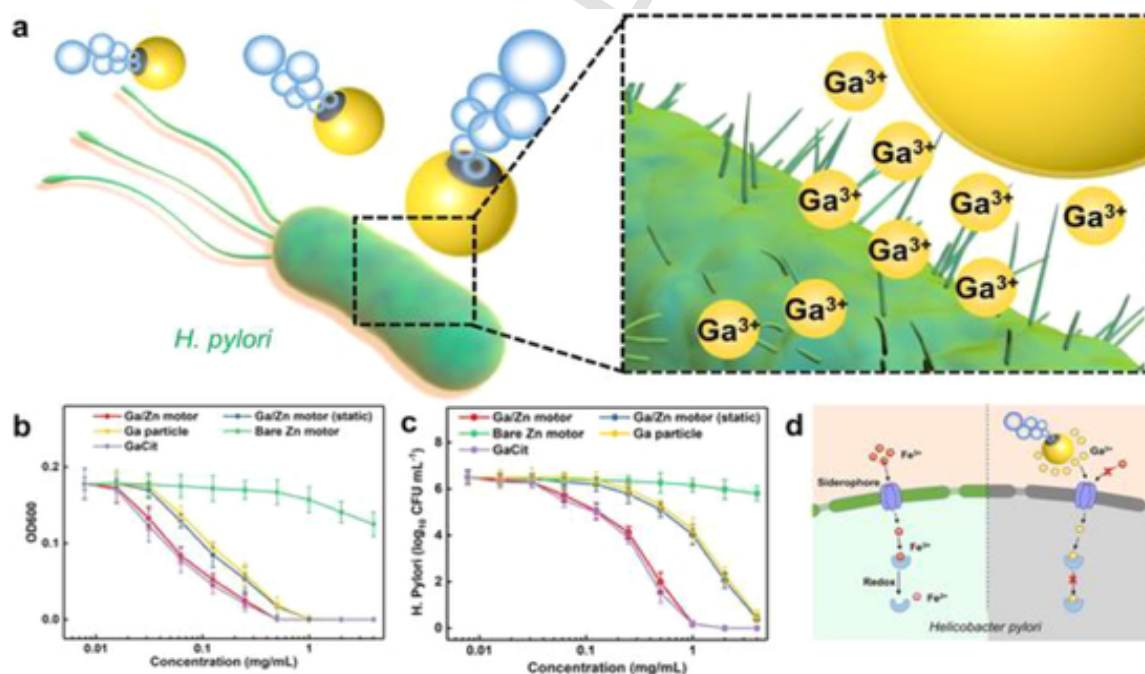


Fig. 47. a) Diagram of motor function and release of Ga^{3+} for the Ga/Zn micromotors. b) Optical density at 600 nm for media containing *H. pylori* after treatment with different Ga and Zn motors or nanoparticles. c) Inhibition of *H. pylori* growth measured by \log_{10} colony forming units (CFU)/mL 72 h after treatment. d) Mechanism of antibacterial activity for the Ga/Zn micromotors. Reproduced from Ref. [274] with permission from John Wiley & Sons, Copyright © 2021 Wiley-VCH GmbH.

nism is shown in Fig. 29. The antibacterial activity against Gram-positive *S. aureus* and *Bacillus anthracoides* and Gram-negative *E. coli* and *Pasteurella multocida* was measured. When compared with GO-Ag and GO-TiO₂@ZnO nanocomposites, the GO-Ag-TiO₂@ZnO nanocomposite showed the largest zones of inhibition against Gram-positive bacteria, but only moderate efficacy against Gram-negative bacteria, while GO-Ag and GO-TiO₂@ZnO showed the strongest inhibitory effects against Gram-negative bacteria. These nanocomposites therefore showed potential as therapeutic agents with tunable activity against different species of bacteria.

ZrO₂ nanoparticles were doped with Te⁴⁺ and Er³⁺ to provide photocatalytic and antibacterial activities [249]. The ZrO₂ NPs in-

duced oxidative stress in *E. faecalis* and *E. coli* bacteria after exposure to visible light, resulted in over 97 % and 94 % inhibition rates, respectively, and a zone of inhibition of 3 mm for each. The ZrO₂ nanoparticles could be a potential technique to treat contaminated wastewater so it can be used for irrigation.

In a study by Steinerová *et al.*, the researchers focused on developing environmentally friendly coatings with antimicrobial properties [250]. Waterborne coatings, specifically acrylic latex paints, were chosen as a suitable platform due to their easy preparation, low toxicity, and compatibility with various surfaces. To achieve antimicrobial properties, the researchers incorporated metal oxide nanoparticles into the acrylic latex binders. The nanoparticles used included magnesium oxide

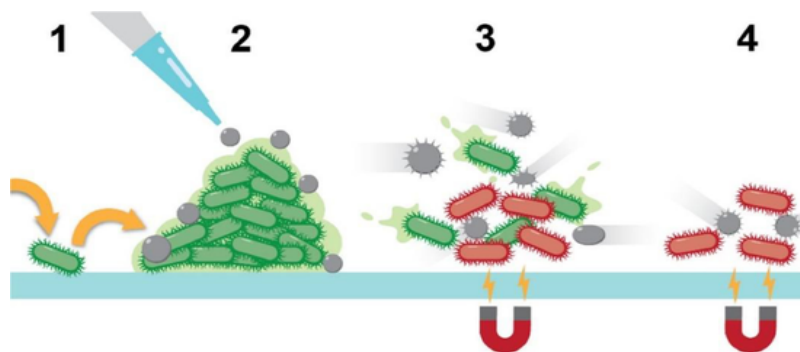


Fig. 48. Illustration of the physical mechanism of GLM-Fe nanoparticles under a magnetic field in four steps: 1. Adhesion of planktonic cells (green). 2. Treatment of active biofilm using GLM-Fe (grey). 3. Addition of a magnetic field that physically disrupts the extracellular matrix of the biofilm and lyses bacterial cells, rendering them inactive (red). 4. Biofilm mass is reduced and the remaining cells are mostly deactivated. Reproduced with permission from Ref. [276] Copyright 2020, American Chemical Society.

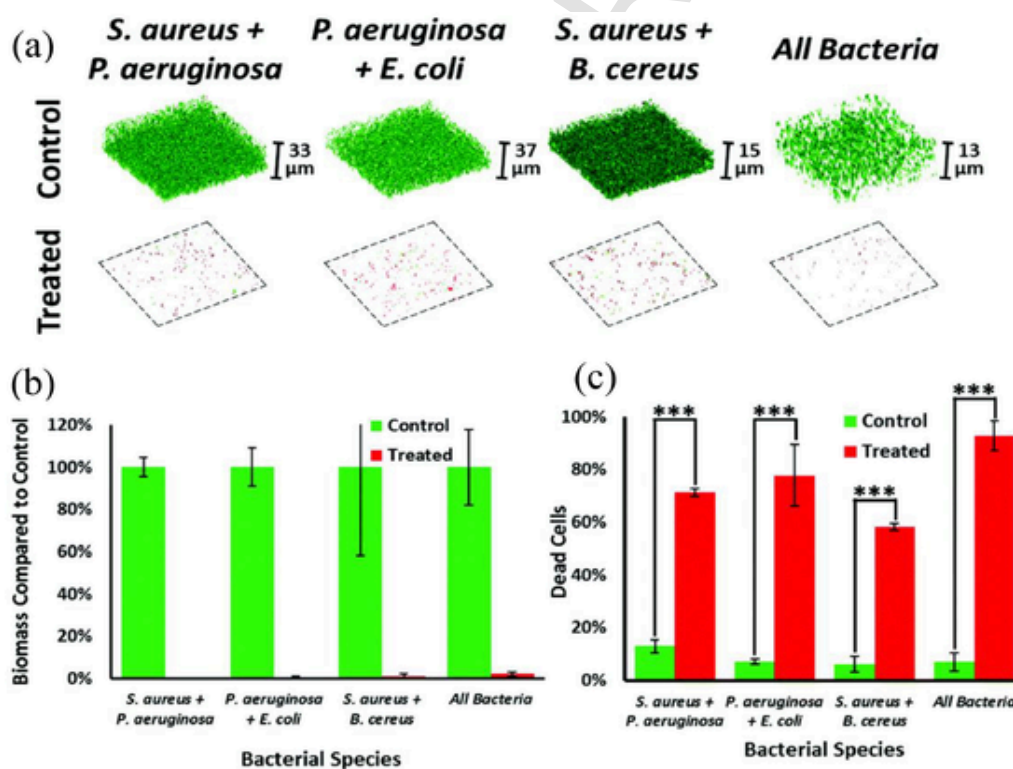


Fig. 49. Antibiofilm activity of GLM-Fe nanomaterials. a) Inhibition of biofilms containing multiple bacterial species. b) Bacterial biomass after treatment. c) Percentage of dead cells after GLM-Fe treatment. Reproduced from Ref. [277] with permission from the Royal Society of Chemistry.

(MgO), zinc oxide (ZnO), lanthanum oxide (La_2O_3), and combinations of MgO and ZnO. These nanoparticles were selected for their known antimicrobial properties and their potential to enhance the physical and mechanical properties of the coatings. Different concentrations of nanoparticles, ranging from 0.5 % to 1.3 % relative to the polymer content, were used to assess their impact on the properties of the latexes. The results of the study demonstrated that all nanoparticles exhibited promising properties and that there was an improvement in the properties of the coatings, corresponding to the increasing nanoparticle concentration. The latexes containing nanoparticles produced smooth, transparent films with high gloss and suitable physical-mechanical properties. These coatings showed significant antimicrobial activity against various bacterial and fungal strains. Additionally, the coatings

exhibited good resistance to solvents, making them suitable for various applications. The latexes containing MgO nanoparticles showed a significant decrease in the minimum temperature at which the film formed, indicating improved film formation at lower temperatures. Furthermore, the coatings based on latexes with a concentration of approximately 1.3 % MgO showed no flash corrosion on a steel substrate. The latex coatings containing nanoparticles were examined for their antimicrobial properties against Gram-negative *E. coli*, *K. pneumoniae*, *E. faecalis*, *S. aureus*, *Penicillium chrysogenum* and *Aspergillus brasiliensis*, and all coatings were found to show significant bactericidal activity. Only the coatings with high MgO concentration were effective against *E. faecalis*, while only ZnO-containing coatings showed fungicidal activity against *P. chrysogenum* or *A. brasiliensis*. Overall, the study highlights

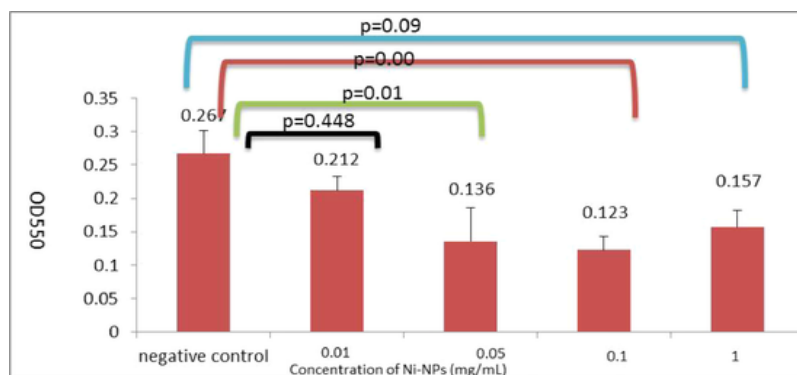


Fig. 50. Biofilm growth measured by OD₅₅₀ of crystal violet stain for *S. epidermidis* taken from biofilms treated with Ni NPs. Reproduced from Ref. [278], <https://ijm.tums.ac.ir/index.php/ijm/article/view/915>, under the terms of the CC BY 4.0 license, <http://creativecommons.org/licenses/by/4.0/>

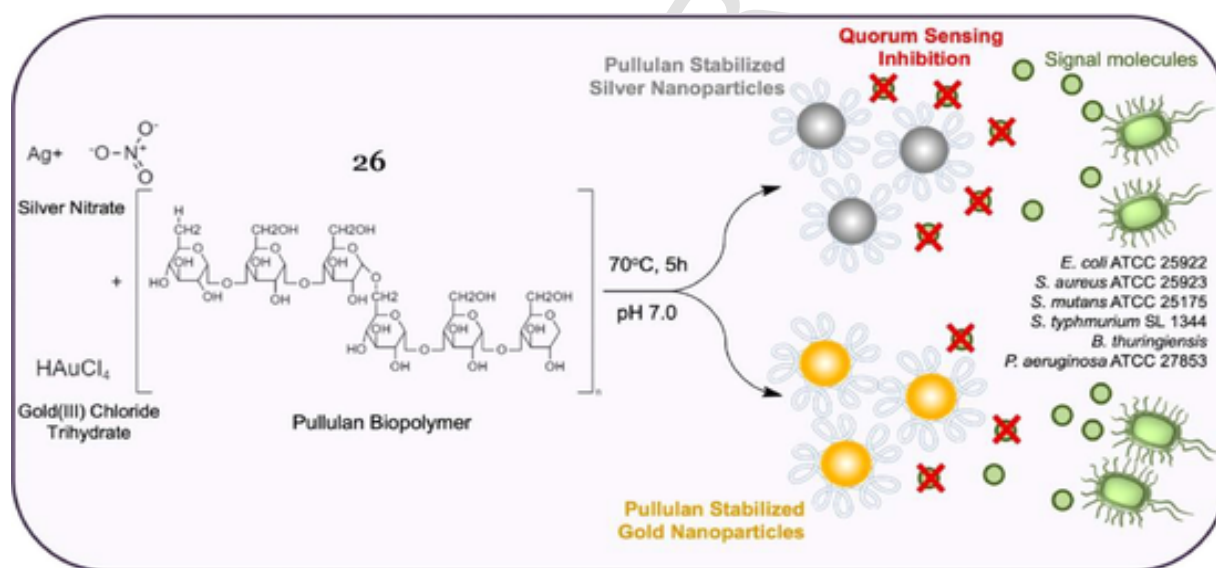


Fig. 51. Preparation of pullulan-stabilized Ag and Au nanoparticles for quorum sensing inhibition. Reproduced from Ref. [279], <https://doi.org/10.1021/acsabm.1c00964>, under the terms of the CC BY 4.0 license, <http://creativecommons.org/licenses/by/4.0/>

the potential of metal oxide nanoparticles, such as MgO, ZnO, and La₂O₃, as effective antimicrobial additives in waterborne coating binders. Such environmentally friendly coatings with antimicrobial properties have significant potential in various industries, including healthcare, food processing, and building materials.

During the COVID-19 pandemic, the limitations of existing N95 masks, including their filtration capabilities and compatibility with individuals with medical conditions, became a notable issue. To address these challenges, Mills and coworkers proposed the development of an antimicrobial filtration system using metal-coated halloysite nanotubes (HNTs) and PLA [251]. They used an electrodeposition method to coat HNTs with copper, silver, and zinc, known for their antimicrobial properties. These metal-coated HNTs, referred to as mHNTs, were then incorporated into PLA and processed into a composite 3D printer filament. The composite filament was used to create an N95-style mask with an interchangeable and replaceable filter designed to kill bacteria and inactivate viruses on contact, thereby reducing the risk of infections. The mask itself is reusable and can be sanitized. The researchers conducted *in vitro* tests to assess the antimicrobial properties of the filaments containing each of the nanoparticle types, or all three of them,

and demonstrated their effectiveness against both Gram-negative *E. coli* and Gram-positive *S. aureus*, as illustrated in Fig. 30.

The preparation and characterization of a chitosan-based gold nanoparticle composite (Chi/AuNPs) has been described [252]. Chitosan served as both a reducing and stabilizing agent for the gold nanoparticles. Chitosan can also inhibit microbial growth in addition to the ROS production by the Au NPs, via disruption of microbial membranes as a result of the negatively charged membranes interacting with positively charged chitosan in an acidic environment. Chi/AuNPs were synthesized by chemically reducing gold ions in the presence of chitosan. The nanoparticles formed were spherical and between 20–120 nm in diameter. Characterization techniques like TEM, SEM, FTIR, XRD, and zeta potential measurements confirmed the successful formation of stable Chi/AuNPs. Cytotoxicity testing showed Chi/AuNPs were non-toxic to normal human skin cells. Chi/AuNPs demonstrated promising antibacterial activity against both Gram-positive (*S. aureus* and *B. subtilis*) and Gram-negative (*P. aeruginosa* and *Klebsiella oxytoca*) bacteria. They also exhibited antifungal activity, especially against the yeast *C. albicans* (Fig. 31). *In vitro* wound healing assays revealed that Chi/AuNPs could promote rapid and effective wound closure. The authors concluded that the chitosan-gold nanoparticle composite showed

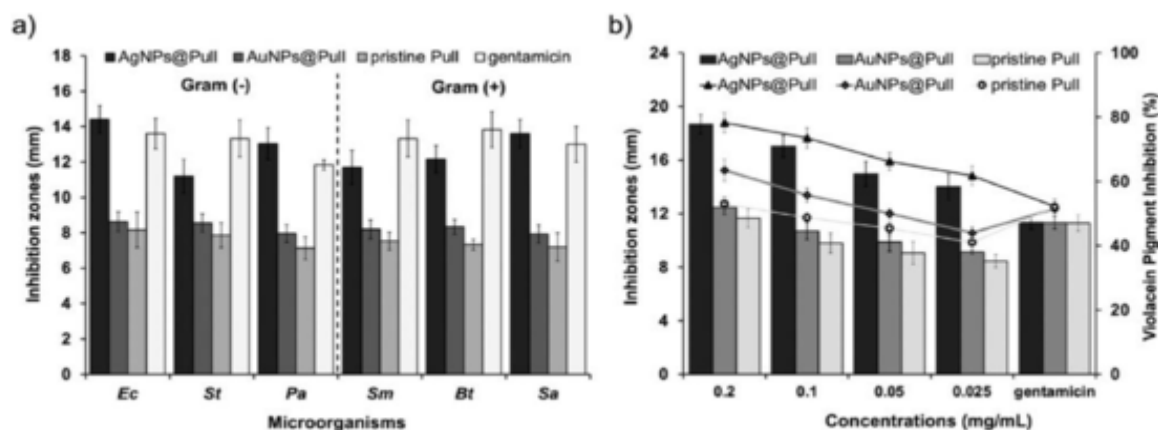


Fig. 52. Inhibition zones for pullulan nanoparticles, pullulan, and gentamicin a) against various Gram-positive and Gram-negative bacteria (Ec = *E. coli*, St = *Salmonella enterica* typhimurium, Pa = *P. aeruginosa*, Sm = *Streptococcus*, Bt = *Bacillus thuringiensis*, Sa = *S. aureus*) and b) at different concentrations to inhibit quorum sensing in the reporter bacterial strain *Chromobacterium violaceum* CV026. Reproduced from Ref. [279], <https://doi.org/10.1021/acsabm.1c00964>, under the terms of the CC BY 4.0 license, <http://creativecommons.org/licenses/by/4.0/>

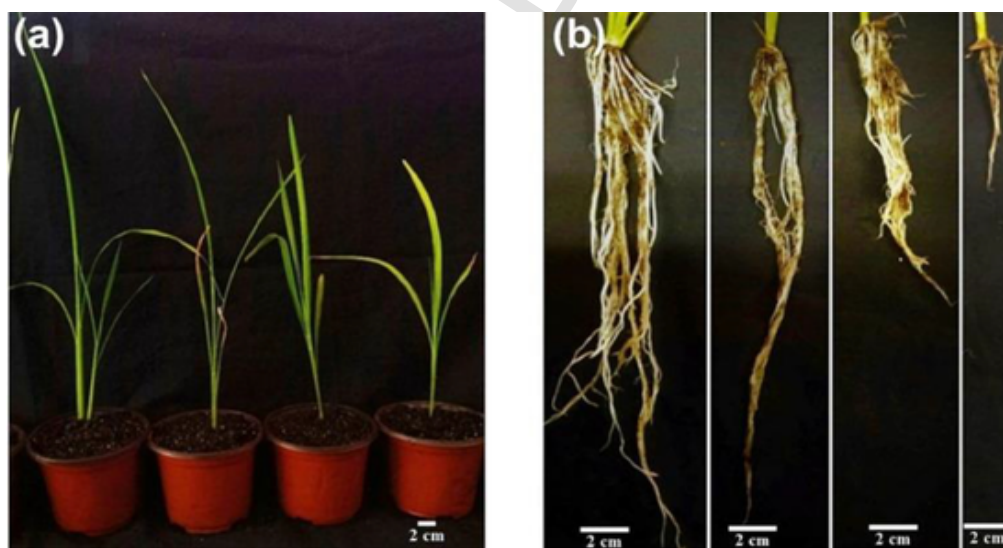


Fig. 53. a) Foliage and b) root growth for rice plants given: (from left to right), NiO NPs alone, NiO NPs and infected with *X. oryzae*, negative control, and infected with *X. oryzae* alone. Reproduced from Ref. [284] with permission from Elsevier, Copyright © 2024.

potential as an improved antimicrobial and wound dressing material. Key benefits included its antibacterial and antifungal effects, biocompatibility, and wound healing capacity.

3.3.2. Therapeutic applications

Metal-containing nanomaterials have been investigated as antimicrobial drugs [253–256]. However, while the use of these nanomaterials has been used to discover new drugs to target drug-resistant microbes, it should be noted that metal and metal oxide nanomaterials can still result in the evolution of antimicrobial resistance [257,258]. It was therefore concluded that additional research is necessary not only regarding the mechanisms of action of these nanomaterials, but also the mechanisms of resistance. While there are many examples of metallic nanoparticles as antibacterial and antifungal agents, in this section, we will only highlight a few examples to demonstrate their potential applications.

Saad *et al.* prepared manganese (IV) oxide NPs, by reduction of manganese ions using green tea extract, and examined their antibacterial

activity [259]. The MnO₂ NPs showed high activity against Gram-negative bacteria *E. coli*, *Klebsiella pneumoniae* and *P. aeruginosa*. Also, Jayandran *et al.* showed that lemon extract could be used in the green synthesis of manganese nanoparticles [260]. These nanoparticles showed similar levels of activity against various species of bacteria (*S. aureus*, *Bacillus subtilis*, *E. coli* and *Staphylococcus bacillus*) and fungi (*C. albicans*, *Curvularia lunata*, *A. niger* and *Trichophyton simii*). Composites of manganese nanoparticles with sodium bentonite clay have shown antibacterial activity against *S. aureus* and *P. aeruginosa* and antifungal activity against *C. albicans* [261]. Lopez-Abarrategui *et al.* prepared manganese ferrite nanoparticles coated with citric acid (MNPs) and conjugated them with the antifungal peptide Cm-p5 to form MNPs-Cm-p5 nanoparticles, which were more effective than either MNPs or Cm-p5 alone (Fig. 32) [262].

Xu *et al.* described a process to convert natural organosulfur compounds into nano-iron polysulfides (nFeS) by a solvothermal method [263]. The resulting nFeS exhibited significant antibacterial properties against the dental pathogen *S. mutans* UA159 in Fig. 33a, while iron ox-

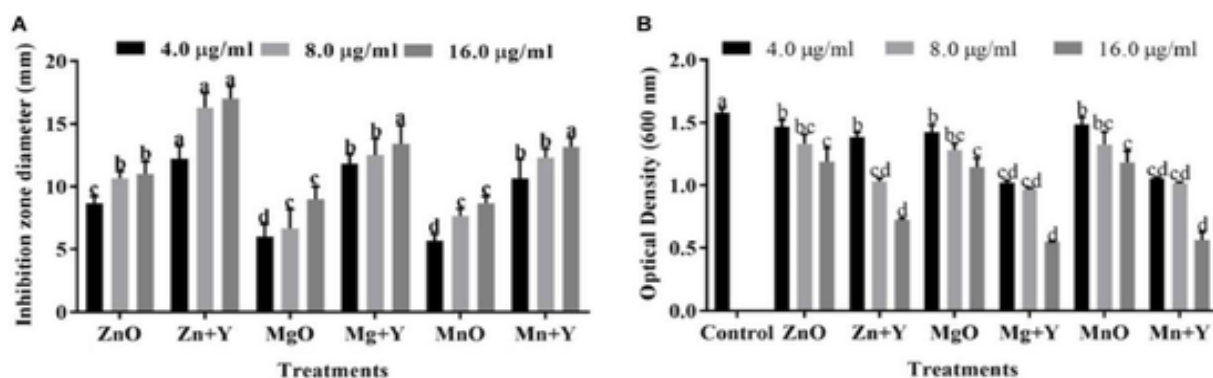
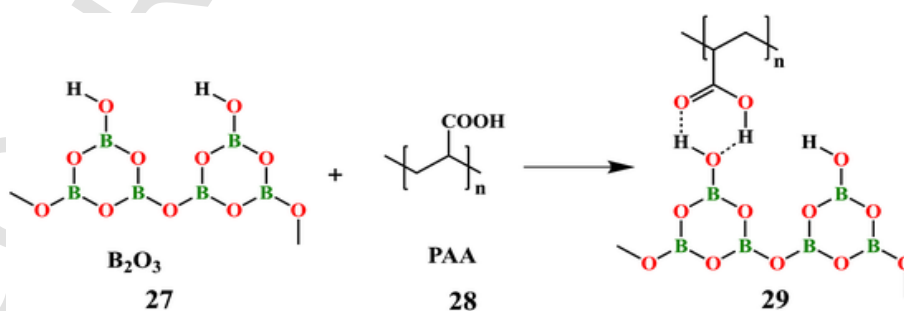


Fig. 54. A) inhibition zone diameter and B) optical density of *X. oryzae* treated with bulk metal oxides (ZnO, MgO, MnO) or metal oxide nanoparticles (Zn + Y, Mg + Y, Mn + Y). n = 3, p < 0.05. Reproduced from Ref. [285], <https://doi.org/10.3389/fmicb.2020.588326>, under the terms of the CC BY 4.0 license, <http://creativecommons.org/licenses/by/4.0/>



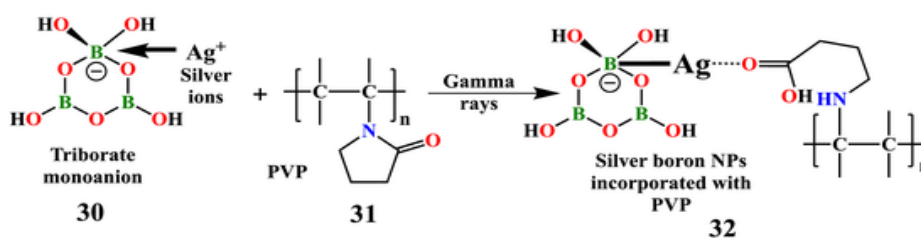
Fig. 55. Routes for synergistic antibacterial activity of boron nitride nanosheets with ionic liquid and ammonium dimolybdate. Reproduced with permission from Ref. [286]. Copyright 2023, American Chemical Society.



Scheme 2. Synthesis of B_2O_3 /PAA nanocomposite.

ide (Fig. 33a) and the organosulfur compounds alone showed minimal antibacterial activity (Fig. 33b). Fig. 33c shows the effect of nFeS with different sulfur content normalized to the same sulfur content in 0.1, 0.25, 0.5, 0.75 or 1.0 gm of cysteine, and $\text{Cys}_{0.5}\text{-nFeS}$ demonstrated the largest decrease in bacterial viability. $\text{Cys}_{0.5}\text{-nFeS}$ was then also tested against *P. aeruginosa*, *E. coli*, and *S. enteritidis*, as well as regular and multidrug-resistant *S. aureus* (Fig. 33d–h), and significant antibacterial

activities were observed for each bacterial strain. This suggested a broad activity with a mechanism that could target Gram-positive and Gram-negative bacteria and could overcome existing drug resistance. An increased level of ROS and lipid peroxidation in *S. mutans* treated with $\text{Cys}_{0.5}\text{-nFeS}$ (Fig. 33i–j) and degradation of DNA (Fig. 33k) were observed, as well as changes to the morphology and integrity of bacterial membranes, as shown by SEM (Fig. 33l). Together, these findings



Scheme 3. Incorporation of PVP into AgB NPs via ring opening of PVP after irradiation with gamma rays.



Fig. 56. Summary of synthesis, size, and osteogenic, antibacterial, and antimycotic effects of hydroxyapatite nanoparticles doped with germanium. Reproduced from Ref. [300], <https://doi.org/10.1021/acsanm.3c05974>, under the terms of the CC BY 4.0 license, <http://creativecommons.org/licenses/by/4.0/>

suggest a number of potential mechanisms for the observed antibacterial effects.

Cotton fabrics treated with epichlorohydrin-modified aramid (AEP) nanofibers, Cu ions, and ionic liquid (IL), referred to as Cot/AEP/IL/Cu, were investigated for their flame-retardant and antibacterial properties [264]. The preparation of the fabric from aramid nanofibers (AF) is shown in Fig. 34. Cot/AEP/IL/Cu not only showed low flammability, but also reduced peak smoke release rate by 77.0 % and generation of CO by 40.5 %. The antibacterial activity of the Cu ions resulted in the fabric exhibiting strong inhibition of both *S. aureus* and *E. coli* growth via an ROS mechanism, as shown in the plates in Fig. 35a and the illustration in Fig. 35b.

In a study by Pormohammad *et al.*, the researchers used purple cabbage extract to synthesize copper nanoparticles (Cu NPs) [265]. The use of plant extracts in the synthesis of Cu NPs makes this approach more environmentally friendly and sustainable compared to traditional methods. The synthesis of the Cu NPs was carried out by mixing purple cabbage extract with copper sulfate solution. A 1,3,5-triazine Schiff base ligand (23) was prepared by reaction of salicylaldehyde (20) with melamine (21), which was then followed by the addition of AgNO₃ to the intermediate 22 to yield the silver complex (23). The Cu NPs were then loaded onto complex 23 to form the Cu@Ag-CPX nanocomposite, as seen in Fig. 36. The formation of the nanocomposite was confirmed by FTIR and XRD analysis.

The antimicrobial activity of the Cu@Ag-CPX nanocomposite was evaluated against several bacterial and fungal strains using the agar diffusion method [265]. The results showed that the nanocomposite had broad-spectrum antimicrobial activity, which was attributed to the release of both Cu²⁺ and Ag⁺ ions from the nanocomposite (Fig. 37).

Yttrium oxide (Y₂O₃) nanoparticles were synthesized using a sol-gel technique from extracts of *Lantana camara* leaves [266]. These nanoparticles were designed to target cancer cells for use in the treatment of cervical cancer. The prepared nanoparticles showed photocatalytic degradation of rhodamine B dye. *In vitro* studies of antibacterial activity were carried out against Gram-positive *B. subtilis* and Gram-negative *E. coli* exhibited maximum inhibition zones of 15 mm and 11 mm, respectively, which were comparable to the reference antibiotics.

A report on the development and testing of antimicrobial and biocompatible wound dressing materials made from polyhydroxyoctanoate (PHO) polymer embedded with silver or copper oxide nanoparticles was made by Balucho *et al.* [267]. A PHO polymer was biosynthesized using *Pseudomonas putida* bacteria. This biopolymer from the polyhydroxyalkanoate family has useful properties like biocompatibility and flexibility. Silver nanoparticles (AgNPs) and/or copper oxide nanoparticles (CuONPs) were also biosynthesized using *P. putida* bacteria to reduce silver nitrate and then incorporated into the PHO polymer matrix. PHO films with 3.5 mM Bio-AgNPs showed the strongest antimicrobial activity, almost completely inhibiting the growth of MRSA, as shown in Fig. 38. The CuONP films did not inhibit MRSA. The PHO-Bio-AgNP films showed good biocompatibility when tested with human fibroblast cells, with > 79 % cell viability and no increased DNA strand breaks, although some increased oxidative DNA damage was seen. Haemolysis testing showed the PHO films were haemocompatible. Platelet aggregation was promoted, which is desirable for wound healing. The results demonstrate these biosynthesized PHO-Bio-AgNP composites have potential uses in antimicrobial wound dressings, specifically for treating infections by bacteria like MRSA.

Table 2

Examples of metal- and metalloid-containing MOFs and nanomaterials with antimicrobial activities.

| Metal | Molecular Structure | Microorganisms | Mechanism of Action | Reference |
|-------|---------------------|---|---|---------------|
| Mg | Nanoparticles | <i>E. coli</i> , <i>K. pneumoniae</i> , <i>E. faecalis</i> , <i>S. aureus</i> , <i>S. pyogenes</i> , <i>P. chrysogenum</i> , <i>A. brasiliensis</i> , <i>X. oryzae</i> | Photocatalytic, ROS | [246,250,285] |
| Ca | MOFs | <i>E. coli</i> | Drug delivery | [104] |
| Sr | MOFs | <i>E. coli</i> | Drug delivery | [104] |
| Ti | MOFs | <i>S. aureus</i> , <i>P. aeruginosa</i> | Photocatalytic | [115] |
| | Nanocomposites | <i>E. coli</i> , <i>S. aureus</i> , <i>B. anthracoides</i> | ROS | [245,248] |
| | Nanoparticles | <i>E. coli</i> , <i>S. aureus</i> | ROS | [247] |
| Mo | Nanosheets | <i>E. coli</i> , <i>S. aureus</i> | ROS, disruption of cell membrane | [286] |
| Mn | Nanoparticles | <i>E. coli</i> , <i>K. pneumoniae</i> , <i>P. aeruginosa</i> , <i>S. bacillus</i> , <i>C. albicans</i> , <i>C. lunata</i> , <i>A. niger</i> , <i>T. simii</i> , <i>X. oryzae</i> | Drug delivery, ROS | [259,262,285] |
| Fe | MOFs | <i>E. coli</i> , <i>S. aureus</i> , <i>S. haemolyticus</i> , <i>R. equi</i> , <i>S. agalactiae</i> , <i>P. aeruginosa</i> , <i>S. dysenteriae</i> , <i>C. albicans</i> , <i>A. niger</i> | Photocatalytic, disruption of cell membrane | [136,139,141] |
| | Nanoparticles | <i>E. coli</i> , <i>S. aureus</i> , <i>P. aeruginosa</i> , <i>S. mutans</i> , <i>S. enteritidis</i> | ROS | [263,269] |
| | Nanocomposite | <i>E. coli</i> , <i>S. aureus</i> | Unknown | [245] |
| Co | MOFs/ composite | <i>P. aeruginosa</i> | ROS | [138] |
| | MOFs | <i>E. coli</i> , <i>S. aureus</i> , <i>B. cereus</i> , <i>Streptococcus</i> , <i>P. mirabilis</i> , <i>Acinetobacter</i> , <i>F. oxysporum</i> , <i>C. albicans</i> , <i>A. fumigatus</i> | Unknown | [140] |
| Ni | MOFs | <i>S. aureus</i> , <i>Streptococcus</i> , <i>E. coli</i> , <i>P. aeruginosa</i> , <i>A. flocculosus</i> , <i>A. nigricans</i> | Unknown, maybe ROS | [130] |
| | Nanoparticles | <i>S. epidermidis</i> , <i>X. oryzae</i> | ROS | [278,284] |

(continued on next page)

Table 2 (continued)

| Metal | Molecular Structure | Microorganisms | Mechanism of Action | Reference |
|-------|---------------------|--|--|-----------------------|
| Cu | MOFs | <i>S. aureus</i> , <i>E. coli</i> , <i>K. pneumoniae</i> , <i>B. cereus</i> , <i>Streptococcus</i> , <i>P. mirabilis</i> , <i>A. baumannii</i> , <i>F. oxysporum</i> , <i>C. albicans</i> , <i>A. fumigatus</i> , <i>A. oryzae</i> | ROS, disruption of cell membrane, unknown | [126,134,143,236] |
| | Nanotubes | <i>E. coli</i> , <i>S. aureus</i> | Unknown, possibly ROS | [251] |
| | Nanoparticles | <i>E. coli</i> , <i>K. pneumoniae</i> , <i>A. baumannii</i> , <i>S. pyogenes</i> , <i>S. epidermidis</i> , <i>S. aureus</i> , <i>L. monocytogenes</i> , <i>B. subtilis</i> , <i>C. perfringens</i> , <i>C. albicans</i> , <i>A. fumigatus</i> , <i>C. tropicalis</i> , <i>F. verticillioides</i> | ROS, disruption of cell membrane, photothermal | [220,265,268] |
| | Nanofibers | <i>E. coli</i> , <i>S. aureus</i> | ROS | [264] |
| | Nanocomposites | <i>S. aureus</i> | ROS | [267] |
| Ag | MOFs | <i>E. coli</i> , <i>P. aeruginosa</i> , <i>K. pneumoniae</i> , <i>S. aureus</i> , <i>S. enteritidis</i> , <i>S. lutea</i> , <i>B. cereus</i> , <i>C. albicans</i> | ROS, photocatalytic | [131,135,144] |
| | Nanotubes | <i>E. coli</i> , <i>S. aureus</i> | Unknown, possibly ROS | [251] |
| | Nanocomposites | <i>E. coli</i> , <i>S. aureus</i> , <i>B. anthracoides</i> | ROS | [245,248,267,270,272] |
| | Nanoparticles | <i>L. monocytogenes</i> , <i>E. coli</i> , <i>P. aeruginosa</i> , <i>S. enterica</i> , <i>Streptococcus</i> , <i>B. thuringiensis</i> , <i>S. aureus</i> , <i>C. violaceum</i> , <i>C. albicans</i> | ROS, inhibition of quorum sensing | [219,279,291] |
| | MOFs | <i>E. coli</i> , <i>S. aureus</i> | Ultrasound-induced ROS generation | [149] |
| Au | Nanocomposites | <i>P. aeruginosa</i> , <i>S. aureus</i> , <i>C. albicans</i> , <i>A. terreus</i> , <i>A. niger</i> , <i>A. fumigatus</i> | Disruption of microbial membrane, ROS | [252] |
| | Nanoparticles | <i>E. coli</i> , <i>P. aeruginosa</i> , <i>S. enterica</i> , <i>Streptococcus</i> , <i>B. thuringiensis</i> , <i>S. aureus</i> , <i>C. violaceum</i> | Inhibition of quorum sensing, ROS | [279] |
| | Nanocomposites | <i>E. coli</i> , <i>S. aureus</i> | Unknown | [245] |
| W | Nanocomposites | <i>E. coli</i> , <i>S. aureus</i> | Unknown | [245] |
| Zn | MOFs | <i>E. coli</i> , <i>S. aureus</i> , <i>P. aeruginosa</i> , <i>K. pneumoniae</i> , <i>C. albicans</i> , <i>A. niger</i> , | Photocatalytic, photothermal, ROS, drug delivery | [128,133,134,137,142] |

(continued on next page)

Table 2 (continued)

| Metal | Molecular Structure | Microorganisms | Mechanism of Action | Reference |
|-----------|-----------------------------|--|--|------------------------|
| | Nanotubes | <i>E. coli</i> , <i>S. aureus</i> | Unknown, possibly ROS | [251] |
| | Micromotor Nanoparticles | <i>H. pylori</i> <i>E. coli</i> , <i>K. pneumoniae</i> , <i>E. faecalis</i> , <i>S. aureus</i> , <i>P. chrysogenum</i> , <i>A. brasiliensis</i> , <i>Alternaria</i> , <i>X. oryzae</i> | Motor ROS | [274] [250,271,285] |
| | Nanocomposites | <i>E. coli</i> , <i>S. aureus</i> , <i>B. anthracoides</i> | ROS | [245,248] |
| Al | MOFs | <i>E. hirae</i> , <i>S. aureus</i> , <i>K. pneumoniae</i> | Unknown | [112,134] |
| Ga | MOFs | <i>E. coli</i> , <i>P. aeruginosa</i> , <i>S. aureus</i> | Photocatalytic | [113–115] |
| | Micromotor Nanoparticles | <i>H. pylori</i> <i>E. coli</i> , <i>P. aeruginosa</i> , <i>S. aureus</i> | Competition with Fe ³⁺ Unknown, mechanical damage to membranes | [274] [273,276,277] |
| Sn | Nanoparticles | <i>E. coli</i> , <i>B. subtilis</i> | Unknown, possibly interactions with bacterial proteins | [280] |
| Y | Nanoparticles | <i>E. coli</i> , <i>B. subtilis</i> | ROS | [266] |
| Zr | MOFs | <i>E. coli</i> , <i>P. aeruginosa</i> , <i>K. pneumoniae</i> , <i>S. aureus</i> , <i>S. enteritidis</i> , <i>S. lutea</i> , <i>B. cereus</i> , <i>C. albicans</i> | Drug delivery | [127,129,131] |
| | Nanoparticles | <i>E. coli</i> , <i>E. faecalis</i> | ROS | [249] |
| La | Nanoparticles | <i>E. coli</i> , <i>K. pneumoniae</i> , <i>E. faecalis</i> , <i>S. aureus</i> , <i>P. chrysogenum</i> , <i>A. brasiliensis</i> | Unknown, possibly ROS | [250] |
| Ce | MOFs | <i>E. coli</i> , <i>S. aureus</i> | Ultrasound-induced ROS | [149] |
| Metalloid | Molecular Structure | Microorganisms | Mechanism of Action | Reference |
| B | Nanosheets | <i>E. coli</i> , <i>P. aeruginosa</i> , <i>S. aureus</i> , <i>C. albicans</i> , <i>A. brasiliensis</i> | Mechanical damage to membranes, possibly ROS | [286,287,290] |
| | Nanocomposites | <i>E. coli</i> , <i>S. aureus</i> | Unknown | [288] |
| | Nanoparticles | <i>P. aeruginosa</i> , <i>E. coli</i> , <i>K. pneumoniae</i> , <i>S. enterica</i> , <i>P. mirabilis</i> , <i>E. faecalis</i> , <i>B. cereus</i> , <i>S. aureus</i> , <i>S. agalactiae</i> , <i>C. albicans</i> | Drug delivery, unknown | [291,292] |
| Si | Nanobrushes | <i>E. coli</i> , <i>P. aeruginosa</i> , <i>S. aureus</i> | Unknown | [296] |

(continued on next page)

Table 2 (continued)

| Metal | Molecular Structure | Microorganisms | Mechanism of Action | Reference |
|-------|---------------------|---|--------------------------------|-----------|
| | Nanoparticles | <i>E. coli</i> , <i>L. monocytogenes</i> <i>B. subtilis</i> , <i>C. perfringens</i> , <i>C. tropicalis</i> , <i>F. verticillioides</i> , <i>G. graminis</i> | Drug delivery | [268,297] |
| Ge | Nanoparticles | <i>E. coli</i> , <i>S. aureus</i> , <i>C. albicans</i> | Unknown | [300] |
| Te | Nanorods | <i>E. coli</i> | Mechanical damage to membranes | [302] |
| Bi | MOFs | <i>E. coli</i> , <i>S. aureus</i> , <i>S. haemolyticus</i> | Photocatalytic | [139,144] |

Porta *et al.* reported on the development of copper nanoparticles capped with aminosilane groups (APTMS) referred to as Cu-APTMS NPs [268]. These nanoparticles were synthesized using a chemical reduction method and shown to be stable colloidal suspensions for up to four months in ethylene glycol. The Cu-APTMS NPs were characterized using techniques like UV-Vis spectroscopy, TEM, XRD, and FTIR. These analyses confirmed the nanoparticles were spherical, monocrystalline metallic copper with a size of ~25 nm and had surface functionalization with siloxane groups. The antimicrobial activity of the Cu-APTMS NPs was evaluated against several bacteria, both Gram-positive (*Listeria monocytogenes*, *B. subtilis*, *S. aureus* and *Clostridium perfringens*) and Gram-negative (*P. aeruginosa*), bacterial spores, and fungi (*Candida tropicalis* and *Fusarium verticillioides*) and the particles showed potent broad microbicidal effects at low concentrations for all. The sporicidal effect of Cu-APTMS NPs was tested against spores of *B. subtilis* and *Clostridium perfringens* and showed a significantly stronger effect than either APTMS or cuprous oxide alone, as displayed in Fig. 39. Mechanistic studies indicated the antimicrobial effect involves DNA degradation, which is known to be a consequence of ROS produced by Cu. The nanoscale copper was found to be more effective than cuprous oxide nanoparticles. The authors conclude that the developed aminosilane-functionalized copper nanoparticles have significant potential as stable and effective antimicrobial agents against a wide range of microbes and could find applications in areas like biomedicine and functional coatings.

Iron oxide NPs (IONPs) with photothermal activity and peroxidase-like activity were used to treat infected wounds [269]. The photothermal effect can directly lead to heat stress in bacterial cells, resulting in DNA, RNA, and protein dysfunction that causes cell death. Meanwhile, the peroxidase-like activity converts hydrogen peroxide into superoxide radicals that cause oxidative stress. These effects are synergistic, as not only do both kill bacteria, but the increased heat from the photothermal effect enhances the catalytic production of superoxide radicals. *In vitro*, both *E. coli* and *S. aureus* treated with 1000 µg/mL IONPs and 808 nm NIR irradiation showed high bactericidal effects, with 100 % and 90.1 % cell death, respectively. This suggested that the effect may be greater for Gram-negative bacteria (such as *E. coli*). A summary of the photothermal/catalytic therapy experiment in mice is shown in Fig. 40. Not only did the IONPs with NIR irradiation clear the infection from the wounds, allowing the tissue to heal, but no change was observed for mouse body weight and no inflammatory response was observed in the organs of the mice after the experiment was concluded, demonstrating the biosafety of the IONPs treatment with NIR irradiation.

Vasil'kov *et al.* presented a novel approach to creating hybrid materials with antimicrobial properties by incorporating silver nanoparticles (Ag NPs) into a hyperbranched polyaminopropylalkoxysiloxane (HB-PAPES) polymer matrix [270]. The Ag NPs were synthesized using a method called metal vapor synthesis (MVS), which involves the condensation of metal and organic ligand vapor on the cooled walls of a reaction vessel under vacuum conditions. The nanoparticles were then in-

corporated into the HB-PAPES matrix on cotton to form the nanocomposites Ag NPs/HB-PAPES/cotton, as shown in Fig. 41. The nanocomposites were found to have an average size of 5.3 nm. One-third of the volume of the nanocomposites was then re-impregnated using organosol to improve the antimicrobial effect. Both the nanocomposites and the re-impregnated samples and exhibited antifungal activity against *A. niger*, as well as antibacterial activity against *B. subtilis* and *E. coli*. The authors suggested that the MVS method is a promising approach for synthesizing metal nanoparticles and that the resulting nanocomposites could have potential applications in medically relevant textiles or related fields.

A study by Walunj *et al.* focused on the synthesis of ZnO NPs using a method in which zinc acetate dihydrate precursor was refluxed in ethylene glycol without the presence of sodium acetate [271]. The refluxing and cooling rates were optimized to obtain the desired phase and unique morphology of polyol-mediated ZnO NPs. The capping agent tetra-butyl ammonium bromide (TBAB) was used along with the precursor to achieve the desired results. The results indicated that the nanoparticles were pure spheres with an average particle size of 18.09 nm. Additionally, annealing under heat enhanced the crystallites and promoted a monocrystalline state. These nanoparticles exhibit antibacterial activity against *E. coli* and antifungal activity against *Alternaria*.

AgNPs prepared from *E. diffusum* extract demonstrated good antibacterial activity against both Gram-positive (*Listeria monocytogenes*) and Gram-negative (*E. coli*) bacteria [219]. ED-AgNPs showed larger inhibition zones compared to controls, as can be seen in Fig. 42. ED-functionalized AgNPs were proposed to detect Hg²⁺ via a redox reaction mechanism between Hg²⁺ and AgNPs, which caused visible discoloration of the AgNP suspension for rapid sensing. Overall, the green synthesized ED-AgNPs provide a simple, eco-friendly platform for selective Hg²⁺ sensing and antibacterial applications, avoiding use of hazardous chemicals.

The development of a photo-reactive silver-containing supramolecular polymer called Ag-Cy-PPG (24) was described by Fesseha *et al.* [272]. The polymer was synthesized by combining a hydrophilic backbone, composed of oligomeric polypropylene glycol, with cytosine-silver-cytosine linkages. The polymer can self-assemble into spherical nanogels in water, and irradiation with UV light causes the nanogels to undergo photocrosslinking resulting in polymer 25, as shown in Fig. 43. These irradiated nanogels exhibit unique transition and photophysical properties and demonstrate strong antibacterial activity.

The Ag-Cy-PPG nanogels undergo structural changes in the bacterial microenvironment, leading to the release of silver ions and potent antibacterial effects. For a microplate Alamar Blue (Resazurin) assay (MABA) for both *S. aureus* and *E. coli*, the unirradiated nanogels showed low levels of antibacterial activity up to 200 µg/mL, while the irradiated nanogels showed no observed bacterial colonies at 50 µg/mL (Fig. 44a). Further, for *E. coli* grown on agar plates and treated with the irradiated nanogels, less than 10 CFU/mL were left after treatment, in comparison to the ~10⁷ CFU/mL of *E. coli* in the control or unirradiated

nanogel treatment groups (Fig. 44b and c). The Ag-Cy-PPG nanogels also showed pH-responsive characteristics and controlled release of silver ions that enhanced the antibacterial activity of the nanogels. This study highlighted the potential of this metallo-supramolecular system for effective antibacterial therapy and enhancing the therapeutic effectiveness of antibacterial treatments.

Ga₂(HPO₄)₃ NPs were synthesized using two methods: a coprecipitation method with PVP coating and a top-down sonication method with PEG (polyethylene glycol) coating [273]. Both PVP- and PEG-coated Ga₂(HPO₄)₃ NPs showed potent antibacterial activity against the Gram-negative bacterium *P. aeruginosa*, with minimum inhibitory concentrations (MICs) comparable to that of gallium nitrate, which is shown in Fig. 45 for PVP-coated NPs and Fig. 46 for PEG-coated NPs. However, the nanoparticles did not show antibacterial activity against the Gram-positive bacterium *S. aureus*, limiting their potential as broad-spectrum antimicrobial agents. Importantly, the Ga₂(HPO₄)₃ NPs did not show any Ga-resistance development in *P. aeruginosa* even after 30 passes, unlike gallium nitrate which rapidly develops resistance. This makes the nanoparticles better suited as antibacterial agents. The study suggested that Ga-based nanoparticles could help overcome the limitations of molecular gallium compounds while retaining their antimicrobial potency and avoiding rapid resistance development. The results support further development of Ga₂(HPO₄)₃ NPs as antibacterial agents against Gram-negative bacteria.

To increase the concentration of Ga³⁺ at the therapeutic site, Lin *et al.* developed a micromotor using gallium and zinc [274]. Ga³⁺ can compete with Fe³⁺ for binding to bacterial proteins, which inhibits metabolic processes in the bacterial cells. These micromotors were prepared through coating Zn microparticles with liquid metal gallium, which can then generate H₂ bubbles that propel the motors. The Ga-Zn galvanic effect enhances this reaction, increasing the force propelling the micromotors. The Ga-Zn micromotors were then tested against *Helicobacter pylori*, a well known gastroenteric bacterium implicated in gastric cancers, and showed better antibacterial activity than Ga particles or gallium citrate (Fig. 47). These effects were present whether the motors were static or not.

In addition to the antimicrobial activity of Ga³⁺, nanomaterials containing liquid metal nanoparticles of Ga (Ga LMs) have also been studied for their biomedical applications [275]. For example, GLM-Fe (liquid metal gallium-iron) nanomaterials are magnetoresponsive and could be moved by a rotating magnetic field to mechanically damage biofilms of *S. aureus* and *P. aeruginosa*, as well as the individual cell walls, as shown in Fig. 48 [276].

Another example of the physical antimicrobial mechanism of gallium was described by Cheeseman *et al.*, who prepared nanomaterials of gallium liquid metal with encapsulated iron droplets to yield GLM-Fe nanomaterials [277]. An advantage to these nanomaterials was that they could also target multispecies biofilms composed of different bacteria, bypassing biological resistance to chemical antimicrobial agents. For example, the antibacterial effects caused by treatment with the GLM-Fe nanomaterials are shown in Fig. 49 and demonstrate a significant change in cell death in biofilms of *S. aureus* and *P. aeruginosa*, *E. coli* and *P. aeruginosa*, *S. aureus* and *B. cereus*, and biofilms composed of all three bacterial species. These results show the versatility of this magnetophysical approach.

Pure nickel nanoparticles have also been investigated for their inhibitory effects against biofilms of *Staphylococcus epidermidis* [278]. Biofilm growth was determined using quantification of crystal violet staining by optical density measurements at 550 nm. At concentrations above 0.05 mg/mL, *S. epidermidis* biofilms were significantly disrupted, as observed in Fig. 50.

CuO NPs biosynthesized from *Lantana camara* flowers were employed for the treatment of bacteria isolates from infected burns [236]. The main strains identified were Gram-positive *S. aureus* and *S. epidermidis* and Gram-negative *P. aeruginosa* and *Acinetobacter baumannii*. The

CuO NPs were more effective against the Gram-positive bacteria than the Gram-negative species, with MIC values of 125 µg/mL for *S. aureus*, 250 µg/ml for *A. baumannii* and 1000 µg/ml for *P. aeruginosa*. The mechanism was believed to be due to ROS generation or disruption of the microbial membrane. These nanoparticles have potential in therapeutic formulations, such as antimicrobial cream, and would be cost-effective to produce, due to the simple preparation and low cost of cultivating *Lantana camara*.

Ghaffarlou *et al.* aimed to synthesize silver and gold nanoparticles stabilized with pullulan (27) and evaluate their potential as inhibitory agents against quorum sensing in bacteria [279]. The synthesis of pullulan-decorated silver and gold nanoparticles was achieved using a simple and environmentally friendly method using Au(III) chloride trihydrate and silver nitrate, respectively, with pullulan (see Fig. 51). The SEM images revealed highly oriented microforms of pullulan, which were attributed to the supramolecular self-assembling behavior of pullulan chains. The antimicrobial and quorum sensing inhibition activities of the pullulan-decorated nanoparticles were tested against six pathogenic bacteria (*E. coli*, *Salmonella enterica* typhimurium, *P. aeruginosa*, *Streptococcus*, *Bacillus thuringiensis*, and *S. aureus*) and a reporter biomonitor strain (*Chromobacterium violaceum*). It was observed that the pullulan decorated with nanoparticles, particularly the silver-modified ones, exhibited improved performance compared to pristine pullulan. The cell proliferation was evaluated using an MTT assay, and the nanoparticle-decorated pullulan showed potential as an inhibitor of bacterial signal molecules. The study highlighted the promising performance of silver nanoparticles decorated with pullulan, which outperformed the commercial antibiotic gentamicin, as seen in Fig. 52a. Fig. 52b also showed the increase in the inhibitory effect the Ag pullulan nanoparticles had on quorum sensing when compared with pullulan alone or the reference gentamicin. This suggested that the pullulan-decorated nanoparticles could be a potential therapeutic approach to overcome bacterial resistance to conventional antibiotics. Overall, the research demonstrates a green and facile method for synthesizing pullulan-stabilized silver and gold nanoparticles and highlights their potential as antimicrobial agents and inhibitors of quorum sensing in bacteria.

Antibacterial tin (IV) oxide nanoparticles were synthesized from two species of marine algae, *Padina gymnospora* and *Turbinaria ornata* [280]. The largest zones of inhibition were observed for Gram-negative *E. coli* at 75 µg/mL and Gram-positive *B. subtilis* at 100 µg/mL. The interactions between the SnO₂ nanoparticles and penicillin-binding proteins (PBPs) necessary for bacterial growth were analyzed by molecular docking experiments and the SnO₂ nanoparticles showed strong binding interactions with PBP1a and PBP1b of *E. coli* and PBP2d and PBP4 of *Bacillus subtilis*. This suggested that the PBPs may be involved in the antibacterial mechanism of the tin nanoparticles.

3.3.3. Phytomedicine

Metal-containing nanomaterials have been studied for their applications in agriculture [281,282]. Metal oxides have especially been studied in phytomedicine (plant medicine) to inhibit growth of plant pathogens against key crops to improve their growth and crop yields [283]. A balance is required to have effective antimicrobial activity without being toxic to the plants themselves. A few examples of metallic nanoparticles with antimicrobial activity against plant pathogens are given below.

Nanoparticles of nickel oxide were prepared for antibacterial activity against the Gram-negative rice pathogen *Xanthomonas oryzae* pv. *oryzae* [284]. Biological synthesis of the nanoparticles was achieved using an aqueous extract from stigmas of *Crocus sativus* L (saffron) and bulk NiO. The NiO nanoparticles generated ROS in *X. oryzae* cells, with a significant difference in ROS levels between a negative control group and cells given 200 µg/mL nickel oxide nanoparticles. The same concentration of nanoparticles sprayed onto rice plants also improved fo-

liage growth, whether healthy or infected with *X. oryzae* (Fig. 53a), as well as root growth (Fig. 53b). The diseased leaf area also decreased for the infected plants, going from 74 % in untreated plants to only 22 % in those treated with the nanoparticles. Levels of ROS were also measured using fluorescent 2,7-dichlorofluorescein diacetate and were shown to be increased in cells treated with Ni compared to negative control cells or cells treated with the antioxidant rotenone. It was therefore concluded that the antibacterial activity likely involved ROS.

Ogunyemi *et al.* used rhizophytic bacteria *Paenibacillus polymyxa* extracts for production of ZnO, MnO₂ and MgO nanoparticles to target *X. oryzae* responsible for leaf blight in rice [285]. As can be observed in Fig. 54a, although inhibition zone diameters for *X. oryzae* (Xoo) were concentration-dependent for the bulk metal oxides and the metal oxide nanoparticles, the nanoparticles improved the inhibition at all three concentrations. The largest inhibition zones were observed at the highest concentration of 16 µg/mL and were 17, 13, and 13 mm for ZnO, MnO₂ and MgO nanoparticles, respectively. As would be expected, the inverse of this effect was shown for the optical density at 600 nm (Fig. 54b). Similarly, biofilm production by the bacteria decreased by 74.5, 74.4, and 80.2 % of the untreated control for ZnO, MnO₂ and MgO nanoparticles, respectively. These findings show the potential use of metal oxide nanoparticles in treatment of rice leaf blight.

3.4. Antibacterial and antifungal activities of metalloidal nanoparticles and composites

Hao *et al.* designed boron nitride nanosheets (BNNS) with ionic liquid and ammonium dimolybdate (ADM) ions [286]. The nanosheets (BNNS-IL-ADM) were three to four layers thick, with intercalated Mo groups that were slowly released, which allowed for longer antibacterial activity. The antibacterial activity of the nanosheets was improved by synergistic effects with boron nitride. Boron nitride nanosheets have also shown mechanical antibacterial activity by physical damage caused by their sharp edges, which did not result in the development of antimicrobial resistance [287]. As can be observed in Fig. 55, the ADM entered the cells via three routes: adhesion to the bacterial cell wall through hydrophobic, electrostatic and van der Waals interactions, the nanosheets removing lipids from the cell wall to increase its permeability, and nanochannels within the nanosheets that protect ADM and allow its release into the cytoplasm [286]. Thanks to these synergistic effects, the nanosheets exhibited a 92 % reduction in MIC needed for either Gram-negative *E. coli* or Gram-positive *S. aureus*, showing a broad range of bacteria could be targeted while maintaining high human cell viability (>80 %) even at the highest concentration tested (750 µg/mL).

Beyli *et al.* prepared boron oxide (B₂O₃)/poly(acrylic acid) (PAA) nanocomposites (29) as shown in Scheme 2 and investigated their thermal stability and antibacterial activity against *S. aureus* and *E. coli* [288]. The nanocomposites were prepared by a solution intercalation method, where B₂O₃ (27) was dispersed into a PAA (28) solution in xylene. The thermal stability of the polymers increased when B₂O₃ was added, in part due to the change in the decomposition of PAA. The B₂O₃/PAA nanocomposites exhibited greater antimicrobial activity against *E. coli* and *S. aureus* compared to pure PAA, with the antimicrobial properties increasing with higher B₂O₃ content.

Borophene is a two-dimensional nanostructure composed of single-atom-thick layers of boron that resembles its carbon analogue graphene, but is lighter and possesses a variety of different types of bonding [289]. β-borophene nanosheets have demonstrated antibacterial activity against *S. aureus*, *P. aeruginosa* and *E. coli*, as well as antifungal activity against *C. albicans* and *Aspergillus brasiliensis* [290]. Zones of inhibition were as follows: 18.0 mm for *S. aureus*, 19.5 mm for *P. aeruginosa*, 25.3 mm for *E. coli*, 23.4 mm for *C. albicans* and 22.8 mm for *A. brasiliensis*. The authors concluded that borophene had potential for

biomedical applications given its strong antimicrobial properties, in addition to its reported high biocompatibility.

El-Batal *et al.* prepared silver boron nanoparticles (AgB NPs) with incorporated PVP (32) via gamma ray-induced reaction of 30 with PVP (31), as seen in Scheme 3 [291]. The antimicrobial and antibiofilm activities of these AgB NPs were then assayed against three species of microbes responsible for urinary tract infections (UTIs). The AgB NPs exhibited strong antimicrobial activity with the largest zone of inhibition against *C. albicans* (20 mm), followed by *E. coli* (18 mm) and *S. aureus* (16 mm), as well as excellent antibiofilm activity, inhibiting biofilm formation by 87 %, 85.3 %, and 69.4 % against *S. aureus*, *E. coli*, and *C. albicans*, respectively.

Boron nitride and chitosan-coated boron nitride (BN) nanoparticles were evaluated against a variety of Gram-positive (*B. cereus*, *S. aureus*, *E. faecalis*, *Streptococcus agalactiae*, *Proteus mirabilis*) and Gram-negative (*E. coli*, *K. pneumoniae*, *P. aeruginosa*, *P. mirabilis*, and *S. enterica typhimurium*) bacterial strains [292]. Chitosan coating improved antibacterial activity by changing the electrostatic surface of the nanoparticles to be more positive. The negative zeta potential of BN NPs that was observed was not present in the chitosan-coated NPs, which showed positive charge. The increased activity thanks to the chitosan coating may allow for potential therapeutic use of the BN NPs, as the required dose would be lower, increasing the biocompatibility of this treatment.

Silicon-containing materials and nanocomposites have been investigated as scaffolds for antimicrobial agents [293–295]. Jiang *et al.* prepared nanoparticle-pinned polymer brushes (NPPBs) composed of silica nanospheres covalently bonded to hydrophilic polymers [296]. The polymer brushes are against non-toxic mammalian cells but exhibit antibacterial activity against *E. coli*, *P. aeruginosa* and *S. aureus*. Small nanoparticles were shown to possess antibacterial activity, which decreased as the size increased. The authors determined that for a silicon nanoparticle diameter < 50 nm, the NPPBs self-organize into a two-dimensional columnar phase, which can be used to form a membrane pore. This may explain why the 50 nm diameter was a threshold above which the antibacterial activity began to rapidly drop off. The mechanism of this activity is still unknown but warrants further study.

Sattary *et al.* used mesoporous silica to nanoencapsulate two types of essential oils, lemongrass oil and clove oil, to improve their antifungal activity against *Gaeumannomyces graminis* var. *tritici* (Ggt), the pathogen responsible for take-all disease in wheat [297]. Take-all disease is the most damaging root disease found in wheat worldwide and is therefore a global target for research [298]. The nanoparticles had 80 % encapsulation efficiency for the oils and resulted in up to three times the antifungal activity against Ggt *in vitro*. *In vivo*, clove oil showed only 49 % and lemongrass oil showed only 57.44 % inhibition of Ggt growth on wheat seeds, while the nanoparticles with clove oil showed 71.27 % and with lemongrass oil showed 74.44 % inhibition. These findings were comparable to the 70 % inhibition exhibited by the commercial fungicide Mancozeb against Ggt. Further encapsulation of the nanoparticles with sodium alginate further improved these results to 84 % for nanoparticles containing either clove or lemongrass oil.

Germanium has also been shown to be active for antimicrobial activity, including in the form of nonionic surfactants [299]. With respect to nanoparticles, germanium has been doped as an ion into nanoparticles of hydroxyapatite (HAp), a calcium phosphate complex [300]. The antibacterial effect of HAp against MRSA was slightly decreased by the Ge doping, but still significantly lower than the untreated cells. Although the Ge-HAp showed no improvement for antibacterial activity against *E. coli*, it should be noted that HAp also showed no significant activity overall, suggesting that HAp is ineffective against *E. coli* or Gram-negative bacteria generally. On the other hand, the antifungal effect against *C. albicans* was significantly improved by doping with Ge⁴⁺ to such a degree that it eliminated the fungal growth. In addition to their antimicrobial activities, Ge-HAp also showed low cytotoxicity

against dental pulp stem cells. Further, Ge-HAp was demonstrated to induce mRNA expression for osteogenic differentiation in these stem cells, which is the process by which stem cells mature into bone tissue cells. Therefore, these nanoparticles showed excellent potential for their use in regenerative medicine, as they can exhibit simultaneous tissue regeneration and antimicrobial effects, as shown in Fig. 56.

Tellurium nanorods derived from tellurite (TeO_3^{2-}) have been prepared and examined for their antibacterial and antifungal activities [301]. In 2022, Tang *et al.* prepared biogenic tellurium nanorods (BioTe) from tellurite using the tellurite-resistant bacterial species *Acinetobacter pittii* and examined their antibacterial activity against *E. coli* [302]. The antibacterial activity of BioTe in *E. coli* was superior to spherical Te nanoparticles, with an MIC 700 times lower than that of the Te NPs. The antibacterial mechanism was determined to be mechanical damage to the cell membrane. The leakage of β -galactosidase in a strain of *E. coli* that overexpresses the protein was used as a measure for cytoplasmic leakage. There was a 465 % increase in leakage of β -galactosidase compared to untreated cells, which is a dramatic improvement over tellurite treatment. The authors suggested that BioTe would be attracted electrostatically to the bacterial cell membranes, followed by physically damaging it with the sharp ends of the nanorods. While ROS were also produced, they were within levels that the *E. coli* could degrade under normal growth, demonstrating that the main bactericidal mechanism was the mechanical disruption of membranes.

4. Conclusion and future directions

This review has highlighted the rapidly growing field of metal- and metalloid-containing materials for antimicrobial and antifungal applications. From the design and synthesis of metal-organic frameworks (MOFs) to the preparation and characterization of metallic and metalloid nanoparticles and nanocomposites, significant advances have been made in overcoming the threat of drug-resistant pathogens. MOFs can be designed to encapsulate antimicrobial agents or release metallic ions that have antimicrobial activity. These materials are tunable and can be designed for a variety of applications. Furthermore, metallic and metalloid nanoparticles are gaining interest due to their high surface-to-volume ratio and unique physicochemical properties. They have been demonstrated to be potent against a wide variety of bacterial and fungal strains, as well as being highly effective in preventing the formation of biofilms. This review has also surveyed the use of green synthesis techniques for nanoparticles, which have advantages such as using readily available resources and being environmentally friendly. These materials hold promise for applications in industrial settings, such as wastewater remediation and fabrication of antimicrobial textiles, and in therapeutic settings to treat infections, particularly those caused by multidrug-resistant strains. Further investigation into their safety, efficacy, and mechanisms of action is required for clinical use. While the global threat of drug resistance has accelerated the study of novel antimicrobial agents, it has been shown that some of these nanomaterials, particularly metal nanoparticles and nanocomposites, can still contribute to the evolution of antimicrobial resistance. Further research is necessary to develop nanomaterials that would not promote the evolution of drug resistance. For example, antibacterial nanomaterials with mechanisms such as mechanical damage to membranes or photothermal activity can prevent evolution of drug resistance, but require further research to use effectively. Several challenges remain in understanding the exact mechanisms of action and the risk of potential toxicity for metal- and metalloid-containing nanomaterials. Nevertheless, these nanomaterials have proven to be promising antimicrobial agents for clinical translation, and design of new nanocomposites based on principles of nanoarchitectonics may further advance this field of research. A summary of the antibacterial activities of the MOFs and nanomaterials containing metals and metalloids described in this review is shown in Table 2. Based on the literature review and recent developments in this field, it is clear

that while a tremendous amount of work has been undertaken by many scientists searching for new and efficient antibacterial and antifungal agents, there is still more research to be done and many new materials to be discovered.

CRediT authorship contribution statement

Ahmad Abd-El-Aziz: Writing – review & editing, Writing – original draft. **Jian Li:** Writing – review & editing, Writing – original draft. **Moustafa M.G. Fouda:** Writing – review & editing, Writing – original draft. **Carmen M. Sharaby:** Writing – review & editing, Writing – original draft. **Xinyue Zhang:** Writing – review & editing, Writing – original draft. **Ning Ma:** Writing – review & editing, Writing – original draft. **Spiros N. Agathos:** Writing – review & editing, Writing – original draft. **Alaa S. Abd-El-Aziz:** Writing – review & editing, Writing – original draft.

Declaration of competing interest

The authors declare that they have no known competing financial interests or personal relationships that could have appeared to influence the work reported in this paper.

Data availability

No data was used for the research described in the article.

Acknowledgements

The authors would like to sincerely acknowledge Harbin Engineering University (HEU), the National Research Centre (NRC), and Al-Azhar University for their support.

References

- [1] World Health Organization (WHO), Antimicrobial resistance, (n.d.). <https://www.who.int/news-room/fact-sheets/detail/antimicrobial-resistance> (accessed 2024).
- [2] Antimicrobial resistance collaborators, global burden of bacterial antimicrobial resistance in 2019: a systematic analysis, *Lancet* 399 (2022) 629–655, [https://doi.org/10.1016/S0140-6736\(21\)02724-0](https://doi.org/10.1016/S0140-6736(21)02724-0).
- [3] B. Xianyu, H. Xu, Dynamic covalent bond-based materials: From construction to biomedical applications, *Supramol. Mater.* 3 (2024) 100070, <https://doi.org/10.1016/j.supmat.2024.100070>.
- [4] L.X. Yip, J. Wang, Y. Xue, K. Xing, C. Sevensan, K. Ariga, D.T. Leong, Cell-derived nanomaterials for biomedical applications, *Sci. Technol. Adv. Mater.* 25 (2024) 2315013, <https://doi.org/10.1080/14686996.2024.2315013>.
- [5] B. Xianyu, S. Pan, S. Gao, H. Xu, T. Li, Selenium-containing nanocomplexes achieve dual immune checkpoint blockade for NK cell reinvigoration, *Small* 20 (2024) 2306225, <https://doi.org/10.1002/smll.202306225>.
- [6] A.S. Abd-El-Aziz, A.M. Youssef, A. Abd-El-Aziz, Transition metal-containing dendrimers in biomedicine: current trends, *Royal Soc. Chem.* (2023), <https://doi.org/10.1039/9781837671441>.
- [7] A. Wang, M. Walden, R. Ettlinger, F. Kiessling, J.J. Gassensmith, T. Lammers, S. Wuttke, Q. Peña, Biomedical metal–organic framework materials: perspectives and challenges, *Adv. Funct. Mater.* (2023) 2308589, <https://doi.org/10.1002/adfm.202308589>.
- [8] Y. Dai, J. Guan, S. Zhang, S. Pan, B. Xianyu, Z. Ge, J. Si, C. He, H. Xu, Tellurium-containing polymers: recent developments and trends, *Prog. Polym. Sci.* 141 (2023) 101678, <https://doi.org/10.1016/j.progpolymsci.2023.101678>.
- [9] X. Shen, K. Ariga, Disease diagnosis with chemosensing, artificial intelligence, and prospective contributions of nanoarchitectonics, *Chemosensors* 11 (2023) 528, <https://doi.org/10.3390/chemosensors11100528>.
- [10] X. Jia, J. Chen, W. Lv, H. Li, K. Ariga, Engineering dynamic and interactive biomaterials using material nanoarchitectonics for modulation of cellular behaviors, *Cell Rep. Phys. Sci.* 4 (2023), <https://doi.org/10.1016/j.xcrp.2023.101251>.
- [11] M. Komiya, N. Shigi, K. Ariga, DNA-based nanoarchitectures as eminent vehicles for smart drug delivery systems, *Adv. Funct. Mater.* 32 (2022) 2200924, <https://doi.org/10.1002/adfm.202200924>.
- [12] D. Franco, G. Calabrese, S.P.P. Guglielmino, S. Conoci, Metal-based nanoparticles: antibacterial mechanisms and biomedical application, *Microorganisms* 10 (2022) 1778, <https://doi.org/10.3390/microorganisms10091778>.
- [13] E. Zhang, X. Zhao, J. Hu, R. Wang, S. Fu, G. Qin, Antibacterial metals and alloys

- for potential biomedical implants, *Bioact. Mater.* 6 (2021) 2569–2612, <https://doi.org/10.1016/j.bioactmat.2021.01.030>.
- [14] V. Karthick, D. Kumar, K. Ariga, C.M. Vineeth Kumar, V. Ganesh Kumar, K. Vasanth, T. Stalin Dhas, M. Ravi, J. Baalamurugan, Incorporation of 5-nitrosatin for tailored hydroxyapatite nanorods and its effect on cervical cancer cells: a nanoarchitectonics approach, *J. Inorg. Organomet. Polym.* 31 (2021) 1946–1953, <https://doi.org/10.1007/s10904-021-01891-9>.
- [15] A.S. Abd-El-Aziz, A.A. Abdelghani, A.K. Mishra, Optical and biological properties of metal-containing macromolecules, *J. Inorg. Organomet. Polym. Mater.* 30 (2020) 3–41, <https://doi.org/10.1007/s10904-019-01293-y>.
- [16] D.A. Dias, K.A. Kouremenos, D.J. Beale, D.L. Callahan, O.A.H. Jones, Metal and metalloid containing natural products and a brief overview of their applications in biology, biotechnology and biomedicine, *Biomaterials* 29 (2016) 1–13, <https://doi.org/10.1007/s10534-015-9892-2>.
- [17] A.S. Abd-El-Aziz, C.E.C. Jr, C.U.P. Jr, J.E. Sheats, M. Zeldin, *Macromolecules Containing Metal and Metal-Like Elements, Volume 3: Biomedical Applications*, John Wiley & Sons, 2004.
- [18] M. Niinomi, Recent metallic materials for biomedical applications, *Metall. Mater. Trans. A* 33 (2002) 477–486, <https://doi.org/10.1007/s11661-002-0109-2>.
- [19] K. Gold, B. Slay, M. Knackstedt, A.K. Gaharwar, Antimicrobial activity of metal and metal-oxide based nanoparticles, *Adv. Therap.* 1 (2018) 1700033, <https://doi.org/10.1002/adtp.201700033>.
- [20] W. Gao, L. Zhang, Nanomaterials arising amid antibiotic resistance, *Nat. Rev. Microbiol.* 19 (2021) 5–6, <https://doi.org/10.1038/s41579-020-00469-5>.
- [21] Y. Zhao, L. Chen, Y. Wang, X. Song, K. Li, X. Yan, L. Yu, Z. He, Nanomaterial-based strategies in antimicrobial applications: progress and perspectives, *Nano Res.* 14 (2021) 4417–4441, <https://doi.org/10.1007/s12274-021-3417-4>.
- [22] V. Alimardani, S. Abolmaali, S. Borandeh, Antifungal and antibacterial properties of graphene-based nanomaterials: a mini-review, *J. Nanostruct.* 9 (2019) 402–413, <https://doi.org/10.22052/JNS.2019.03.002>.
- [23] M. Xie, M. Gao, Y. Yun, M. Malmsten, V.M. Rotello, R. Zboril, O. Akhavan, A. Kraskouski, J. Amalraj, X. Cai, J. Lu, H. Zheng, R. Li, Antibacterial nanomaterials: mechanisms, impacts on antimicrobial resistance and design principles, *Angew. Chem. Int. Ed.* 62 (2023) e202217345, <https://doi.org/10.1002/anie.202217345>.
- [24] J.-L. Xu, Y.-X. Luo, S.-H. Yuan, L.-W. Li, N.-N. Liu, Antifungal nanomaterials: current progress and future directions, *Innov. Digit. Health Diagn. Biomark.* 1 (2020) 3–7, <https://doi.org/10.36401/IDDB-20-03>.
- [25] S.C. Warangkar, M.R. Deshpande, N.D. Totewad, A.A. Singh, S.C. Warangkar, M.R. Deshpande, N.D. Totewad, A.A. Singh, Antibacterial, antifungal and antiviral nanocomposites: recent advances and mechanisms of action, in: *bio-composites - recent advances*, IntechOpen (2022), <https://doi.org/10.5772/intechopen.108994>.
- [26] Y.P. Li, I.B. Fekih, E.C. Fru, A. Moraleda-Munoz, X. Li, B.P. Rosen, M. Yoshinaga, C. Rensing, Antimicrobial activity of metals and metalloids, *Annu. Rev. Micro.* 75 (2021) 175–197, <https://doi.org/10.1146/annurev-micro-032921-123231>.
- [27] K. Ariga, K. Minami, M. Ebara, J. Nakanishi, What are the emerging concepts and challenges in NANO? Nanoarchitectonics, hand-operating nanotechnology and mechanobiology, *Polym. J.* 48 (2016) 371–389, <https://doi.org/10.1038/pj.2016.8>.
- [28] D. Gupta, B.S. Varghese, M. Suresh, C. Panwar, T.K. Gupta, Nanoarchitectonics: functional nanomaterials and nanostructures—a review, *J. Nanopart. Res.* 24 (2022) 196, <https://doi.org/10.1007/s11051-022-05577-2>.
- [29] O. Azzaroni, K. Ariga (Eds.), *Concepts and design of materials nanoarchitectonics*, Concepts and design of materials nanoarchitectonics, Royal Soc. Chem. (2022), <https://doi.org/10.1039/9781788019613>.
- [30] K. Ariga, X. Jia, J. Song, J.P. Hill, D.T. Leong, Y. Jia, J. Li, Nanoarchitectonics beyond self-assembly: challenges to create bio-like hierarchic organization, *Angew. Chem. Int. Ed.* 59 (2020) 15424–15446, <https://doi.org/10.1002/anie.202000802>.
- [31] X. Shen, J. Song, K. Kawakami, K. Ariga, Molecule-to-Material-to-bio nanoarchitectonics with biomedical fullerene nanoparticles, *Materials* 15 (2022) 5404, <https://doi.org/10.3390/ma15155404>.
- [32] L. Huang, J. Yang, Y. Asakura, Q. Shuai, Y. Yamauchi, Nanoarchitectonics of hollow covalent organic frameworks: synthesis and applications, *ACS Nano* 17 (2023) 8918–8934, <https://doi.org/10.1021/acsnano.3c01758>.
- [33] Z. Wang, M. Gao, J. Peng, L. Miao, W. Chen, T. Ao, Nanoarchitectonics of heteroatom-doped hierarchical porous carbon derived from carboxymethyl cellulose carbon aerogel and metal-organic framework for capacitive deionization, *Int. J. Biol. Macromol.* 241 (2023) 124596, <https://doi.org/10.1016/j.ijbiomac.2023.124596>.
- [34] K. Ariga, Nanoarchitectonics revolution and evolution: from small science to big technology, *Small Sci.* 1 (2021) 2000032, <https://doi.org/10.1002/smssc.202000032>.
- [35] H. Cai, M. Li, X.-R. Lin, W. Chen, G.-H. Chen, X.-C. Huang, D. Li, Spatial, hysteretic, and adaptive host–guest chemistry in a metal–organic framework with open watson–crick sites, *Angew. Chem. Int. Ed.* 54 (2015) 10454–10459, <https://doi.org/10.1002/anie.201502045>.
- [36] F. Khan, M. Shariq, M. Asif, M.A. Siddiqui, P. Malan, F. Ahmad, Green nanotechnology: plant-mediated nanoparticle synthesis and application, *Nanomaterials* 12 (2022) 673, <https://doi.org/10.3390/nano12040673>.
- [37] V. Selvarajan, S. Obuobi, P.L.R. Ee, Silica nanoparticles—a versatile tool for the treatment of bacterial infections, *Front. Chem.* 8 (2020) 00602, <https://doi.org/10.3389/fchem.2020.00602>.
- [38] Y. Li, J. Tian, C. Yang, B.S. Hsiao, Nanocomposite film containing fibrous cellulose scaffold and Ag/TiO₂ nanoparticles and its antibacterial activity, *Polymers* 10 (2018) 1052, <https://doi.org/10.3390/polym10101052>.
- [39] N. Koralkar, S. Mehta, A. Upadhyay, G. Patel, K. Deshmukh, MOF-based nanoarchitectonics for lithium-ion batteries: a comprehensive review, *J. Inorg. Organomet. Polym. Mater.* 34 (2024) 903–929, <https://doi.org/10.1007/s10904-023-02898-0>.
- [40] A. Rajabizadeh, M. Alihosseini, H.I.M. Amin, H.A. Almarshhadani, F. Mousazadeh, M.A.L. Nobre, M.D. Soltani, S. Sharaki, A.T. Jalil, M.M. Kadhim, The recent advances of metal–organic frameworks in electric vehicle batteries, *J. Inorg. Organomet. Polym.* 33 (2023) 867–884, <https://doi.org/10.1007/s10904-022-02467-x>.
- [41] A.F. Sahayaraj, H.J. Prabu, J. Maniraj, M. Kannan, M. Bharathi, P. Diwahaar, J. Salamon, Metal–organic frameworks (MOFs): The next generation of materials for catalysis, gas storage, and separation, *J. Inorg. Organomet. Polym. Mater.* 33 (2023) 1757–1781, <https://doi.org/10.1007/s10904-023-02657-1>.
- [42] J.D. Bhaliya, V.R. Shah, G. Patel, K. Deshmukh, Recent advances of MOF-based nanoarchitectonics for chemiresistive gas sensors, *J. Inorg. Organomet. Polym. Mater.* 33 (2023) 1453–1494, <https://doi.org/10.1007/s10904-023-02597-w>.
- [43] V.F. Yusuf, N.I. Malek, S.K. Kailasa, Review on metal–organic framework classification, synthetic approaches, and influencing factors: applications in energy, drug delivery, and wastewater treatment, *ACS Omega* 7 (2022) 44507–44531, <https://doi.org/10.1021/acsomega.2c05310>.
- [44] S. Shao, L. Zhang, W. Liu, Y. Zhang, X. Shen, Y. Nie, W. Yang, H. Liu, S. Li, S. Li, Synthesis of hierarchical porous MOFs via ligand thermolysis for high-performance supercapacitor, *J. Inorg. Organomet. Polym. Mater.* 32 (2022) 4412–4421, <https://doi.org/10.1007/s10904-022-02427-5>.
- [45] M.Y. Zorainy, S. Kaliaguine, M. Gobara, S. Elbasuney, D.C. Boffito, Microwave-assisted synthesis of the flexible iron-based MIL-88B metal–organic framework for advanced energetic systems, *J. Inorg. Organomet. Polym. Mater.* 32 (2022) 2538–2556, <https://doi.org/10.1007/s10904-022-02353-6>.
- [46] A. Mariyam, M. Shahid, I. Mantasha, M.S. Khan, M.S. Ahmad, Tetrazole based porous metal organic framework (MOF): topological analysis and dye adsorption properties, *J. Inorg. Organomet. Polym. Mater.* 30 (2020) 1935–1943, <https://doi.org/10.1007/s10904-019-01334-6>.
- [47] R.F. Mendes, F. Figueira, J.P. Leite, L. Gales, F.A.A. Paz, Metal–organic frameworks: a future toolbox for biomedicine? *Chem. Soc. Rev.* 49 (2020) 9121–9153, <https://doi.org/10.1039/D0CS00883D>.
- [48] H. Cai, Y.-L. Huang, D. Li, Biological metal–organic frameworks: Structures, host–guest chemistry and bio-applications, *Coord. Chem. Rev.* 378 (2019) 207–221, <https://doi.org/10.1016/j.ccr.2017.12.003>.
- [49] H.M. Abd El Salam, H.N. Nassar, A.S.A. Khidir, T. Zaki, Antimicrobial activities of green synthesized Ag nanoparticles @ Ni-MOF nanosheets, *J. Inorg. Organomet. Polym. Mater.* 28 (2018) 2791–2798, <https://doi.org/10.1007/s10904-018-0950-4>.
- [50] S. Dang, Q.-L. Zhu, Q. Xu, Nanomaterials derived from metal–organic frameworks, *Nat. Rev. Mater.* 3 (2017) 1–14, <https://doi.org/10.1038/natrevmats.2017.75>.
- [51] W. Zhou, L. Wang, F. Li, W. Zhang, W. Huang, F. Huo, H. Xu, Selenium-containing polymer@metal-organic frameworks nanocomposites as an efficient multiresponsive drug delivery system, *Adv. Funct. Mater.* 27 (2017) 1605465, <https://doi.org/10.1002/adfm.201605465>.
- [52] N.L. Torad, M. Hu, S. Ishihara, H. Sukegawa, A.A. Belik, M. Imura, K. Ariga, Y. Sakka, Y. Yamauchi, Direct synthesis of MOF-derived nanoporous carbon with magnetic Co nanoparticles toward efficient water treatment, *Small* 10 (2014) 2096–2107, <https://doi.org/10.1002/smll.201302910>.
- [53] W. Chaikittisilp, K. Ariga, Y. Yamauchi, A new family of carbon materials: synthesis of MOF-derived nanoporous carbons and their promising applications, *J. Mater. Chem. A* 1 (2012) 14–19, <https://doi.org/10.1039/C2TA00278G>.
- [54] A.C. McKinlay, R.E. Morris, P. Horcajada, G. Férey, R. Gref, P. Couvreur, C. Serre, BioMOFs: metal–organic frameworks for biological and medical applications, *Angew. Chem. Int. Ed.* 49 (2010) 6260–6266, <https://doi.org/10.1002/anie.201000048>.
- [55] H.-C. Zhou, J.R. Long, O.M. Yaghi, Introduction to metal–organic frameworks, *Chem. Rev.* 112 (2012) 673–674, <https://doi.org/10.1021/cr300014x>.
- [56] J. Yang, Y.-W. Yang, Metal–organic frameworks for biomedical applications, *Small* 16 (2020) 1906846, <https://doi.org/10.1002/smll.201906846>.
- [57] H.-S. Wang, Y.-H. Wang, Y. Ding, Development of biological metal–organic frameworks designed for biomedical applications: from bio-sensing/bio-imaging to disease treatment, *Nanoscale Adv.* 2 (2020) 3788–3797, <https://doi.org/10.1039/D0NA00557F>.
- [58] L. Jiao, J.Y.R. Seow, W.S. Skinner, Z.U. Wang, H.-L. Jiang, Metal–organic frameworks: structures and functional applications, *Mater. Today* 27 (2019) 43–68, <https://doi.org/10.1016/j.mattod.2018.10.038>.
- [59] X. Zhang, X. Tian, N. Wu, S. Zhao, Y. Qin, F. Pan, S. Yue, X. Ma, J. Qiao, W. Xu, W. Liu, J. Liu, M. Zhao, K. (Ken) Ostrikov, Z. Zeng, Metal-organic frameworks with fine-tuned interlayer spacing for microwave absorption, *Sci. Adv.* (2024), <https://doi.org/10.1126/sciadv.adl6498>.
- [60] C.Y. Wong, W.Y. Wong, W. Sudarsono, K.S. Loh, K.L. Lim, W. Bo, Tuning the functionality of metal–organic frameworks (MOFs) for fuel cells and hydrogen storage applications, *J. Mater. Sci.* 58 (2023) 8637–8677, <https://doi.org/10.1007/s10853-023-08552-x>.
- [61] M. Ahmadi, M. Ebrahimi, M.-A. Shahbazi, R. Keçili, F. Ghorbani-Bidkorbeh, Microporous metal–organic frameworks: synthesis and applications, *J. Ind. Eng. Chem.* 115 (2022) 1–11, <https://doi.org/10.1016/j.jiec.2022.07.047>.
- [62] Q. Xiong, Y. Chen, D. Yang, K. Wang, Y. Wang, J. Yang, L. Li, J. Li, Constructing strategies for hierarchically porous MOFs with different pore sizes and

- applications in adsorption and catalysis, *Mater. Chem. Front.* 6 (2022) 2944–2967, <https://doi.org/10.1039/D2QM00557C>.
- [63] L. Liu, D. Zhang, Y. Zhu, Y. Han, Bulk and local structures of metal–organic frameworks unravelled by high-resolution electron microscopy, *Commun. Chem.* 3 (2020) 1–14, <https://doi.org/10.1038/s42004-020-00361-6>.
- [64] N. Stock, S. Biswas, Synthesis of metal–organic frameworks (MOFs): routes to various MOF topologies, morphologies, and composites, *Chem. Rev.* 112 (2012) 933–969, <https://doi.org/10.1021/cr200304e>.
- [65] D.Y. Heo, H.H. Do, S.H. Ahn, S.Y. Kim, Metal–organic framework materials for perovskite solar cells, *Polymers* 12 (2020), <https://doi.org/10.3390/polym12092061>.
- [66] D. Ma, X. Huang, Y. Zhang, L. Wang, B. Wang, Metal–organic frameworks: synthetic methods for industrial production, *Nano Res.* 16 (2023) 7906–7925, <https://doi.org/10.1007/s12274-023-5441-4>.
- [67] M. Rubio-Martinez, C. Avci-Camur, A.W. Thornton, I. Imaz, D. Maspocho, M.R. Hill, New synthetic routes towards MOF production at scale, *Chem. Soc. Rev.* 46 (2017) 3453–3480, <https://doi.org/10.1039/C7CS00109F>.
- [68] R. Udaya Rajesh, T. Mathew, H. Kumar, A. Singhal, L. Thomas, Metal–organic frameworks: recent advances in synthesis strategies and applications, *Inorg. Chem. Commun.* 162 (2024) 112223, <https://doi.org/10.1016/j.inoche.2024.112223>.
- [69] N.A. Khan, S.H. Jung, Synthesis of metal–organic frameworks (MOFs) with microwave or ultrasound: rapid reaction, phase-selectivity, and size reduction, *Coord. Chem. Rev.* 285 (2015) 11–23, <https://doi.org/10.1016/j.ccr.2014.10.008>.
- [70] A. Mansar, H. Serier-Brault, Microwave-assisted synthesis to prepare metal–organic framework for luminescence thermometry, *J. Solid State Chem.* 312 (2022) 123183, <https://doi.org/10.1016/j.jssc.2022.123183>.
- [71] Z. Ni, R.I. Masel, Rapid production of metal–organic frameworks via microwave-assisted solvothermal synthesis, *J. Am. Chem. Soc.* 128 (2006) 12394–12395, <https://doi.org/10.1021/ja0635231>.
- [72] H. Wei, Y. Tian, Q. Chen, D. Estevez, P. Xu, H.-X. Peng, F. Qin, Microwave absorption performance of 2D iron–quinoid MOF, *Chem. Eng. J.* 405 (2021) 126637, <https://doi.org/10.1016/j.cej.2020.126637>.
- [73] R. Vakkil, S. Xu, N. Al-Janabi, P. Gorgojo, S.M. Holmes, X. Fan, Microwave-assisted synthesis of zirconium-based metal organic frameworks (MOFs): optimization and gas adsorption, *Micropor. Mesopor. Mater.* 260 (2018) 45–53, <https://doi.org/10.1016/j.micromeso.2017.10.028>.
- [74] B.-X. Jiang, H. Wang, Y.-T. Zhang, S.-B. Li, Microwave-assisted synthesis of Zr-based metal–organic frameworks and metal–organic cages, *Polyhedron* 243 (2023) 116569, <https://doi.org/10.1016/j.poly.2023.116569>.
- [75] H. Wen, B. Lei, W. Zhang, Preparation and investigation of high-efficiency ZIF-67/MoS₂-based microwave absorbers, *Mater. Res. Bull.* 172 (2024) 112671, <https://doi.org/10.1016/j.materresbull.2024.112671>.
- [76] C. Vaitis, G. Sourkouni, C. Argiris, Metal organic frameworks (MOFs) and ultrasound: a review, *Ultrason. Sonochem.* 52 (2019) 106–119, <https://doi.org/10.1016/j.ultrsonch.2018.11.004>.
- [77] F.Lo Presti, A.L. Pellegrino, N. Consoli, G. Malandrino, Green ultrasound-assisted synthesis of rare-earth-based MOFs, *Molecules* 28 (2023) 6088, <https://doi.org/10.3390/molecules28166088>.
- [78] A. Taghipour, A. Rahimpour, M. Rastgar, M. Sadrzadeh, Ultrasonically synthesized MOFs for modification of polymeric membranes: a critical review, *Ultrason. Sonochem.* 90 (2022) 106202, <https://doi.org/10.1016/j.ultrsonch.2022.106202>.
- [79] U. Müller, H. Pütter, M. Hesse, H. Wessel, M. Schubert, J. Huff, M. Guzmán, Method for electrochemical production of a crystalline porous metal organic skeleton material, 2005. <https://patentscope.wipo.int/search/en/detail.jsf?docId=WO2005049892> (accessed May 6, 2024).
- [80] J.L. Hauser, M. Tso, K. Fitchmun, S.R.J. Oliver, Anodic electrodeposition of several metal organic framework thin films on indium tin oxide glass, *Crys. Growth Des.* 19 (2019) 2358–2365, <https://doi.org/10.1021/acs.cgd.9b00054>.
- [81] A.M. Antonio, J. Rosenthal, E.D. Bloch, Electrochemically mediated synthesis of titanium(III)-based metal–organic frameworks, *J. Am. Chem. Soc.* 141 (2019) 11383–11387, <https://doi.org/10.1021/jacs.9b05035>.
- [82] W. Wu, G.E. Decker, A.E. Weaver, A.I. Arnoff, E.D. Bloch, J. Rosenthal, Facile and rapid room-temperature electrosynthesis and controlled surface growth of Fe-MIL-101 and Fe-MIL-101-NH₂, *ACS Cent. Sci.* 7 (2021) 1427–1433, <https://doi.org/10.1021/acscentsci.1c00686>.
- [83] J. Zheng, M.B. Solomon, A. Rawal, Y. Chi, R. Yu, L. Liu, J. Tang, G. Mao, D.M. D' Alessandro, P.V. Kumar, M.A. Rahim, K. Kalantar-Zadeh, Passivation-free, liquid-metal-based electrosynthesis of aluminum metal–organic frameworks mediated by light metal activation, *ACS Nano* 17 (2023) 25532–25541, <https://doi.org/10.1021/acsnano.3c09472>.
- [84] M. Stodolka, J.Y. Choi, X. Fang, C. Lu, H.T.B. Pham, B. Check, J. Park, Electrosynthesis of a nickel-based conductive metal–organic framework with controlled morphology for enhanced capacitance, *ACS Mater. Lett.* 6 (2024) 49–55, <https://doi.org/10.1021/acsmaterialslett.3c01224>.
- [85] Y. Chen, S. Li, X. Pei, J. Zhou, X. Feng, S. Zhang, Y. Cheng, H. Li, R. Han, B. Wang, A solvent-free hot-pressing method for preparing metal–organic-framework coatings, *Angew. Chem. Int. Ed.* 55 (2016) 3419–3423, <https://doi.org/10.1002/anie.201511063>.
- [86] D. Turetsky, D.M. Alzate-Sánchez, M.C. Wasson, A. Yang, H. Noh, A. Atilgan, T. Islamoglu, O.K. Farha, W.R. Dichtel, Hot press synthesis of MOF/textile composites for nerve agent detoxification, *ACS Mater. Lett.* 4 (2022) 1511–1515, <https://doi.org/10.1021/acsmaterialslett.2c00258>.
- [87] Y.-J. Tang, Y. Chen, H.-J. Zhu, A.-M. Zhang, X.-L. Wang, L.-Z. Dong, S.-L. Li, Q. Xu, Y.-Q. Lan, Solid-phase hot-pressing synthesis of POMOFs on carbon cloth and derived phosphides for all pH value hydrogen evolution, *J. Mater. Chem. A* 6 (2018) 21969–21977, <https://doi.org/10.1039/C8TA02219D>.
- [88] J. Beamish-Cook, K. Shankland, C.A. Murray, P. Vaquerio, Insights into the mechanochemical synthesis of MOF-74, *Crys. Growth Des.* 21 (2021) 3047–3055, <https://doi.org/10.1021/acs.cgd.1c00213>.
- [89] T. Friščić, Metal–Organic Frameworks: Mechanochemical Synthesis Strategies, in: *Encyclopedia of Inorganic and Bioinorganic Chemistry*, John Wiley & Sons, Ltd, 2014, pp. 1–19, <https://doi.org/10.1002/9781119951438.eibc2202>.
- [90] B. Nath, Chapter 6 - Mechanochemical synthesis of metal–organic frameworks, in: Y. Azim, S.-U. Rather, S.A. Bhawani, P.M. Bhatt (Eds.), *Synthesis of Metal–Organic Frameworks Via Water-Based Routes*, Elsevier, 2024, pp. 93–120, <https://doi.org/10.1016/B978-0-323-95939-1.00014-9>.
- [91] Z. Wang, Z. Li, M. Ng, P.J. Milner, Rapid mechanochemical synthesis of metal–organic frameworks using exogenous organic base, *Dalton Trans.* 49 (2020) 16238–16244, <https://doi.org/10.1039/D0DT01240H>.
- [92] J. Troyano, C. Çamur, L. Garzón-Tovar, A. Carné-Sánchez, I. Imaz, D. Maspocho, Spray-drying synthesis of MOFs, COFs, and related composites, *Acc. Chem. Res.* (2020), <https://doi.org/10.1021/acs.accounts.0c00133>.
- [93] G.L. Denisov, P.V. Primakov, A.A. Korlyukov, V.V. Novikov, Y.V. Nelyubina, Solvothermal synthesis of the metal–organic framework MOF-5 in autoclaves prepared by 3D printing, *Russ. J. Coord. Chem.* 45 (2019) 836–842, <https://doi.org/10.1134/S1070328419120030>.
- [94] C. McKinstry, R.J. Cathcart, E.J. Cussen, A.J. Fletcher, S.V. Patwardhan, J. Sefcik, Scalable continuous solvothermal synthesis of metal organic framework (MOF-5) crystals, *Chem. Eng. J.* 285 (2016) 718–725, <https://doi.org/10.1016/j.cej.2015.10.023>.
- [95] K.A.S. Usman, J.W. Maina, S. Seyedin, M.T. Conato, L.M. Payawan, L.F. Dumée, J.M. Razal, Downsizing metal–organic frameworks by bottom-up and top-down methods, *NPG Asia Mater.* 12 (2020) 1–18, <https://doi.org/10.1038/s41427-020-00240-5>.
- [96] N. Al Amery, H.R. Abid, S. Al-Saadi, S. Wang, S. Liu, Facile directions for synthesis, modification and activation of MOFs, *Mater. Today Chem.* 17 (2020) 100343, <https://doi.org/10.1016/j.mtchem.2020.100343>.
- [97] Y. Liu, L. Zhou, Y. Dong, R. Wang, Y. Pan, S. Zhuang, D. Liu, J. Liu, Recent developments on MOF-based platforms for antibacterial therapy, *RSC Med. Chem.* 12 (2021) 915–928, <https://doi.org/10.1039/D0MD000416B>.
- [98] D. Bagchi, A. Bhattacharya, T. Dutta, S. Nag, D. Wulferding, P. Lemmens, S.K. Pal, Nano MOF entrapping hydrophobic photosensitizer for dual-stimuli-responsive unprecedented therapeutic action against drug-resistant bacteria, *ACS Appl. Bio Mater.* 2 (2019) 1772–1780, <https://doi.org/10.1021/acsbam.9b00223>.
- [99] W. Zou, L. Zhang, J. Lu, D. Sun, Recent development of metal–organic frameworks in wound healing: current status and applications, *Chem. Eng. J.* 480 (2024) 148220, <https://doi.org/10.1016/j.cej.2023.148220>.
- [100] S. Chen, J. Lu, T. You, D. Sun, Metal–organic frameworks for improving wound healing, *Coord. Chem. Rev.* 439 (2021) 213929, <https://doi.org/10.1016/j.ccr.2021.213929>.
- [101] Y. Zang, L.-K. Li, S.-Q. Zang, Recent development on the alkaline earth MOFs (AEMOFs), *Coord. Chem. Rev.* 440 (2021) 213955, <https://doi.org/10.1016/j.ccr.2021.213955>.
- [102] G. Ye, C. Chen, J. Lin, X. Peng, A. Kumar, D. Liu, J. Liu, Alkali/alkaline earth-based metal–organic frameworks for biomedical applications, *Dalton Trans.* 50 (2021) 17438–17454, <https://doi.org/10.1039/D1DT02814F>.
- [103] M.A. Matlinska, M. Ha, B. Hughton, A.O. Oliynyk, A.K. Iyer, G.M. Bernard, G. Lambkin, M.C. Lawrence, M.J. Katz, A. Mar, V.K. Michaelis, Alkaline earth metal–organic frameworks with tailorable ion release: a path for supporting biomineralization, *ACS Appl. Mater. Interfaces* 11 (2019) 32739–32745, <https://doi.org/10.1021/acsaami.9b11004>.
- [104] A. Vadivelmurugan, R. Sharmila, W.-L. Pan, S.-W. Tsai, Preparation and evaluation of aminomalononitrile-coated Ca–Sr metal–organic frameworks as drug delivery carriers for antibacterial applications, *ACS Omega* 8 (2023) 41909–41917, <https://doi.org/10.1021/acsomega.3c06991>.
- [105] W. Fan, K.-Y. Wang, C. Welton, L. Feng, X. Wang, X. Liu, Y. Li, Z. Kang, H.-C. Zhou, R. Wang, D. Sun, Aluminum metal–organic frameworks: from structures to applications, *Coord. Chem. Rev.* 489 (2023) 215175, <https://doi.org/10.1016/j.ccr.2023.215175>.
- [106] K.H. Cho, D.D. Borges, U.-H. Lee, J.S. Lee, J.W. Yoon, S.J. Cho, J. Park, W. Lombardo, D. Moon, A. Sapienza, G. Maurin, J.-S. Chang, Rational design of a robust aluminum metal–organic framework for multi-purpose water-sorption-driven heat allocations, *Nat. Commun.* 11 (2020) 5112, <https://doi.org/10.1038/s41467-020-18968-7>.
- [107] N. Tannert, C. Jansen, S. Nießing, C. Janiak, Robust synthesis routes and porosity of the Al-based metal–organic frameworks Al-fumarate, CAU-10-H and MIL-160, *Dalton Trans.* 48 (2019) 2967–2976, <https://doi.org/10.1039/C8DT04688C>.
- [108] M. Gaab, N. Trukhan, S. Maurer, R. Gummaraju, U. Müller, The progression of Al-based metal–organic frameworks – From academic research to industrial production and applications, *Micropor. Mesopor. Mater.* 157 (2012) 131–136, <https://doi.org/10.1016/j.micromeso.2011.08.016>.
- [109] J. Benecke, A. Fuß, T.A. Engesser, N. Stock, H. Reinsch, A flexible and porous ferrocene-based gallium MOF with MIL-53 architecture, *Eur. J. Inorg. Chem.* 2021 (2021) 713–719, <https://doi.org/10.1002/ejic.202001085>.
- [110] T. Rhauderwiek, S. Waitschat, S. Wuttke, H. Reinsch, T. Bein, N. Stock, Nanoscale synthesis of two porphyrin-based MOFs with gallium and indium, *Inorg. Chem.* 55 (2016) 5312–5319, <https://doi.org/10.1021/acs.inorgchem.5b02111>.

- acs.inorgchem.6b00221.
- [111] J. Liu, Y. Chen, X. Huang, Y. Ren, M. Hamsch, D. Bodesheim, D. Pohl, X. Li, M. Deconinck, B. Zhang, M. Löffler, Z. Liao, F. Zhao, A. Dianat, G. Cuniberti, Y. Vaynzof, J. Gao, J. Hao, S.C.B. Mannsfeld, X. Feng, R. Dong, On-liquid-gallium surface synthesis of ultra-smooth conductive metal-organic framework thin films, (2024). <https://doi.org/10.48550/arXiv.2404.15357>.
- [112] C. Geggel, S. Gonca, M. Turabik, S. Özdemir, An aluminum-based MOF and its amine form as novel biological active materials for antioxidant, DNA cleavage, antimicrobial, and biofilm inhibition activities, *Mater. Today Sustain.* 19 (2022) 100204, <https://doi.org/10.1016/j.mtsust.2022.100204>.
- [113] K. Huang, J. Wang, Q. Zhang, K. Yuan, Y. Yang, F. Li, X. Sun, H. Chang, Y. Liang, J. Zhao, T. Tang, S. Yang, Sub 150 nm nanoscale gallium based metal-organic frameworks armored antibiotics as super penetrating bombs for eradicating persistent bacteria, *Adv. Funct. Mater.* 32 (2022) 2204906, <https://doi.org/10.1002/adfm.202204906>.
- [114] S. Liu, Y. Ji, H. Zhu, Z. Shi, M. Li, Q. Yu, Gallium-based metal-organic frameworks loaded with antimicrobial peptides for synergistic killing of drug-resistant bacteria, *J. Mater. Chem. B* 11 (2023) 10446–10454, <https://doi.org/10.1039/D3TB01754K>.
- [115] J. Yang, C. Wang, X. Liu, Y. Yin, Y.-H. Ma, Y. Gao, Y. Wang, Z. Lu, Y. Song, Gallium-carbenicillin framework coated defect-rich hollow TiO₂ as a photocatalyzed oxidative stress amplifier against complex infections, *Adv. Funct. Mater.* 30 (2020) 2004861, <https://doi.org/10.1002/adfm.202004861>.
- [116] T. Li, Y. Bai, Y. Wang, H. Xu, H. Jin, Advances in transition-metal (Zn, Mn, Cu)-based MOFs and their derivatives for anode of lithium-ion batteries, *Coord. Chem. Rev.* 410 (2020) 213221, <https://doi.org/10.1016/j.ccr.2020.213221>.
- [117] V. Pascanu, G. González Miera, A.K. Inge, B. Martín-Matute, Metal-organic frameworks as catalysts for organic synthesis: a critical perspective, *J. Am. Chem. Soc.* 141 (2019) 7223–7234, <https://doi.org/10.1021/jacs.9b00733>.
- [118] P. Horcajada, R. Gref, T. Baati, P.K. Allan, G. Maurin, P. Couvreur, G. Férey, R.E. Morris, C. Serre, Metal-organic frameworks in biomedicine, *Chem. Rev.* 112 (2012) 1232–1268, <https://doi.org/10.1021/cr200256v>.
- [119] A. Ayati, M.N. Shahrak, B. Tanhaei, M. Sillanpää, Emerging adsorptive removal of azo dye by metal-organic frameworks, *Chemosphere* 160 (2016) 30–44, <https://doi.org/10.1016/j.chemosphere.2016.06.065>.
- [120] B.M. Connolly, J.P. Mehta, P.Z. Moghadam, A.E.H. Wheatley, D. Fairen-Jimenez, From synthesis to applications: metal-organic frameworks for an environmentally sustainable future, *Curr. Opin. Green Sustain. Chem.* 12 (2018) 47–56, <https://doi.org/10.1016/j.cogsc.2018.06.012>.
- [121] Y. Hu, L. Dai, D. Liu, W. Du, Y. Wang, Progress & prospect of metal-organic frameworks (MOFs) for enzyme immobilization (enzyme/MOFs), *Renew. Sustain. Energy Rev.* 91 (2018) 793–801, <https://doi.org/10.1016/j.rser.2018.04.103>.
- [122] A. Kumari, S. Kaushal, P.P. Singh, Bimetallic metal organic frameworks heterogeneous catalysts: design, construction, and applications, *Mater. Today Energy* 20 (2021) 100667, <https://doi.org/10.1016/j.mtener.2021.100667>.
- [123] A. Dhakshinamoorthy, A.M. Asiri, H. García, Metal-organic framework (MOF) compounds: photocatalysts for redox reactions and solar fuel production, *Angew. Chem. Int. Ed.* 55 (2016) 5414–5445, <https://doi.org/10.1002/anie.201505581>.
- [124] S. Kaushal, G. Kaur, J. Kaur, P.P. Singh, First transition series metal-organic frameworks: synthesis, properties and applications, *Mater. Adv.* 2 (2021) 7308–7335, <https://doi.org/10.1039/D1MA00719J>.
- [125] Y.C. López, H. Viltres, N.K. Gupta, P. Acevedo-Peña, C. Leyva, Y. Ghaffari, A. Gupta, S. Kim, J. Bae, K.S. Kim, Transition metal-based metal-organic frameworks for environmental applications: a review, *Environ. Chem. Lett.* 19 (2021) 1295–1334, <https://doi.org/10.1007/s10311-020-01119-1>.
- [126] M. Barjasteh, S.M. Dehnavi, S. Ahmadi Seyedkhan, M. Akrami, Cu-vitamin B3 donut-like MOFs incorporated into TEMPO-oxidized bacterial cellulose nanofibers for wound healing, *Int. J. Pharm.* 646 (2023) 123484, <https://doi.org/10.1016/j.ijpharm.2023.123484>.
- [127] S.F. Aden, L.A.M. Mahmoud, E.H. Ivanovska, L.R. Terry, V.P. Ting, M.G. Katsikogianni, S. Nayak, Controlled delivery of ciprofloxacin using zirconium-based MOFs and poly-caprolactone composites, *J. Drug Deliv. Sci. Technol.* 88 (2023) 104894, <https://doi.org/10.1016/j.jddst.2023.104894>.
- [128] K. Shoueir, A.R. Wassel, M.K. Ahmed, M.E. El-Naggar, Encapsulation of extremely stable polyaniline onto Bio-MOF: Photo-activated antimicrobial and depletion of ciprofloxacin from aqueous solutions, *J. Photochem. Photobiol. A* 400 (2020) 112703, <https://doi.org/10.1016/j.jphotochem.2020.112703>.
- [129] B. Xue, X. Geng, H. Cui, H. Chen, Z. Wu, H. Chen, H. Li, Z. Zhou, M. Zhao, C. Tan, J. Li, Size engineering of 2D MOF nanosheets for enhanced photodynamic antimicrobial therapy, *Chin. Chem. Lett.* 34 (2023) 108140, <https://doi.org/10.1016/j.ccl.2023.108140>.
- [130] Ahmed.A.G. El-Shahawy, E.M. Dief, S.I. El-Dek, A.A. Farghali, F.I. Abo El-Ela, Nickel-gallate metal-organic framework as an efficient antimicrobial and anticancer agent: in vitro study, *Cancer Nanotechnol.* 14 (2023) 60, <https://doi.org/10.1186/s12645-023-00207-5>.
- [131] E.Y. Kayhan, A. Yildirim, M.B. Kocer, A. Uysal, M. Yilmaz, A cellulose-based material as a fluorescent sensor for Cr(VI) detection and investigation of antimicrobial properties of its encapsulated form in two different MOFs, *Int. J. Biol. Macromol.* 240 (2023) 124426, <https://doi.org/10.1016/j.ijbiomac.2023.124426>.
- [132] A. Yildirim, M.B. Kocer, A. Uysal, M. Yilmaz, Synthesis of new fluorescent metal-organic framework (4-sulfo-1,8-naphthalimide-UiO66) for detection of Cr(III)/Cr(VI) ions in aqueous media and its antimicrobial studies, *Mater. Today Commun.* 32 (2022) 104117, <https://doi.org/10.1016/j.mtcomm.2022.104117>.
- [133] Y. Wu, Y. Luo, B. Zhou, L. Mei, Q. Wang, B. Zhang, Porous metal-organic framework (MOF) carrier for incorporation of volatile antimicrobial essential oil, *Food Control* 98 (2019) 174–178, <https://doi.org/10.1016/j.foodcont.2018.11.011>.
- [134] M. López-R, Y. Barrios, L.D. Perez, C.Y. Soto, C. Sierra, Metal-organic framework (MOFs) tethered to cotton fibers display antimicrobial activity against relevant nosocomial bacteria, *Inorg. Chim. Acta* 537 (2022) 120955, <https://doi.org/10.1016/j.ica.2022.120955>.
- [135] T. Kuang, L. Deng, S. Shen, H. Deng, Z. Shen, Z. Liu, Z. Zhao, F. Chen, M. Zhong, Nano-silver-modified polyphosphazene nanoparticles with different morphologies: Design, synthesis, and evaluation of antibacterial activity, *Chin. Chem. Lett.* 34 (2023) 108584, <https://doi.org/10.1016/j.ccl.2023.108584>.
- [136] B.S. Bashar, H.A. Kareem, Y.M. Hasan, N. Ahmad, A.M. Alshehri, K. Al-Majidi, S.K. Hadrawi, M.M.R.A. Kubaisy, M.T. Qasim, Application of novel Fe₃O₄/Zn-metal organic framework magnetic nanostructures as an antimicrobial agent and magnetic nanocatalyst in the synthesis of heterocyclic compounds, *Front. Chem.* 10 (2022) 1014731, <https://doi.org/10.3389/fchem.2022.1014731>.
- [137] B. Wu, J. Fu, Y. Zhou, Y. Shi, J. Wang, X. Feng, Y. Zhao, G. Zhou, C. Lu, G. Quan, X. Pan, C. Wu, Metal-organic framework-based chemo-photothermal combinational system for precise, rapid, and efficient antibacterial therapeutics, *Pharmaceutics* 11 (2019) 463, <https://doi.org/10.3390/pharmaceutics11090463>.
- [138] Y. Zhan, Y. Yu, P. Wu, P. Ding, Study on the synthesis and antibacterial activity of cobalt-metal organic framework, *J. Phys.: Conf. Ser.* 2393 (2022) 012034, <https://doi.org/10.1088/1742-6596/2393/1/012034>.
- [139] L. Pulvirenti, C. Lombardo, M. Salmeri, C. Bongiorno, G. Mannino, F.Lo Presti, M.T. Cambria, G.G. Condorelli, Self-assembled BiFeO₃/MIL-101 nanocomposite for antimicrobial applications under natural sunlight, *Discover Nano* 18 (2023) 113, <https://doi.org/10.1186/s11671-023-03883-9>.
- [140] M. Asiri, Y. Jawad BahrAluloom, M. Abdullateef Alzubaidi, I. Mourad Mohammed, M. Suliman, E. Ramzy Muhammad, A.S. Abed, F. Abodi Ali, S.K. Hadrawi, A.H. Alsalamy, M. Alwase, Synthesis of Cu/Co-hybrid MOF as a multifunctional porous compound in catalytic applications, synthesis of new nanofibers, and antimicrobial and cytotoxicity agents, *Front. Mater.* 10 (2023), <https://doi.org/10.3389/fmats.2023.1214426>.
- [141] S.M. Sheta, S.R. Salem, S.M. El-Sheikh, A novel iron(III)-based MOF: Synthesis, characterization, biological, and antimicrobial activity study, *J. Mater. Res.* 37 (2022) 2356–2367, <https://doi.org/10.1557/s43578-022-00644-9>.
- [142] T. Asadollahi, N. Moatakef Kazemi, S. Halajian, Alginate-zinc composite modified with metal organic framework for sulfasalazine delivery, *Chem. Pap.* 78 (2024) 565–575, <https://doi.org/10.1007/s11696-023-03110-w>.
- [143] S. Bouson, A. Krittayavathananon, N. Phattharasupakun, P. Siwayaprahm, M. Sawangphruk, Antifungal activity of water-stable copper-containing metal-organic frameworks, *R. Soc. Open Sci.* 4 (2017) 170654, <https://doi.org/10.1098/rsos.170654>.
- [144] Y. Li, Y. Han, H. Li, X. Niu, X. Liu, D. Zhang, H. Fan, K. Wang, Study of bismuth metal organic skeleton composites with photocatalytic antibacterial activity, *J. Coll. Interface Sci.* 653 (2024) 764–776, <https://doi.org/10.1016/j.jcis.2023.09.130>.
- [145] L. Ding, Y. Ding, F. Bai, G. Chen, S. Zhang, X. Yang, H. Li, X. Wang, In situ growth of Cs₃Bi₂Br₉ quantum dots on Bi-MOF nanosheets via cosharing bismuth atoms for CO₂ capture and photocatalytic reduction, *Inorg. Chem.* 62 (2023) 2289–2303, <https://doi.org/10.1021/acs.inorgchem.2c04041>.
- [146] J. Panda, S.P. Tripathy, S. Dash, A. Ray, P. Behera, S. Subudhi, K. Parida, Inner transition metal-modulated metal organic frameworks (IT-MOFs) and their derived nanomaterials: a strategic approach towards stupendous photocatalysis, *Nanoscale* 15 (2023) 7640–7675, <https://doi.org/10.1039/D3NR00274H>.
- [147] Y. Zhang, S. Liu, Z.-S. Zhao, Z. Wang, R. Zhang, L. Liu, Z.-B. Han, Recent progress in lanthanide metal-organic framework and their derivatives in catalytic applications, *Inorg. Chem. Front.* 8 (2021) 590–619, <https://doi.org/10.1039/D0QI01191F>.
- [148] R. Zhang, L. Zhu, B. Yue, Luminescent properties and recent progress in applications of lanthanide metal-organic frameworks, *Chin. Chem. Lett.* 34 (2023) 108009, <https://doi.org/10.1016/j.ccl.2022.108009>.
- [149] Q. Zheng, X. Liu, S. Gao, Z. Cui, S. Wu, Y. Liang, Z. Li, Y. Zheng, S. Zhu, H. Jiang, R. Zou, Engineering dynamic defect of CeIII/CeIV-based metal-organic framework through ultrasound-triggered Au electron trapper for sonodynamic therapy of osteomyelitis, *Small* 19 (2023) 2207687, <https://doi.org/10.1002/smll.202207687>.
- [150] M.C. Zambonino, E.M. Quizhpe, L. Mouheb, A. Rahman, S.N. Agathos, S.A. Dahoumane, Biogenic selenium nanoparticles in biomedical sciences: properties, current trends, novel opportunities and emerging challenges in theranostic nanomedicine, *Nanomaterials* 13 (2023) 424, <https://doi.org/10.3390/nano13030424>.
- [151] Z. Sang, L. Xu, R. Ding, M. Wang, X. Yang, X. Li, B. Zhou, K. Gou, Y. Han, T. Liu, X. Chen, Y. Cheng, H. Yang, H. Li, Nanoparticles exhibiting virus-mimic surface topology for enhanced oral delivery, *Nat. Commun.* 14 (2023) 7694, <https://doi.org/10.1038/s41467-023-43465-y>.
- [152] H. Qin, Y. Chen, Z. Wang, N. Li, Q. Sun, Y. Lin, W. Qiu, Y. Qin, L. Chen, H. Chen, Y. Li, J. Shi, G. Nie, R. Zhao, Biosynthesized gold nanoparticles that activate Toll-like receptors and elicit localized light-converting hyperthermia for pleiotropic tumor immunoregulation, *Nat. Commun.* 14 (2023) 5178, <https://doi.org/10.1038/s41467-023-40851-4>.
- [153] T. Lang, R. Zhu, X. Zhu, W. Yan, Y. Li, Y. Zhai, T. Wu, X. Huang, Q. Yin, Y. Li, Combining gut microbiota modulation and chemotherapy by capcitabine-loaded prebiotic nanoparticle improves colorectal cancer therapy, *Nat. Commun.* 14 (2023) 4746, <https://doi.org/10.1038/s41467-023-40439-y>.
- [154] A. Haleem, M. Javaid, R.P. Singh, S. Rab, R. Suman, Applications of nanotechnology in medical field: a brief review, *Glob. Health J.* 7 (2023) 70–77,

- <https://doi.org/10.1016/j.glojih.2023.02.008>.
- [155] S. Archana, D. Radhika, K. Yogesh Kumar, S.B. Benaka Prasad, R. Deepak Kasai, Introduction to biomedical applications in nanotechnology, in: S. Gopi, P. Balakrishnan, N.M. Mubarak (Eds.), *Nanotechnology for Biomedical Applications*, Springer, Singapore, 2022, pp. 1–14, https://doi.org/10.1007/978-981-16-7483-9_1.
- [156] S.A. Dahoumane, C. Jeffryes, M. Mechouet, S.N. Agathos, Biosynthesis of inorganic nanoparticles: a fresh look at the control of shape, size and composition, *Bioengineering* 4 (2017) 14, <https://doi.org/10.3390/bioengineering4010014>.
- [157] M. Todaria, D. Maity, R. Awasthi, Biogenic metallic nanoparticles as game-changers in targeted cancer therapy: recent innovations and prospects, *Futur, J. Pharm. Sci.* 10 (2024) 25, <https://doi.org/10.1186/s43094-024-00601-9>.
- [158] L. Devi, P. Kushwaha, T.M. Ansari, A. Kumar, A. Rao, Recent trends in biologically synthesized metal nanoparticles and their biomedical applications: a review, *Biol. Trace Elem. Res.* (2023), <https://doi.org/10.1007/s12011-023-03920-9>.
- [159] R. Khurshed, K. Dua, S. Vishwas, M. Gulati, N.K. Jha, G.M. Aldhfeeri, F.G. Alanazi, B.H. Goh, G. Gupta, K.R. Paudel, P.M. Hansbro, D.K. Chellappan, S.K. Singh, Biomedical applications of metallic nanoparticles in cancer: Current status and future perspectives, *Biomed. Pharmacother.* 150 (2022) 112951, <https://doi.org/10.1016/j.biopha.2022.112951>.
- [160] S. Sagadevan, S. Imteyaz, B. Murugan, J.A. Lett, N. Sridewi, G.K. Weldegebrail, I. Fatimah, W.-C. Oh, A comprehensive review on green synthesis of titanium dioxide nanoparticles and their diverse biomedical applications, *Green Process. Synth.* 11 (2022) 44–63, <https://doi.org/10.1515/gps-2022-0005>.
- [161] S. Mukherjee, R. Kotcherlakota, S. Haque, D. Bhattacharya, J.M. Kumar, S. Chakravarty, C.R. Patra, Improved delivery of doxorubicin using rationally designed PEGylated platinum nanoparticles for the treatment of melanoma, *Mater. Sci. Eng. C* 108 (2020) 110375, <https://doi.org/10.1016/j.msec.2019.110375>.
- [162] E.R. Evans, P. Bugga, V. Asthana, R. Drezek, Metallic nanoparticles for cancer immunotherapy, *Mater. Today* 21 (2018) 673–685, <https://doi.org/10.1016/j.mattod.2017.11.022>.
- [163] P. Kuppasamy, M.M. Yusoff, G.P. Maniam, N. Govindan, Biosynthesis of metallic nanoparticles using plant derivatives and their new avenues in pharmacological applications – An updated report, *Saudi Pharm. J.* 24 (2016) 473–484, <https://doi.org/10.1016/j.jsps.2014.11.013>.
- [164] I. Khan, K. Saeed, I. Khan, Nanoparticles: properties, applications and toxicities, *Arab. J. Chem.* 12 (2019) 908–931, <https://doi.org/10.1016/j.arabjc.2017.05.011>.
- [165] J. Dolai, K. Mandal, N.R. Jana, Nanoparticle size effects in biomedical applications, *ACS Appl. Nano Mater.* 4 (2021) 6471–6496, <https://doi.org/10.1021/acsnm.1c00987>.
- [166] B. Rezaei, P. Yari, S.M. Sanders, H. Wang, V.K. Chugh, S. Liang, S. Mostufa, K. Xu, J.-P. Wang, J. Gómez-Pastora, K. Wu, Magnetic nanoparticles: a review on synthesis, characterization, functionalization, and biomedical applications, *Small* 20 (2024) 2304848, <https://doi.org/10.1002/sml.202304848>.
- [167] A. Meher, A. Tandi, S. Moharana, S. Chakroborty, S.S. Mohapatra, A. Mondal, S. Dey, P. Chandra, Silver nanoparticle for biomedical applications: a review, *Hybrid Adv.* 6 (2024) 100184, <https://doi.org/10.1016/j.hybadv.2024.100184>.
- [168] V. Kokkarachedu, D.C. Cid, T. Jayaramudu, R. Sadiku, R.C. Congreve, C.P. Quezada, N. Sisubalan, K. Chandrasekaran, Silver nanoparticles: a promising antimicrobial and antiviral material in advanced healthcare applications, in: V. Kokkarachedu, R. Sadiku (Eds.), *Nanoparticles in Modern Antimicrobial and Antiviral Applications*, Springer International Publishing, Cham, 2024, pp. 1–17, https://doi.org/10.1007/978-3-031-50093-0_1.
- [169] T. Patil, R. Gambhir, A. Vibhute, A.P. Tiwari, Gold nanoparticles: synthesis methods, functionalization and biological applications, *J. Clust. Sci.* 34 (2023) 705–725, <https://doi.org/10.1007/s10876-022-02287-6>.
- [170] M.I. Setyawati, Q. Wang, N. Ni, J.K. Tee, K. Ariga, P.C. Ke, H.K. Ho, Y. Wang, D.T. Leong, Engineering tumoral vascular leakiness with gold nanoparticles, *Nat. Commun.* 14 (2023) 4269, <https://doi.org/10.1038/s41467-023-40015-4>.
- [171] S.A. Ahmed, A.K. Nayak, M.T. Ansari, A. Sherikar, M.U.M. Siddique, S. Alkahtani, S. Ali, M. Tabish, S. Khatoon, A.Q. Darraj, M.S. Hasnain, Quantum dots in biomedical applications: recent advancements and future prospects, in: M.S. Hasnain, A.K. Nayak, S. Alkahtani (Eds.), *Carbon Nanostructures in Biomedical Applications*, Springer International Publishing, Cham, 2023, pp. 169–196, https://doi.org/10.1007/978-3-031-28263-8_7.
- [172] N. Le, K. Kim, Current advances in the biomedical applications of quantum dots: promises and challenges, *Int. J. Mol. Sci.* 24 (2023), <https://doi.org/10.3390/ijms241612682>.
- [173] A. Yañez-Aulestia, N.K. Gupta, M. Hernández, G. Osorio-Toribio, E. Sánchez-González, A. Guzmán-Vargas, J.L. Rivera, I.A. Ibarra, E. Lima, Gold nanoparticles: current and upcoming biomedical applications in sensing, drug, and gene delivery, *Chem. Commun.* 58 (2022) 10886–10895, <https://doi.org/10.1039/D2CC04826D>.
- [174] L. Zhang, Y. Dai, S. Pan, Y. Tan, C. Sun, M. Cao, H. Xu, Copper-selenocysteine quantum dots for NIR-II photothermally enhanced chemodynamic therapy, *ACS Appl. Bio Mater.* 5 (2022) 1794–1803, <https://doi.org/10.1021/acsbm.2c00150>.
- [175] M.I. Anik, N. Mahmud, A. Al Masud, M. Hasan, Gold nanoparticles (GNPs) in biomedical and clinical applications: a review, *Nano Select* 3 (2022) 792–828, <https://doi.org/10.1002/nano.202100255>.
- [176] A. Mittal, I. Roy, S. Gandhi, Magnetic nanoparticles: an overview for biomedical applications, *Magnetochemistry* 8 (2022), <https://doi.org/10.3390/magnetochemistry8090107>.
- [177] E.M. Materón, C.M. Miyazaki, O. Carr, N. Joshi, P.H.S. Picciani, C.J. Dalmaschio, F. Davis, F.M. Shimizu, Magnetic nanoparticles in biomedical applications: a review, *Appl. Surf. Sci. Adv.* 6 (2021) 100163, <https://doi.org/10.1016/j.apsadv.2021.100163>.
- [178] P.M. Martins, A.C. Lima, S. Ribeiro, S. Lanceros-Mendez, P. Martins, Magnetic nanoparticles for biomedical applications: from the soul of the earth to the deep history of ourselves, *ACS Appl. Bio Mater.* 4 (2021) 5839–5870, <https://doi.org/10.1021/acsbm.1c00440>.
- [179] R. Vakayil, S. Muruganantham, N. Kaberdass, M. Rajendran, A. Mahadeo palve, S. Ramasamy, T. Awad Alahmadi, H.S. Almoallim, V. Manikandan, M. Mathanmohun, *Acorus calamus*-zinc oxide nanoparticle coated cotton fabrics shows antimicrobial and cytotoxic activities against skin cancer cells, *Process Biochem.* 111 (2021) 1–8, <https://doi.org/10.1016/j.procbio.2021.08.024>.
- [180] P. Amuthavalli, J.-S. Hwang, H.-U. Dahms, L. Wang, J. Anitha, M. Vasanthakumaran, A.D. Gandhi, K. Murugan, J. Subramaniam, M. Paulpandi, B. Chandramohan, S. Singh, Zinc oxide nanoparticles using plant *Lawsonia inermis* and their mosquitocidal, antimicrobial, anticancer applications showing moderate side effects, *Sci. Rep.* 11 (2021) 8837, <https://doi.org/10.1038/s41598-021-88164-0>.
- [181] B. Khodashenas, M. Ardjmand, A.S. Rad, M.R. Esfahani, Gelatin-coated gold nanoparticles as an effective pH-sensitive methotrexate drug delivery system for breast cancer treatment, *Mater. Today Chem.* 20 (2021) 100474, <https://doi.org/10.1016/j.mtchem.2021.100474>.
- [182] A. Almatroudi, Silver nanoparticles: synthesis, characterisation and biomedical applications, *Open Life Sci.* 15 (2020) 819–839, <https://doi.org/10.1515/biol-2020-0094>.
- [183] A.C. Gomathi, S.R. Xavier Rajarathinam, A.M. Sadiq, S. Rajesh kumar, Anticancer activity of silver nanoparticles synthesized using aqueous fruit shell extract of *Tamarindus indica* on MCF-7 human breast cancer cell line, *J. Drug Deliv. Sci. Technol.* 55 (2020) 101376, <https://doi.org/10.1016/j.jddst.2019.101376>.
- [184] J. Lou-Franco, B. Das, C. Elliott, C. Cao, Gold nanozymes: from concept to biomedical applications, *Nano-Micro Lett.* 13 (2020) 10, <https://doi.org/10.1007/s40820-020-00532-z>.
- [185] A.M. Wagner, J.M. Knipe, G. Orive, N.A. Peppas, Quantum dots in biomedical applications, *Acta Biomater.* 94 (2019) 44–63, <https://doi.org/10.1016/j.actbio.2019.05.022>.
- [186] A.-C. Burduşel, O. Gherasim, A.M. Grumezescu, L. Mogoantă, A. Fica, E. Andronescu, Biomedical applications of silver nanoparticles: an up-to-date overview, *Nanomaterials* 8 (2018), <https://doi.org/10.3390/nano8090681>.
- [187] Y.K. Mohanta, S.K. Panda, K. Biswas, A. Tamang, J. Bandyopadhyay, D. De, D. Mohanta, A.K. Bastia, Biogenic synthesis of silver nanoparticles from *Cassia fistula* (Linn.): in vitro assessment of their antioxidant, antimicrobial and cytotoxic activities, *IET Nanobiotechnol.* 10 (2016) 438–444, <https://doi.org/10.1049/iet-nbt.2015.0104>.
- [188] Y. Gao, Y. Liu, C. Xu, Magnetic nanoparticles for biomedical applications: from diagnosis to treatment to regeneration, in: W. Cai (Ed.), *Engineering in Translational Medicine*, Springer, London, 2014, pp. 567–583, https://doi.org/10.1007/978-1-4471-4372-7_21.
- [189] E.S. Day, L.R. Bickford, J.H. Slater, N.S. Riggall, R.A. Drezek, J.L. West, Antibody-conjugated gold-gold sulfide nanoparticles as multifunctional agents for imaging and therapy of breast cancer, *Int. J. Nanomed.* 5 (2010) 445–454, <https://doi.org/10.2147/IJN.S10881>.
- [190] J.M. Klostranec, W.C.W. Chan, Quantum dots in biological and biomedical research: recent progress and present challenges, *Adv. Mater.* 18 (2006) 1953–1964, <https://doi.org/10.1002/adma.200500786>.
- [191] K.E. Alzahrani, A.A. Niazy, A.M. Alswieleh, R. Wahab, A.M. El-Toni, H.S. Alghamdi, Antibacterial activity of trimetal (CuZnFe) oxide nanoparticles, *Int. J. Nanomed.* 13 (2017) 77–87, <https://doi.org/10.2147/IJN.S154218>.
- [192] T. Batsalova, A. Vasil'kov, D. Moten, A. Voronova, I. Teneva, A. Naumkin, B. Dzhabazov, Bimetallic gold-iron oxide nanoparticles as carriers of methotrexate: perspective tools for biomedical applications, *Appl. Sci.* 13 (2023) 12894, <https://doi.org/10.3390/app132312894>.
- [193] S. Murthy, P. Effiong, C.C. Fei, 11 - Metal oxide nanoparticles in biomedical applications, in: Y. Al-Douri (Ed.), *Metal Oxide Powder Technologies*, Elsevier, 2020, pp. 233–251, <https://doi.org/10.1016/B978-0-12-817505-7.00011-7>.
- [194] M.P. Nikolova, M.S. Chavali, Metal oxide nanoparticles as biomedical materials, *biomimetics* 5 (2020) 27, <https://doi.org/10.3390/biomimetics5020027>.
- [195] K.R. Singh, V. Nayak, J. Singh, A.K. Singh, R.P. Singh, Potentialities of bioinspired metal and metal oxide nanoparticles in biomedical sciences, *RSC Adv.* 11 (2021) 24722–24746, <https://doi.org/10.1039/D1RA04273D>.
- [196] F. Naushin, S. Sen, M. Kumar, H. Bairagi, S. Maiti, J. Bhattacharya, S. Sen, Structural and surface properties of pH-varied Fe₂O₃ nanoparticles: correlation with antibacterial properties, *ACS Omega* 9 (2024) 464–473, <https://doi.org/10.1021/acsomega.3c05930>.
- [197] E. Ren, C. Zhang, D. Li, X. Pang, G. Liu, Leveraging metal oxide nanoparticles for bacteria tracing and eradicating, *VIEW* 1 (2020) 20200052, <https://doi.org/10.1002/view.20200052>.
- [198] B. Ates, S. Koytepe, A. Ulu, C. Gurses, V.K. Thakur, Chemistry, structures, and advanced applications of nanocomposites from biorenewable resources, *Chem. Rev.* 120 (2020) 9304–9362, <https://doi.org/10.1021/acs.chemrev.9b00553>.
- [199] E. Omanović-Miklićanin, A. Badnjević, A. Kazlagić, M. Hajlovač, Nanocomposites: a brief review, *Health Technol.* 10 (2020) 51–59, <https://doi.org/10.1007/s12553-019-00380-x>.
- [200] K. Ravichandran, P.K. Praseetha, T. Arun, S. Gopalakrishnan, Chapter 6 - synthesis of nanocomposites, in: S.M. Bhagyaraj, O.S. Oluwafemi, N. Kalarikkal, S. Thomas (Eds.), *Synthesis of Inorganic Nanomaterials*, Woodhead Publishing,

- 2018, pp. 141–168, <https://doi.org/10.1016/B978-0-08-101975-7.00006-3>.
- [201] B. Arora, R. Bhatia, P. Attri, 28 - Bionanocomposites: green materials for a sustainable future, in: C.M. Hussain, A.K. Mishra (Eds.), *New Polymer Nanocomposites for Environmental Remediation*, Elsevier, 2018, pp. 699–712, <https://doi.org/10.1016/B978-0-12-811033-1.00027-5>.
- [202] G. Velmurugan, V.S. Shankar, S.G. Shree, M. Abarna, B. Rupa, Review and challenges of green polymer-based nanocomposite materials, in: B. Sethuraman, P. Jain, M. Gupta (Eds.), *Recent Advances in Mechanical Engineering*, Springer Nature, Singapore, 2023, pp. 613–624, https://doi.org/10.1007/978-981-99-2349-6_55.
- [203] N. Gendelberg, D. Bird, N.M. Ravindra, Chapter 7 - nanocomposites for biomedical applications, in: K. Song, C. Liu, J.Z. Guo (Eds.), *Polymer-Based Multifunctional Nanocomposites and Their Applications*, Elsevier, 2019, pp. 175–199, <https://doi.org/10.1016/B978-0-12-815067-2.00007-X>.
- [204] S. Murugesan, T. Scheibel, Copolymer/clay nanocomposites for biomedical applications, *Adv. Funct. Mater.* 30 (2020) 1908101, <https://doi.org/10.1002/adfm.201908101>.
- [205] S. Patra, K.M. Sahu, S.S. Purohit, S.K. Swain, Two-dimensional nanomaterials-based polymer nanocomposites for biomedical applications, in: *Two-Dimensional Nanomaterials-Based Polymer Nanocomposites*, 2024: pp. 579–608, <https://doi.org/10.1002/9781119905110.ch16>.
- [206] A.K. Nayak, S. Alkahtani, M.S. Hasnain, *Biomedical nanocomposites*, in: A.K. Nayak, M.S. Hasnain (Eds.), *Biomedical Composites: Perspectives and Applications*, Springer, Singapore, 2021, pp. 35–69, https://doi.org/10.1007/978-981-33-4753-3_3.
- [207] A.E. Shalan, A.S.H. Makhlof, S. Lanceros-Méndez, Nanocomposites materials and their applications: current and future trends, in: A.E. Shalan, A.S. Hamdy Makhlof, S. Lanceros-Méndez (Eds.), *Advances in Nanocomposite Materials for Environmental and Energy Harvesting Applications*, Springer International Publishing, Cham, 2022, pp. 3–14, https://doi.org/10.1007/978-3-030-94319-6_1.
- [208] T. Cele, Preparation of nanoparticles, in: *engineered nanomaterials - health and safety*, IntechOpen (2020), <https://doi.org/10.5772/intechopen.90771>.
- [209] M. Pourmadadi, R. Holghoomi, A. shamsabadipour, R. Maleki-baladi, A. Rahdar, S. Pandey, Copper nanoparticles from chemical, physical, and green synthesis to medicinal application: a review, *Plant Nano Biol.* 8 (2024) 100070, <https://doi.org/10.1016/j.plana.2024.100070>.
- [210] A. Nyabadza, É. McCarthy, M. Makhesana, S. Heidarinasab, A. Plouze, M. Vazquez, D. Brabazon, A review of physical, chemical and biological synthesis methods of bimetallic nanoparticles and applications in sensing, water treatment, biomedicine, catalysis and hydrogen storage, *Adv. Colloid Interface Sci.* 321 (2023) 103010, <https://doi.org/10.1016/j.cis.2023.103010>.
- [211] K.A. Altammar, A review on nanoparticles: characteristics, synthesis, applications, and challenges, *Front. Microbiol.* 14 (2023) 1155622, <https://doi.org/10.3389/fmicb.2023.1155622>.
- [212] S. Ying, Z. Guan, P.C. Ofoegbu, P. Clubb, C. Rico, F. He, J. Hong, Green synthesis of nanoparticles: current developments and limitations, *Environ. Technol. Innov.* 26 (2022) 102336, <https://doi.org/10.1016/j.eti.2022.102336>.
- [213] I. Ijaz, E. Gilani, A. Nazir, A. Bukhari, Detail review on chemical, physical and green synthesis, classification, characterizations and applications of nanoparticles, *Green Chem. Lett. Rev.* 13 (2020) 223–245, <https://doi.org/10.1080/17518253.2020.1802517>.
- [214] A. Q. Malik, T. ul G. Mir, D. Kumar, I.A. Mir, A. Rashid, M. Ayoub, S. Shukla, A review on the green synthesis of nanoparticles, their biological applications, and photocatalytic efficiency against environmental toxins, *Environ. Sci. Pollut. Res.* 30 (2023) 69796–69823, <https://doi.org/10.1007/s11356-023-27437-9>.
- [215] S. Kazemi, A. Hosseingholian, S.D. Gohari, F. Feirahi, F. Moammeri, G. Mesbahian, Z.S. Moghaddam, Q. Ren, Recent advances in green synthesized nanoparticles: from production to application, *Mater. Today Sustain.* 24 (2023) 100500, <https://doi.org/10.1016/j.mtsust.2023.100500>.
- [216] M. Mohammadlou, H. Jafarizadeh-Malmiri, H. Maghsoudi, Hydrothermal green synthesis of silver nanoparticles using Pelargonium/Geranium leaf extract and evaluation of their antifungal activity, *Green Process. Synth.* 6 (2017) 31–42, <https://doi.org/10.1515/gps-2016-0075>.
- [217] A. Roy, S. Datta, R. Luthra, M.A. Khan, A. Gacem, M.A. Hasan, K.K. Yadav, Y. Ahn, B.-H. Jeon, Green synthesis of metalloids nanoparticles and its biological applications: a review, *Front. Chem.* 10 (2022) 994724, <https://doi.org/10.3389/fchem.2022.994724>.
- [218] B.B. Ahire, S.M. Kasabe, Synthesis, characterization and antimicrobial activities of bio functionalized Ag and Au metal nanoparticles: a review, *Orient. J. Chem.* 37 (2021) 281–284, <https://doi.org/10.13005/ojc/370203>.
- [219] A. Jabbar, A. Abbas, N. Assad, M. Naem-ul-Hassan, H.A. Alhazmi, A. Najmi, K. Zoghebi, M.A. Bratty, A. Hanbashi, H.M.A. Amin, A highly selective Hg²⁺ colorimetric sensor and antimicrobial agent based on green synthesized silver nanoparticles using Equisetum diffusum extract, *RSC Adv.* 13 (2023) 28666–28675, <https://doi.org/10.1039/D3RA05070J>.
- [220] N. Choudhary, J. Chaudhari, V. Mochi, P. Patel, D. Ali, S. Alarifi, D.K. Sahoo, A. Patel, V.K. Yadav, Phytanofabrication of copper oxide from Albizia saman and its potential as an antimicrobial agent and remediation of Congo Red dye from wastewater, *Water* 15 (2023) 3787, <https://doi.org/10.3390/w15213787>.
- [221] E.R.A. Begum, R. Shenbagarathai, U. Lavanya, K. Bhavan, Synthesis, characterization, and antimicrobial activity of extracted chitosan-based silver nanoparticles, *J. Microbiol. Biotechnol. Food Sci.* 12 (2023) <https://doi.org/10.55251/jmbfs.4215>, e4215–e4215.
- [222] B.H. Shnawa, P.J. Jailil, S.M. Hamad, M.H. Ahmed, Antioxidant, protocoelical, hemocompatibility, and antibacterial activity of nickel oxide nanoparticles synthesized by ziziphus spina-christi, *BioNanoSci* 12 (2022) 1264–1278, <https://doi.org/10.1007/s12668-022-01028-3>.
- [223] L. Safavinia, M.R. Akhgar, B. Tahamipour, S.A. Ahmadi, Green synthesis of highly dispersed zinc oxide nanoparticles supported on silica gel matrix by daphne oleoides extract and their antibacterial activity, *Iran. J. Biotechnol.* 19 (2021) 86–95, <https://doi.org/10.30498/IJB.2021.2598>.
- [224] D.N. Chandrani, S. Ghosh, A.R. Tanna, Green synthesis for fabrication of cobalt ferrite nanoparticles with photocatalytic dye degrading potential as a sustainable effluent treatment strategy, *J. Inorg. Organomet. Polym. Mater.* (2024), <https://doi.org/10.1007/s10904-023-02981-6>.
- [225] Z.A. Sandhu, M.A. Raza, A. Alqurashi, S. Sajid, S. Ashraf, K. Imtiaz, F. Aman, A.H. Alessa, M.B. Shamsi, M. Latif, Advances in the optimization of Fe nanoparticles: unlocking antifungal properties for biomedical applications, *Pharmaceutics* 16 (2024) 645, <https://doi.org/10.3390/pharmaceutics16050645>.
- [226] N.B. Guerra, J. Bortoluz, A.R. Bystronski, A.E.D. Maddalozzo, D. Restelatto, M. Roesch-Ely, D.M. Devine, M. Giovanna, J.S. Crespo, Recent progress on natural rubber-based materials containing metallic and metal oxide nanoparticles: state of the art and biomedical applications, *Compounds* 3 (2023) 310–333, <https://doi.org/10.3390/compounds3020023>.
- [227] F. Liaqat, M.I. Khazi, A.S. Awan, R. Eltem, J. Li, 15 - antimicrobial studies of metal oxide nanomaterials, in: M.A. Chaudhry, R. Hussain, F.K. Butt (Eds.), *Metal Oxide-Carbon Hybrid Materials*, Elsevier, 2022, pp. 407–435, <https://doi.org/10.1016/B978-0-12-822694-0.00020-X>.
- [228] V. Chandrakala, V. Aruna, G. Angajala, Review on metal nanoparticles as nanocarriers: current challenges and perspectives in drug delivery systems, *Emergent Mater.* 5 (2022) 1593–1615, <https://doi.org/10.1007/s42247-021-00335-x>.
- [229] M.A. Islam, M.V. Jacob, E. Antunes, A critical review on silver nanoparticles: From synthesis and applications to its mitigation through low-cost adsorption by biochar, *J. Environ. Manage.* 281 (2021) 111918, <https://doi.org/10.1016/j.jenvman.2020.111918>.
- [230] E. Matras, A. Gorczyca, S.W. Przemieniecki, M. Oćwieja, Surface properties-dependent antifungal activity of silver nanoparticles, *Sci. Rep.* 12 (2022) 18046, <https://doi.org/10.1038/s41598-022-22659-2>.
- [231] A. Gibała, P. Żeliszewska, T. Gosiewski, A. Krawczyk, D. Duraczynska, J. Szaleniec, M. Szaleniec, M. Oćwieja, Antibacterial and antifungal properties of silver nanoparticles—effect of a surface-stabilizing agent, *Biomolecules* 11 (2021) 1481, <https://doi.org/10.3390/biom11101481>.
- [232] H.F. Hetta, I.M.S. Al-Kadmy, S.S. Khazaal, S. Abbas, A. Suhail, M.A. El-Mokhtar, N.H.A. Ellah, E.A. Ahmed, R.B. Abd-ellatif, E.A. El-Masry, G.E.-S. Batiha, A.A. Elkady, N.A. Mohamed, A.M. Algamal, Antibiofilm and antiviral potential of silver nanoparticles against multidrug-resistant *Acinetobacter baumannii*, *Sci. Rep.* 11 (2021) 10751, <https://doi.org/10.1038/s41598-021-90208-4>.
- [233] M.C. Chen, P.W. Koh, V.K. Ponnusamy, S.L. Lee, Titanium dioxide and other nanomaterials based antimicrobial additives in functional paints and coatings: review, *Prog. Org. Coat.* 163 (2022) 106660, <https://doi.org/10.1016/j.porgcoat.2021.106660>.
- [234] X. Ma, S. Zhou, X. Xu, Q. Du, Copper-containing nanoparticles: Mechanism of antimicrobial effect and application in dentistry—a narrative review, *Front. Surg.* 9 (2022) 905892, <https://doi.org/10.3389/fsurg.2022.905892>.
- [235] C.R. Mendes, G. Dilarri, C.F. Forsan, V.de M.R. Sapata, P.R.M. Lopes, P.B. de Moraes, R.N. Montagnoli, H. Ferreira, E.D. Bidoia, Antibacterial action and target mechanisms of zinc oxide nanoparticles against bacterial pathogens, *Sci. Rep.* 12 (2022) 2658, <https://doi.org/10.1038/s41598-022-06657-y>.
- [236] L.M. Hussein, A.Y. Hasan, The antibacterial activity of the biosynthesized copper oxide nanoparticles by lantana camara flowers extract against some bacterial isolated from burns, *Al-Mustansiriyah J. Sci.* 33 (2022) 39–52, <https://doi.org/10.23851/mjs.v33i5.1311>.
- [237] M. Azizi-Lalabadi, A. Ehsani, B. Divband, M. Alizadeh-Sani, Antimicrobial activity of titanium dioxide and zinc oxide nanoparticles supported in 4A zeolite and evaluation the morphological characteristic, *Sci. Rep.* 9 (2019) 17439, <https://doi.org/10.1038/s41598-019-54025-0>.
- [238] P.G. Jamkhande, N.W. Ghule, A.H. Bamer, M.G. Kalaskar, Metal nanoparticles synthesis: an overview on methods of preparation, advantages and disadvantages, and applications, *J. Drug Deliv. Sci. Technol.* 53 (2019) 101174, <https://doi.org/10.1016/j.jddst.2019.101174>.
- [239] F.C. C. K. T, Advances in stabilization of metallic nanoparticle with biosurfactants—a review on current trends, *Heliyon* 10 (2024) e29773, <https://doi.org/10.1016/j.heliyon.2024.e29773>.
- [240] I. Naletova, B. Tomasello, F. Attanasio, V.V. Pleshkan, Prospects for the use of metal-based nanoparticles as adjuvants for local cancer immunotherapy, *Pharmaceutics* 15 (2023) 1346, <https://doi.org/10.3390/pharmaceutics15051346>.
- [241] S. Zahmatkesh, M. Hajiaghahi-Keshтели, A. Bokhari, S. Sundaramurthy, B. Panneerselvam, Y. Rezakhani, Wastewater treatment with nanomaterials for the future: a state-of-the-art review, *Environ. Res.* 216 (2023) 114652, <https://doi.org/10.1016/j.envres.2022.114652>.
- [242] M.I.H. Mondal, F. Ahmed, M.M. Islam, M.N. Pervez, J. Saha, 11 - Metal and metal oxides nanoparticles in healthcare and medical textiles, in: M.I.H. Mondal (Ed.), *Medical Textiles from Natural Resources*, Woodhead Publishing, 2022, pp. 341–371, <https://doi.org/10.1016/B978-0-323-90479-7.00010-5>.
- [243] X. Yang, X. Cao, C. Chen, L. Liao, S. Yuan, S. Huang, Green synthesis of zinc oxide nanoparticles using aqueous extracts of hibiscus cannabinus L.: wastewater purification and antibacterial activity, *Separations* 10 (2023) 466, <https://doi.org/10.3390/separations10090466>.
- [244] S.A. Shilpa, M.S. Subbulakshmi, G.S. Hikku, Nanoparticles of metal/metal oxide

- embedded fabrics to impart antibacterial activity to counteract hospital acquired infections, *Eng. Res. Express* 4 (2022) 032002, <https://doi.org/10.1088/2631-8695/ac8f1c>.
- [245] E. Lizundia, I. Armentano, F. Luzzi, F. Bertoglio, E. Restivo, L. Visai, L. Torre, D. Puglia, Synergic effect of nanolignin and metal oxide nanoparticles into Poly(l-lactide) bionanocomposites: material properties, antioxidant activity, and antibacterial performance, *ACS Appl. Bio Mater.* 3 (2020) 5263–5274, <https://doi.org/10.1021/acsbm.0c00637>.
- [246] S.A. Kumar, M. Jarvin, S. Sharma, A. Umar, S.S.R. Inbanathan, N.P. Lalla, Facile and green synthesis of MgO nanoparticles for the degradation of victoria blue dye under UV irradiation and their antibacterial activity, *ES Food Agroforest.* 5 (2021) 14–19.
- [247] A.K. Shimi, H.M. Ahmed, M. Wahab, S. Katheria, S.M. Wabaidur, G.E. Eldesoky, M.A. Islam, K.P. Rane, Synthesis and applications of green synthesized TiO₂ nanoparticles for photocatalytic dye degradation and antibacterial activity, *J. Nanomater.* 2022 (2022) e7060388, <https://doi.org/10.1155/2022/7060388>.
- [248] N. El-Shafai, M.E. El-Khouly, M. El-Kemary, M. Ramadan, I. Eldesoukey, M. Masoud, Graphene oxide decorated with zinc oxide nanoflower, silver and titanium dioxide nanoparticles: fabrication, characterization, DNA interaction, and antibacterial activity, *RSC Adv.* 9 (2019) 3704–3714, <https://doi.org/10.1039/C8RA09788G>.
- [249] P. Halder, I. Mondal, A. Mukherjee, S. Biswas, S. Sau, S. Mitra, B.K. Paul, D. Mondal, B. Chattopadhyay, S. Das, Te⁴⁺ and Er³⁺ doped ZrO₂ nanoparticles with enhanced photocatalytic, antibacterial activity and dielectric properties: a next generation of multifunctional material, *J. Environ. Manage.* 359 (2024) 120985, <https://doi.org/10.1016/j.jenvman.2024.120985>.
- [250] D. Steinerová, A. Kalendová, J. Machotová, P. Knotek, P. Humpolček, J. Vajdák, S. Slang, A. Krejčová, L. Beneš, F. Wolff-Fabris, Influence of metal oxide nanoparticles as antimicrobial additives embedded in waterborne coating binders based on self-crosslinking acrylic latex, *Coatings* 12 (2022) 1445, <https://doi.org/10.3390/coatings12101445>.
- [251] A.W. McFarland, A. Elumalai, C.C. Miller, A. Humayun, D.K. Mills, Effectiveness and applications of a metal-coated HNT/poly(lactic acid) antimicrobial filtration system, *Polymers* 14 (2022) 1603, <https://doi.org/10.3390/polym14081603>.
- [252] A.H. Hashem, A.M. Shehabeldine, O.M. Ali, S.S. Salem, Synthesis of chitosan-based gold nanoparticles: antimicrobial and wound-healing activities, *Polymers* 14 (2022) 2293, <https://doi.org/10.3390/polym14112293>.
- [253] E. Sánchez-López, D. Gomes, G. Esteruelas, L. Bonilla, A.L. Lopez-Machado, R. Galindo, A. Cano, M. Espina, M. Etcheto, A. Camins, A.M. Silva, A. Durazzo, A. Santini, M.L. Garcia, E.B. Souto, Metal-based nanoparticles as antimicrobial agents: an overview, *Nanomaterials* 10 (2020) 292, <https://doi.org/10.3390/nano10020292>.
- [254] J.M.V. Makabenta, A. Nabawy, C.-H. Li, S. Schmidt-Malan, R. Patel, V.M. Rotello, Nanomaterial-based therapeutics for antibiotic-resistant bacterial infections, *Nat. Rev. Microbiol.* 19 (2021) 23–36, <https://doi.org/10.1038/s41579-020-0420-1>.
- [255] L. Luo, W. Huang, J. Zhang, Y. Yu, T. Sun, Metal-based nanoparticles as antimicrobial agents: a review, *ACS Appl. Nano Mater.* 7 (2024) 2529–2545, <https://doi.org/10.1021/acsnan.3c05615>.
- [256] S. Gautam, D.K. Das, J. Kaur, A. Kumar, M. Ubaidullah, M. Hasan, K.K. Yadav, R.K. Gupta, Transition metal-based nanoparticles as potential antimicrobial agents: recent advancements, mechanistic, challenges, and future prospects, *Discover Nano* 18 (2023) 84, <https://doi.org/10.1186/s11671-023-03861-1>.
- [257] A. Frei, A.D. Verdeso, A.G. Elliott, J. Zuegg, M.A.T. Blaskovich, Metals to combat antimicrobial resistance, *Nat. Rev. Chem.* 7 (2023) 202–224, <https://doi.org/10.1038/s41570-023-00463-4>.
- [258] Q. Zhang, H. Zhou, P. Jiang, X. Xiao, Metal-based nanomaterials as antimicrobial agents: a novel driveway to accelerate the aggravation of antibiotic resistance, *J. Hazard. Mater.* 455 (2023) 131658, <https://doi.org/10.1016/j.jhazmat.2023.131658>.
- [259] W.M. Saod, L.L. Hamid, N.J. Alaallah, A. Ramizy, Biosynthesis and antibacterial activity of manganese oxide nanoparticles prepared by green tea extract, *Biotechnol. Rep.* 34 (2022) e00729, <https://doi.org/10.1016/j.btre.2022.e00729>.
- [260] M. Jayandran, M.M. Haneefa, V. Balasubramanian, Green synthesis and characterization of manganese nanoparticles using natural plant extracts and its evaluation of antimicrobial activity, *J. App. Pharm. Sci.* 5 (2015) 105–110, <https://doi.org/10.7324/JAPS.2015.501218>.
- [261] B. Krishnan, S. Mahalingam, Facile synthesis and antimicrobial activity of manganese oxide/bentonite nanocomposites, *Res. Chem. Intermed.* 43 (2017) 2351–2365, <https://doi.org/10.1007/s11164-016-2765-7>.
- [262] C. Lopez-Abarrategui, V. Figueroa-Espi, M.B. Lugo-Alvarez, C.D. Pereira, H. Garay, J.A. Barbosa, R. Falcão, L. Jiménez-Hernández, O. Estévez-Hernández, E. Reguera, O.L. Franco, S.C. Dias, A.J. Otero-Gonzalez, The intrinsic antimicrobial activity of citric acid-coated manganese ferrite nanoparticles is enhanced after conjugation with the antifungal peptide Cm-p5, *Int. J. Nanomed.* 11 (2016) 3849–3857, <https://doi.org/10.2147/IJN.S107561>.
- [263] Z. Xu, Z. Qiu, Q. Liu, Y. Huang, D. Li, X. Shen, K. Fan, J. Xi, Y. Gu, Y. Tang, J. Jiang, J. Xu, J. He, X. Gao, Y. Liu, H. Koo, X. Yan, L. Gao, Converting organosulfur compounds to inorganic polysulfides against resistant bacterial infections, *Nat. Commun.* 9 (2018) 3713, <https://doi.org/10.1038/s41467-018-06164-7>.
- [264] Y. Wang, J. Ren, M. Ou, J. Cui, H. Guan, R. Lian, C. Jiao, X. Chen, Flame-retardant and antibacterial properties of cotton fabrics treated by epichlorohydrin-modified aramid nanofibers, ionic liquid, and Cu ion, *Polym. Degrad. Stab.* 212 (2023) 110347, <https://doi.org/10.1016/j.polydegradstab.2023.110347>.
- [265] E. Pormohammad, P. Ghamari kargar, G. Bagherzade, H. Beyzaei, Loading of green-synthesized Cu nanoparticles on Ag complex containing 1,3,5-triazine Schiff base with enhanced antimicrobial activities, *Sci. Rep.* 13 (2023) 20421, <https://doi.org/10.1038/s41598-023-47358-4>.
- [266] R. Govindasamy, M. Govindarasu, S.S. Alharthi, P. Mani, N. Bernardshaw, T. Gomathi, M.A. Ansari, M.N. Alomary, B. Atwah, M.S. Malik, V.D. Rajeswari, K. Rekha, S.A. Ahmed, M. Thiruvengadam, Sustainable green synthesis of yttrium oxide (Y₂O₃) nanoparticles using lontana camara leaf extracts: physicochemical characterization, photocatalytic degradation, antibacterial, and anticancer potency, *Nanomaterials* 12 (2022) 2393, <https://doi.org/10.3390/nano12142393>.
- [267] J. Balcucho, D.M. Narváez, N.A. Tarazona, J.L. Castro-Mayorga, Microbially synthesized polymer-metal nanoparticles composites as promising wound dressings to overcome methicillin-resistance *Staphylococcus aureus* infections, *Polymers* 15 (2023) 920, <https://doi.org/10.3390/polym15040920>.
- [268] E. Porta, S. Cogliati, M. Francisco, M.V. Roldán, N. Mamana, R. Grau, N. Pellegri, Stable colloidal copper nanoparticles functionalized with siloxane groups and their microbicidal activity, *J. Inorg. Organomet. Polym. Mater.* 29 (2019) 964–978, <https://doi.org/10.1007/s10904-018-01071-2>.
- [269] J. Guo, W. Wei, Y. Zhao, H. Dai, Iron oxide nanoparticles with photothermal performance and enhanced nanozyme activity for bacteria-infected wound therapy, *Regen. Biomater.* 9 (2022) rbac041, <https://doi.org/10.1093/rb/rbac041>.
- [270] A. Vasil'kov, D. Migulin, A. Naumkin, I. Volkov, I. Butenko, A. Golub, V. Sadykova, A. Muzafarov, Hybrid materials with antimicrobial properties based on hyperbranched polyaminopropylalkoxysiloxanes embedded with Ag nanoparticles, *Pharmaceutics* 15 (2023) 809, <https://doi.org/10.3390/pharmaceutics15030809>.
- [271] P. Walunj, A. Roy, V. Jadhav, P. Athare, A. Dhaygude, J. Aher, J.S. Algethami, D. Lokhande, M.S. Alqahtani, A. Bhagare, S. Alghamdi, L.B. Eltayeb, I.S. Al-Moraya, K.K. Yadav, Y. Ahn, B.-H. Jeon, Polyol-mediated zinc oxide nanoparticles using the refluxing method as an efficient photocatalytic and antimicrobial agent, *Front. Bioeng. Biotechnol.* 11 (2023), <https://doi.org/10.3389/fbioe.2023.1177981>.
- [272] Y.A. Fesseha, A.H. Manayia, P.-C. Liu, T.-H. Su, S.-Y. Huang, C.-W. Chiu, C.-C. Cheng, Photoreactive silver-containing supramolecular polymers that form self-assembled nanogels for efficient antibacterial treatment, *J. Colloid Interface Sci.* 654 (2024) 967–978, <https://doi.org/10.1016/j.jcis.2023.10.119>.
- [273] H. Alamri, G. Chen, S.D. Huang, Development of biocompatible Ga₂(HPO₄)₃ nanoparticles as an antimicrobial agent with improved Ga resistance development profile against *Pseudomonas aeruginosa*, *Antibiotics* 12 (2023) 1578, <https://doi.org/10.3390/antibiotics12111578>.
- [274] Z. Lin, C. Gao, D. Wang, Q. He, Bubble-propelled Janus gallium/zinc micromotors for the active treatment of bacterial infections, *Angew. Chem. Int. Ed.* 60 (2021) 8750–8754, <https://doi.org/10.1002/anie.202016260>.
- [275] T. Huang, S. Huang, D. Liu, W. Zhu, Q. Wu, L. Chen, X. Zhang, M. Liu, Y. Wei, Recent advances and progress on the design, fabrication and biomedical applications of Gallium liquid metals-based functional materials, *Coll. Surf. B: Biointerfaces* 238 (2024) 113888, <https://doi.org/10.1016/j.colsurfb.2024.113888>.
- [276] A. Elbourne, S. Cheeseman, P. Atkin, N.P. Truong, N. Syed, A. Zavabeti, M. Mohiuddin, D. Esrafilzadeh, D. Cozzolino, C.F. McConville, M.D. Dickey, R.J. Crawford, K. Kalantar-Zadeh, J. Chapman, T. Daeneke, V.K. Truong, Antibacterial liquid metals: biofilm treatment via magnetic activation, *ACS Nano* 14 (2020) 802–817, <https://doi.org/10.1021/acsnano.9b07861>.
- [277] S. Cheeseman, A. Elbourne, R. Kariuki, A.V. Ramarao, A. Zavabeti, N. Syed, A.J. Christofferson, K.Y. Kwon, W. Jung, M.D. Dickey, K. Kalantar-Zadeh, C.F. McConville, R.J. Crawford, T. Daeneke, J. Chapman, V.K. Truong, Broad-spectrum treatment of bacterial biofilms using magneto-responsive liquid metal particles, *J. Mater. Chem. B* 8 (2020) 10776–10787, <https://doi.org/10.1039/D0TB01655A>.
- [278] M. Vahedi, N. Hosseini-Jazani, S. Yousefi, M. Gahremani, Evaluation of antibacterial effects of nickel nanoparticles on biofilm production by *Staphylococcus epidermidis*, *Iran J. Microbiol.* 9 (2017) 160–168.
- [279] M. Ghaffarlou, S. İlk, H. Hammamchi, F. Kırac, M. Okan, O. Güven, M. Barsbay, Green and facile synthesis of pullulan-stabilized silver and gold nanoparticles for the inhibition of quorum sensing, *ACS Appl. Bio Mater.* 5 (2022) 517–527, <https://doi.org/10.1021/acsbm.1c00964>.
- [280] N.E. Sunny, A. Kaviya, P. Saravanan, R. Rajeshkannan, M. Rajasimman, S.V. Kumar, In vitro and in silico molecular docking analysis of green synthesized tin oxide nanoparticles using brown algae species of *Padina gymnospora* and *Turbinaria ornata*, *Biomass Conv. Bioref.* (2022), <https://doi.org/10.1007/s13399-022-03253-y>.
- [281] V. Santás-Miguel, M. Arias-Estévez, A. Rodríguez-Seijo, D. Arenas-Lago, Use of metal nanoparticles in agriculture. A review on the effects on plant germination, *Environ. Pollut.* 334 (2023) 122222, <https://doi.org/10.1016/j.envpol.2023.122222>.
- [282] P. Wang, E. Lombi, F.-J. Zhao, P.M. Kopittke, Nanotechnology: a new opportunity in plant sciences, *Trends Plant Sci.* 21 (2016) 699–712, <https://doi.org/10.1016/j.tplants.2016.04.005>.
- [283] R. Bhattacharjee, L. Kumar, N. Mukerjee, U. Anand, A. Dhasmana, S. Preetam, S. Bhaumik, S. Sibi, S. Pal, T. Khare, S. Chattopadhyay, S.A. El-Zahaby, A. Alexiou, E.P. Koshy, V. Kumar, S. Malik, A. Dey, J. Proćków, The emergence of metal oxide nanoparticles (NPs) as a phytomedicine: a two-facet role in plant growth, nano-toxicity and anti-phyto-microbial activity, *Biomed. Pharmacother.* 155 (2022) 113658, <https://doi.org/10.1016/j.biopha.2022.113658>.
- [284] Y. Abdallah, S.O. Ogunyemi, J. Bi, F. Wang, X. Huang, X. Shi, J. Jiang, E. Ibrahim, M. Mohany, S.S. Al-Rejazi, C. Yan, B. Li, Nickel oxide nanoparticles: a

- new generation nanoparticles to combat bacteria *Xanthomonas oryzae* pv. *oryzae* and enhance rice plant growth, *Pestic. Biochem. Phys.* 200 (2024) 105807, <https://doi.org/10.1016/j.pestbp.2024.105807>.
- [285] S.O. Ogunyemi, M. Zhang, Y. Abdallah, T. Ahmed, W. Qiu, M.A. Ali, C. Yan, Y. Yang, J. Chen, B. Li, The bio-synthesis of three metal oxide nanoparticles (ZnO, MnO₂, and MgO) and their antibacterial activity against the bacterial leaf blight pathogen, *Front. Microbiol.* 11 (2020) 588326, <https://doi.org/10.3389/fmicb.2020.588326>.
- [286] L. Hao, Q. Zheng, M. Guan, M. Zhou, Z. Yin, H. Chen, H. Zhou, X. Zhou, Large ultrathin polyoxomolybdate-decorated boron nitride nanosheets with enhanced antibacterial activity for infection control, *ACS Appl. Nano Mater.* 6 (2023) 4754–4769, <https://doi.org/10.1021/acsnano.3c00247>.
- [287] Y. Pan, H. Zheng, G. Li, Y. Li, J. Jiang, J. Chen, Q. Xie, D. Wu, R. Ma, X. Liu, S. Xu, J. Jiang, X. Cai, M. Gao, W. Wang, H. Zuilhof, M. Ye, R. Li, Antibiotic-like activity of atomic layer boron nitride for combating resistant bacteria, *ACS Nano* 16 (2022) 7674–7688, <https://doi.org/10.1021/acsnano.1c11353>.
- [288] P.T. Beyli, M. Doğan, Z. Gündüz, M. Alkan, Y. Turhan, Synthesis, characterization and their antimicrobial activities of boron oxide/poly(acrylic acid) nanocomposites: thermal and antimicrobial properties, *Adv. Mater. Sci.* 18 (2018) 28–36, <https://doi.org/10.1515/adms-2017-0025>.
- [289] R. Yang, M. Sun, Borophenes: monolayer, bilayer and heterostructures, *J. Mater. Chem. C* 11 (2023) 6834–6846, <https://doi.org/10.1039/D3TC00974B>.
- [290] N. Taşaltın, S. Güllülü, S. Karakuş, Dual-role of β borophene nanosheets as highly effective antibacterial and antifungal agent, *Inorg. Chem. Commun.* 136 (2022) 109150, <https://doi.org/10.1016/j.inoche.2021.109150>.
- [291] A.I. El-Batal, G.S. El-Sayyad, N.E. Al-Hazmi, M. Gobara, Antibiofilm and antimicrobial activities of silver boron nanoparticles synthesized by PVP polymer and gamma rays against urinary tract pathogens, *J. Clust. Sci.* 30 (2019) 947–964, <https://doi.org/10.1007/s10876-019-01553-4>.
- [292] R.S. Özakar, M.S. Bingöl, M.C. Adıgüzel, E. Özakar, Preparation, characterization of chitosan-coated/uncoated boron nanoparticles and in-vitro evaluation of their antimicrobial effects, *Polymer (Korea)* 46 (2022) 709–721, <https://doi.org/10.7317/pk.2022.46.6.709>.
- [293] P.T. Tabriz, P.H. Maghsodi, A.J. Afarin, H. Heydari, F. Amiry, M.R. Sazegar, Antibacterial composite: polymeric mesoporous silica nanoparticles and combination of imipenem/meropenem, *J. Mater. Chem. B* 11 (2023) 1971–1977, <https://doi.org/10.1039/D2TB02442J>.
- [294] I. Zarafu, A.A. Jebur Al Taweel, C. Limban, M. Popa, L. Măruțescu, M.C. Chifiriuc, G.G. Pircalabioru, D. Culiță, C. Ghica, P. Ionita, Aminopropyl-silica functionalized with halogen-reactive compounds for antimicrobial applications, *Mater. Chem. Phys.* 241 (2020) 122353, <https://doi.org/10.1016/j.matchemphys.2019.122353>.
- [295] J. Takeshita, S. Aoki, R. Wada, A. Osawa, J. Sawai, Antimicrobial properties of a copper/silicone composite membrane prepared using a two-step immersion process in iodine and copper sulfate solutions, *Membranes* 12 (2022) 1049, <https://doi.org/10.3390/membranes12111049>.
- [296] Y. Jiang, W. Zheng, K. Tran, E. Kamilar, J. Bariwal, H. Ma, H. Liang, Hydrophilic nanoparticles that kill bacteria while sparing mammalian cells reveal the antibiotic role of nanostructures, *Nat. Commun.* 13 (2022) 197, <https://doi.org/10.1038/s41467-021-27193-9>.
- [297] M. Sattary, J. Amini, R. Hallaj, Antifungal activity of the lemongrass and clove oil encapsulated in mesoporous silica nanoparticles against wheat's take-all disease, *Pestic. Biochem. Phys.* 170 (2020) 104696, <https://doi.org/10.1016/j.pestbp.2020.104696>.
- [298] J. Palma-Guerrero, T. Chancellor, J. Spong, G. Canning, J. Hammond, V.E. McMillan, K.E. Hammond-Kosack, Take-all disease: new insights into an important wheat root pathogen, *Trends Plant Sci.* 26 (2021) 836–848, <https://doi.org/10.1016/j.tplants.2021.02.009>.
- [299] M.F. Zaki, S.M. Tawfik, Synthesis, surface properties and antimicrobial activity of some germanium nonionic surfactants, *J. Oleo Sci.* 63 (2014) 921–931, <https://doi.org/10.5650/jos.ess14052>.
- [300] M.M. Lazarević, N.L. Ignjatović, Q. Mahlet, V.V. Bumah, M. Radunović, J. Milašin, D.P. Uskoković, V. Uskoković, Biocompatible germanium-doped hydroxyapatite nanoparticles for promoting osteogenic differentiation and antimicrobial activity, *ACS Appl. Nano Mater.* 7 (2024) 8580–8592, <https://doi.org/10.1021/acsnm.3c05974>.
- [301] M. Shakibaie, M. Adeli-Sardou, T. Mohammadi-Khorsand, M. Zeydabadi-Nejad, E. Amirafzali, S. Amirpour-Rostami, A. Ameri, H. Foroortanfar, Antimicrobial and antioxidant activity of the biologically synthesized tellurium nanorods; a preliminary in vitro study, *Iran. J. Biotechnol.* 15 (2017) 268–276, <https://doi.org/10.15171/ijb.1580>.
- [302] A. Tang, Q. Ren, Y. Wu, C. Wu, Y. Cheng, Investigation into the antibacterial mechanism of biogenic tellurium nanoparticles and precursor tellurite, *Int. J. Mol. Sci.* 23 (2022) 11697, <https://doi.org/10.3390/ijms231911697>.